Estimation of radon and thoron in environmental samples

A thesis submitted to the
University of Calicut, Kerala
for the award of the Degree of
DOCTOR OF PHILOSOPHY
in **PHYSICS**
under the Faculty of Science

by

Ramsiya M

Department of Physics
University of Calicut
Kerala, India
October 2018

CERTIFICATE

This is to certify that the corrections/suggestions from the adjudicators have been incorporated in the thesis entitled "**Estimation of radon and thoron in environmental samples**" submitted to the Department of Physics, University of Calicut by Mrs. Ramsiya M.

Dr. Antony Joseph
Supervising Guide
Department of Physics
University of Calicut

Calicut University
16-08-2019

CERTIFICATE

This is to certify that the thesis entitled "**Estimation of radon and thoron in environmental samples**" submitted to the Department of Physics, University of Calicut by **Mrs. Ramsiya M.** in partial fulfilment of the requirements for the award of the degree of **Doctor of Philosophy** in Physics is the original work carried out by her under my supervision and guidance at the Department of Physics, University of Calicut. This thesis has not been submitted by her for the award of any other degree, diploma, associateship, fellowship etc. of any other university or institute.

Dr. Antony Joseph
Professor, Department of Physics
University of Calicut
Calicut University P.O.
Kerala - 673635, India
(Supervising Guide)

Calicut University
30-10-2018

DECLARATION

I hereby declare that the work presented in this thesis is based on the original work done by me at the Department of Physics, University of Calicut, under the supervision of Dr. Antony Joseph, Professor, Department of Physics. This thesis has not been submitted by me for the award of any other degree, diploma, associateship, fellowship etc. of any other university or institute.

Ramsiya M

Department of Physics

University of Calicut

Calicut University

30-10-2018

List of Publications

Journals

1. Activity concentrations of radionuclides in soil samples along the coastal areas of Kerala, India and the assessment of radiation hazard indices; **Ramsiya M.**, Antony Joseph, K.P.Eappen and A.K. Visnuprasad, Journal of Radioanalytical and Nuclear Chemistry, 320 (2019) 291-298.

2. Estimation of indoor radon and thoron in the dwellings of Palakkad, Kerala, India, using Solid State Nuclear Track Detectors; **Ramsiya M.**, Antony Joseph and Jojo P.J : Journal of Radiation Research and Applied Sciences, 10 (2017) 269-272.

3. Identification of Radio Nuclides in Soil Samples from selected Locations in Kerala, India; **Ramsiya M.** and Antony Joseph : Int. Res. J. Environment Sci. 3 (3) (2014) 55-58.

Seminar/Conference Presentations

- Estimation of radon and thoron in Kappad coastal areas, Kerala, Ramsiya M and Antony joseph, National Conference on Particle Accelerators in Interdisciplinary Research, 11-13, April 2017, Manglore University.

- Radon and thoron levels in coastal belt of Ponnani, Malappuram - an initial report, Ramsiya M and Antony joseph, 29th Kerala Science Congress, 28-30, January 2017, Marthoma college, Thiruvalla, Kerala.

- Radon and thoron levels in coastal belt of Ponnani, Malappuram, Kerala, Ramsiya M and Antony Joseph, National Seminar on Radiation -Medical, Industrial and Research Applications, 26th November 2016, Sir Syed College, Taliparamba, Kerala.

- Estimation of terrestial souce of radioactivity in some areas in Palakkad district, Kerala, India. Ramsiya M., Antony Joseph, Visnuprasad, Monica S. and Jojo P.J., 28th Kerala Science Congress, 28-30 Jaunuary 2016, Calicut University, Kerala.

- Cup mode and Bare mode exposure of LR-115 detectors in dwellings of Palakkad district, Kerala, India. Ramsiya M., Antony Joseph., Visnuprasad, Manu Joseph and Jojo P.J, NSRP-20 October 28-30 2015, Manglore University, Karnataka.

- Computational studies on track Profiles in CR-39 detector, Ramsiya M. and Antony Joseph at Kerala Science Congress, January 2, 2014, Kerala Veterinary and Animal Science, Wayand, Kerala.

- Computational studies on Track Profiles, Ramsiya M. and Antony joseph, 18th National Symposium on Solid State Nuclear Track Detector and Their Applications, 18-20 October 2013, Ballabgarh, Haryana, India.

Acknowledgement

First and foremost I thank the God almighty for the blessings offered.

I am utmost thankful to my research guide Dr. Antony Joseph, Professor, Dept of Physics, University of Calicut for his encouragement to pursue the topic and for the valuable guidance and support offered. He is always patient, supportive, insightful and inspiring to me. I am really indebted to him for the technical help during experimental sessions.

I would like to express sincere thanks to the Head of the Department, Prof. (Dr.) P. P. Pradyumnan for his substantial support and cooperation. His unconditional support as the Head of the Department helped me to submit the thesis on time. I am also thankful to the former heads of the Department, Prof. George Varghese and Dr. M. M. Musthafa for their help and facilitation, offered during the research period. Thanks are also expressed to other faculties Dr. Shahin Tayyil, Dr. C.D. Ravikumar, Dr. A. M. Vinodkumar and the non teaching staff of the department.

Special gratitude is expressed to Dr. Eappen K.P., Ex-BARC and IEC consultant, New Delhi, for sparing his valuable time for the scientific discussions, in spite of his busy schedule. Discussions with him provided many insights into the research work carried out.

I acknowledge with thanks Mrs Rama Prajith and Dr. Rosaline Misra, R.P.A.D, BARC, for providing with valuable suggesions and instruments for the completion of the work. Also, My sincere gratitude is extended to Dr. Jojo P. J., Pofessor, Fatima Matha National College, Kollam, for sharing the experimental facilities and for fruitful discussions. I could never forget the sincere help and discussions offered by Mr. Visnuprasad A.K. My deepest gratitude to him is expressed herewith. I extend the gratitude to Ms. Monica S., Mr. Manu Joseph and Ms. Soniya - research scholars at Fatima Matha National College, Kollam.

Thanks is expressed to Mr. Jamshihas A.P, for the technical help received. Special thanks to Mr. Arjun, for rectifying mistakes in Latex and to Ms. Reshma Bhaskaran for giving suggestions and for the fruitful discussions. I also wish to thank Mr. Vishnu C.V. for his assistence during the experiments.

I acknowledge the financial support (MANF Fellowship) received from the Mistry of Minority Affairs, Govt. of India, during the period of this thesis work. I also express my gratitude for providing me with UGC-SAP DRS II and DST-FIST facilities in Department. The XRF- measurements carried out in CSIF is also acknowledged. My sincere gratitude is extended to Dr. Aslam, Associate Professor, Govt. Arts and science college, Meenchanda, Kozhikode for the facilities extended and the suggestions offered.

My sincere thanks to my research colleagues Mrs. Hajara U., Mr. Midhun C.V, Ms.Jisha P, Ms. Divya N.K., Ms.Jumana, Mr. Shabeer, Ms. Anju Paulson, Mr. Nikhil Nath, Ms. Dhanya Joseph, Ms. Deepthy Maria Joseph, Ms. Nithu Ashok, Ms. Salma Ibrahim R. V., Mr. Habeeb Rahman and Ms.Sitha K Jagan,. Each of them gave valuable support and motivation throughout the research tenure and gifted memorable days.

I am thankful to my parents, and in-laws, sister and brother for their motivation and prayers. I also remember the cooperation offered by my beloved son - Danish Rehan, whose infancy and child hood days are partly shared by my Ph.D tenure.

A special thanks to my husband Ashraf P. for his valuable support and guidance provided to me throughout all the stages of the research life.

Finally I thank all my friends and well wishers for offering motivation to pursue the research.

Dedicated to DANISH REHAN

Abstract

The main objective of this thesis is to study the distribution of radioactive nuclides ^{238}U, ^{232}Th and ^{40}K in soil samples along the costal areas of Kerala, using gamma ray spectrometric technique and hence to evaluate various parameters including the radiological hazard indices. We also aimed to estimate the inhalation dose recieved by the public in the northern districts of Kerala.

Humans are getting exposed continuously to ionizing radiations, emitted by radon (^{222}Rn), thoron (^{220}Rn) and their corresponding progenies, originating from natural and man-made sources. The three pathways by which humans are exposed to radiations contribute to 1) dose due to external gamma rays 2) inhalation dose from radon, thoron gases, their progenies and other radioactive nuclides 3) ingestion dose from radioactive materials through food and water. It is well known that about 50% of the natural radiation exposure results from inhalation pathway and the major contributors are radon, thoron gases and their short lived radioactive decay products. Radon and thoron are the decay products from decay series of uranium (^{238}U) and thorium (^{232}Th) respectively. These gases are found in the atmosphere at varying concentrations depending on the presence of their parents uranium (^{238}U) and thorium (^{232}Th) in soil and rocks and the mechanism of the gas release to the atmosphere. Radon has a half-life of 3.825 days and it decays by alpha emission

having energy 5.5 MeV. In comparison with radon, thoron has a very short half-life of 55 seconds. The alpha particle deposits its entire energy to a small volume due to its low penetration depth. The radon progenies easily get attached to the dust particles present in the air forming aerosols and it reaches the human body through inhalation and ingestion pathways. The inhaled radon daughters are transported to the lung, undergoes radioactive decay and causes changes to DNA structures within the lungs. Also, Several epidemiological studies on lung cancer indicate the role of radon and thoron in causing structural and molecular damages to lung tissues.

Natural radioactivity exists in various geological formations such as soil, water, rocks, sand and air in the earth's environment. The radionuclides ^{238}U, ^{232}Th and ^{40}K are non-uniformly distributed in earth's crust but there are certain areas in the world where high natural radiations are observed due to the presence of minerals like uraninites, monazites etc. The coastal lines of Kerala, India, especially the south west regions are well known for the presence of thorium deposits.

The thesis is divided into 6 chapters, as given below.

Chapter 1 is an introduction, giving the basic information about natural background radiation, decay series of natural radionuclides, with emphasis on radon, thoron and their physical, chemical and nuclear properties. This chapter also depicts the main objectives and relevance of the thesis work.

Chapter 2 contains a review of the radon and thoron measurements carried out in India and other countries, in recent times. The review indicates that in Kerala, the radon measurements were mostly limited to the high background radiation area (HBRA) in the south west coastal part of the state and not much has been carried out in the middle and northern side of Kerala.

Chapter 3 discusses the methodologies and general practices in radon and thoron

measurements and the essential theory behind these techniques.

Chapter 4 illustrates gamma ray measurements in soil collected from the coastal line of Kerala, and the details of the procedures followed in calibration of the experimental setups. We have evaluated the distribution of uranium, thorium and potassium concentrations using High Purity Germanium detector. The coastal regions of Kerala being a monazite deposit area, the study was envisaged to determine the background radiation levels in the area and the findings could be used as a baseline data for future dosimetric or epidemiological studies. The trace level concentration of uranium, thorium and lead in the soil samples were also measured by using energy dispersive X-ray Flourescence method.

Chapter 5 contains the results from indoor radon monitoring studies, discussions and the conclusions drawn therefrom. The first study related to this was done in houses located near the granite quarries of Pirayiri, in Palakkad district. Next we extended the indoor radon monitoring to coastal areas of Ponnani and Kappad. Solid state nuclear track detectors (SSNTD) based twin cup dosimeters were deployed in these areas. The detectors were etched and the tracks were counted with the help of a spark counter. The indoor radon and thoron concentration and the inhalation doses were estimated and compared with those at other areas.

Chapter 6 incudes the summary of research work carried out. The radon measurement results are assumed to be useful as the baseline data for the future dosimetric studies. The gamma ray measuremts carried out in soil samples along the coastal areas of Kerala clearly distinguishes the HBRAs and the NBRAs of Kerala. The future scope on further studies in this field of research, which which will defenitely be beneficial to human beings, is also proposed here.

Contents

List of Tables

List of Figures

Abbreviations

AED : Annual Effective Dose

DCF: Dose Conversion Factor

DRPS: Direct Radon Progeny Sensor

DTPS : Direct Thoron Progeny Sensor

EDXRF: Energy Dispersive X-Ray Fluorescence.

EERC : Equilibrium Equivalent radon Concentration

EETC : Equilibrium Equivalent Thoron Concetration

EID : Effective Inalation Dose

EF : Equilibrium Factor

FTIR : Fourier-transform infrared spectroscopy

HBRA : High Background Radiation Area.

H_{ex} : External Hazard Index

HPGe : Hyper Pure Germanim detector

HV: High Voltage.

IAEA : International Atomic Energy Agency.

ICRP : International Commission on Radiological Protection

MCA : Multi Channel Analyzer

NBRA : Normal Background Radiation Area

NORM : Naturally Occurring Radioactive Materials

Ra_{eq} : Radium Equivalent Activity

SSNTD : Solid State Nuclear Track Detector

UNSCEAR : United Nations Scientific Committee on the Effectsof Atomic Radiation

XRD : X-ray diffraction

Chapter 1

Introduction

1.1 Introduction

Natural background radiation is a perennial source of ionising radiation prevailing in the environment, emitted by various sources. The major sources of natural background radiation are cosmic rays and terrestrial radiations. Cosmic rays usually originate from the sources such as sun and other celestial objects in the universe and they interact with the gaseous components of the atmosphere and form radionuclides. Cosmogenic nuclides are primarily produced in the stratosphere and upper troposphere and serve as tracers for studying the nature of large-scale motions of the atmosphere. The terrestrial sources of radiation are mainly the decay products of uranium and thorium series and singly occurring potassium (^{40}K). According to United Nations Scientific Committee on the Effect of Radiation (UNSCEAR, 2000) report, more than 50% of the dose received from terrestrial radiations is due to radon (^{222}Rn), thoron (^{220}Rn) and their decay products, originating from uranium and thorium series respectively.

In addition to natural radiation exposure received by humans, additional dose can also be received from radiation sources used for medical, military and industrial applications. The man-made or 'anthropogenic' radionuclides in the atmosphere were introduced since 1952 from the detonation of a number of nuclear weapons. With regards to peaceful uses of radiation, medical exposure is almost always voluntary and provides a direct benefit to the exposed individual. The generation of electrical energy by nuclear power plants had been increasing since 1956. The nuclear fuel cycle includes the mining and milling of uranium ore, fuel fabrication, production of energy, storage of irradiated fuel and disposal of radioactive wastes. The dose received from the nuclear industry markedly decreases over time. A small number of accidents related to nuclear fuel cycle have been reported so far. Table 1.1 given below shows various annual dose levels contributed by different natural and artificial sources.

Table 1.1: Total annual radiation dose received by human beings from all sources

Natural source	Dose (mSv)	Artificial source	Dose (mSv)
Inhalation (mainly radon)	1.26	Diagnostic medical examinations	0.6
Extra terrestrial	0.48	Atmospheric nuclear testing	0.005
Cosmic rays	0.39	Nuclear fuel cycle	0.0002
Ingestion	0.29	Occupational exposure	0.005
Total	2.4	Total	0.6

The amount of energy deposited by the ionising radiation in living tissues is expressed in terms of dose and the unit for the dose is expressed as Sievert (Sv). The world average of annual dose received by human beings from natural radiation is 2.4 mSv/y (UNSCEAR, 2000). However, the dose rate received by the humans varies, depending on the geographical location and concentrations of the radionuclides in

various environmental matrices. Natural radiation dose delivered to human beings are generally coming from gamma rays, (outside body) and the deposited activity (inside the body) due to the terrestrial radionuclides. Ingestion, inhalation and injection are the three pathways by which the radionuclides enter the body. Hence it is imperative to evaluate the radioactivity levels in environmental samples and the three pathways for the entry of the radionuclides inside the body. Many standard techniques like gamma ray spectrometry for soil samples, Lucas scintillation based alpha measurements for water samples and Solid State Nuclear Track Detectors for gaseous samples etc. are used for evaluating the radionuclides in the environmental samples.

1.2 Radon, thoron and their progenies

Though radon has no stable isotopes, thirty six radioactive isotopes have been characterized, with atomic masses ranging from 193 to 229. Among these, radon (^{222}Rn), thoron (^{220}Rn) and actinon (^{219}Rn) are constantly produced in the environment from ^{238}U, ^{232}Th and ^{235}U series respectively. Radon is the 7^{th} member of uranium series, and the immediate daughter of ^{226}Ra. Radon has a half life of 3.825 days and it emits alpha particles of energy 5.5 MeV. The radon itself is an inert gas, but the alpha particles emitted by the radon gas are heavy, positively charged and deposits its entire energy to a small volume due to its low penetration depth. The radon isotopes produced will diffuse continuously to the surrounding atmosphere from the soil or get dissolved in water. Figure 1.1 gives the decay series of uranium-238 and thorium-232.

Thoron (^{220}Rn) is the 6^{th} member of thorium series having short half-life (55.83

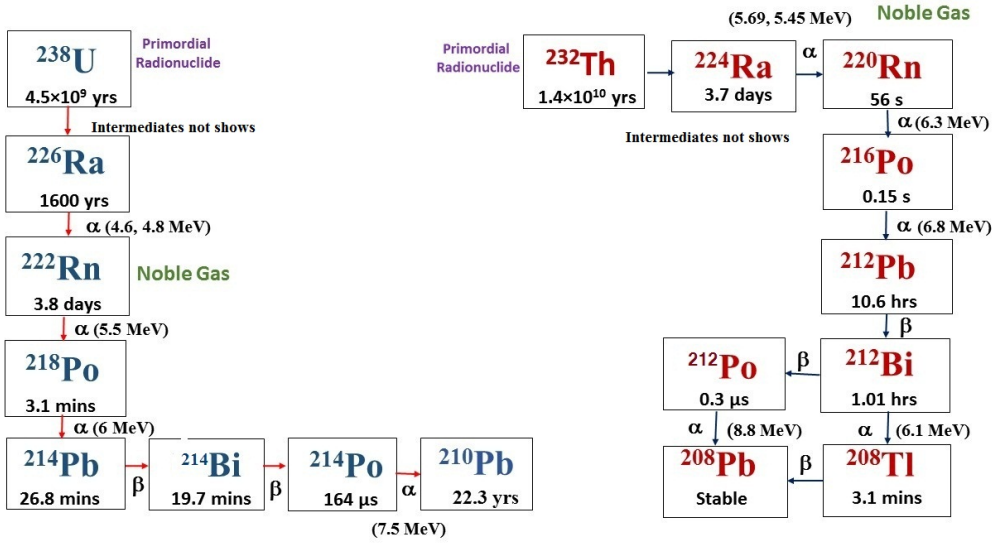

Figure 1.1: Uranium and thorium decay series.

Table 1.2: Nuclear properties of radon and thoron (Baskaran M, 2016 Springer)

Parameter	Radon	Thoron
Half life	3.82 d	55.83 s
Decay constant	2.098 $10^{-6}s^{-1}$	1.242 $10^{-2}s^{-1}$
Average recoil energy on formation	86 keV	103 keV
Diffusion coefficient in air	1×10^{-5} m^2 s^{-1}	
Diffusion coefficient in water	1×10^{-9} m^2 s^{-1}	

seconds). Thoron measurements in indoor environment were neglected in earlier days due its short half-life. Actinon (^{219}Rn), present in ^{235}U series is much less abundant than ^{222}Rn due to the relative low abundance of its parent ^{235}U compared to ^{238}U (^{238}U/ ^{235}U mass ratio = 137.7 (Richter et al., 2010) and its short half-life (3.9 s)). Hence it is not useful for atmospheric studies. The basic nuclear properties of radon and thoron are listed in Table 1.2.

In the periodic table, radon lies between metals and non-metals and exhibit some of the characteristics of both. Hence it is classified as a metalloid element

Table 1.3: The atomic and physical properties of radon(Baskaran M, 2016 springer)

Atomic number	86
Standard atomic weight	222
Desity	9.73 kg/m^3
Melting point(^{0}K)	202
Normal boiling point(^{0}K)	208.2
First ionisation enthalpy (KJ Mol^{-1})	1037
Electronegativity	2.2 (Pauling scale)

along with silicon, boron, germanium, polonium and tellurium. Being an inert gas, radon reacts with other gases in a very feeble way. However, it shows unique reaction with fluoride and forms compounds (Kolthof and Philips, 1966). Radon reacts spontaneously at 250^{0}C or lower temperature with fluorine, halogen fluoride and there is no evidence for the existence of radon compounds or ions in aqueous solutions. Radon dissolves in organic solvents and is less soluble in water. The water containing radon will be released to surrounding air having low radon content due to its flow or thermal agitation (Duncan, 1974). Like other noble gases, radon has closed electronic structure and is highly stable, so that ionisation enthalpies are high. Radon has lower electro negativity, as electro negativity decreases with increasing atomic number in the periodic table. The important characteristics of radon atom are given in Table 1.3.

1.3 Mechanism of radon emanation

Being an inert gas, radon easily gets released from its sources by emanation from the media and then reaches the outside environment by exhalation. In indoor environment radon gas gets distributed from internal walls, floors and ceilings. The meteorological factors like temperature, atmospheric pressure, humidity, character-

Table 1.4: Main sources of radon emanation

Source	Input to Atmosphere
	(T Bq per year)
Soil	7.40×10^7
Ground water	1.85×10^7
Oceans	1.11×10^6
Phosphate residues	1.11×10^5
Uranium mill tailings	7.40×10^4
Coal residues	7.40×10^2
Natural gas	3.70×10^2
Coal combustion	3.70×10^1

istics of the medium (soil, construction materials etc.), geological structure, location etc. affect the radon release to the atmosphere (Swakon et al., 2005). The major sources of radon and thoron emitted to the atmosphere are rocks, soil, sand, ocean water and sediments. When radium atom decays, radon escapes from mineral grains and enter into the interstitial volumes between grains and the gas reach the soil surface through diffusion and advection. Table 1.4 shows the details of emanation of radon to the atmosphere from various sources.

The recoil energy of radon (86 keV) is calculated from the conservation of momentum of a ^{226}Ra (parent) - ^{222}Rn system. The recoil distance travelled by the radon atom is a measure of the distance between the site of generation and the point where its kinetic energy is transferred. The mechanism governing emanation is recoil process and recoil range is 60 micrometre in air (Nazaroff, 1988; Nero et al., 1990). Transport of radon through soil occur by diffusion or with other gases such as CO_2, CH_4 or with water. The physical factors governing the exhalation of radon from soil are soil porosity, soil moisture, soil grain size and the conditions of the soil surface. Radon and thoron enter the atmosphere by crossing soil-air or building material-air boundary. Figure 1.2 shows the mechanism by which radon

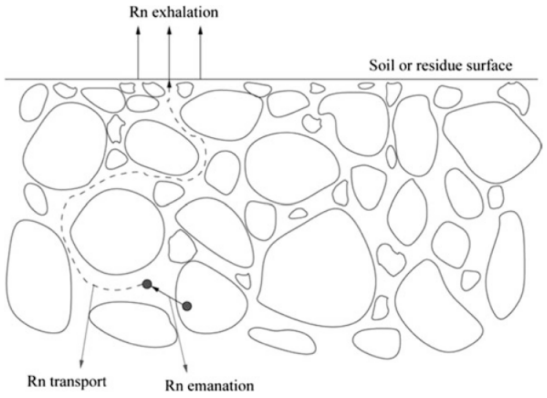

Figure 1.2: Mechanism leading to radon release to atmosphere.

gets released to the atmosphere.

It is established that the transport of radon from soil to atmosphere occurs predominantly by molecular diffusion (Schery et al., 1984; Nazaroff, 1992). The radon flux density is linearly proportional to the concentration gradient .

J^d = -$D_m \nabla$C

where D_m is the molecular diffusion coefficient of the gas (m^2 s^{-1}) and ∇C is the gradient of radon activity concentration (Bq m^{-3}). The rate of radon movement in soil is expected to be slow compared to its movement in homogeneous medium such as air due to its tortuous flow path around particles and relatively smaller fluid volume. Radon diffusion coefficient in soil depends on soil type, pore size distribution, water content and porosity.

The corresponding diffusion length of radon is L= $\sqrt{(D\tau)}$ where τ is the mean life time of radon (5.51 days) and D is the diffusion constant of radon in the medium (m^2 s^{-1}).

The diffusion length (ranges between 0.02-0.2 nm), is generally one to three orders of magnitude lower than that of the recoil distances and hence the escape of radon from mineral grain by diffusion is negligible.

1.4 Radiological properties of radon, thoron and their progenies

Since 1859, scientists were working to find out more radioactive elements and Curies isolated two radioactive elements Polonium and Radium in the year 1899. In 1900, German physicist Friedrich Ernest Dorn found a third radioactive element, from the observations of Curie and his further effort. He observed that when radium is exposed to air, it gives off a radioactive gas and the air become radioactive. At first he colloquially called it as Emanation (emanation refers to something that has been given off). Further, scientists decided to give the name radon. The name is a reminder of the source from which the gas comes, radium. The credit of discovering thoron gas goes to Ernest Rutherford and Robert B. Owens. They first recognised the presence of such radioactive gas from thorium in 1899, which they called thoron emanation, but today it is recognised as a radon isotope. In 1904, French chemist Andre Louis Debierne made a similar discovery of another isotope of radon (^{219}Rn) and he named it as actinon.

The radiogenic lung cancer was first reported among miners in the Schneeberg region of central Europe in 15^{th} and 16^{th} centuries. Possible association of lung cancer with radon was suggested by Ludewing and Lorenzer (1924) when reported a high level of radon in this area. Later it was recognised that inhalation of short lived radon progeny was the major responsible factor for the lung cancer (Shapiro, 1954; Bale and Shapiro 1956). Many epidemiological studies and case controlled studies showed that exposure to short lived radon decay products causes enhanced risk of lung cancer issues.

Radon progenies enter into human body through inhalation of radioactive ma-

terials or through the ingestion path way. Alpha particles emitted from the inhaled radon gas interact with biological tissues in the lungs, leading to DNA damage (WHO, 2009). The progenies have high diffusivities and ability to stick on to the surfaces. They immediately get attached to the dust particles present in the air and forms aerosols. These are classified into two categories based on their size distribution. 1.fine/ unattached fraction (2 nm) 2.coarse/attached fraction (150 nm). The coarse fraction enters the upper respiratory tract during inhalation and leave alveoli during exhalation. At the same time, the fine fractions also reaches the upper respiratory tract and get deposited in the alveoli. This fractions are easily absorbed by the blood compared to coarse particles. The fine and coarse fractions play an important role in radiation damage caused by the cells and thus these two fractions should be evaluated for actual dose calculations (Butterweck, G. et al., 2002). The complex mechanism of cancer arises as a result of two major genetic alterations, gene mutation and chromosomal aberrations (Land et al., 1983).

1.5 The units, standards and definitions

Radiation measurements and the investigation of radiation effects require highly specialised units. The commonly used units are tabulated in Table 1.5.

International Commission on Radiological Protection (ICRP) provides the guidelines for the quantification of the biological effect of radiation and gives the recommendations on radiation protection against ionising radiation. The commonly used parameters and terminologies in inhalation dosimetry are listed below.

Potential Alpha Energy (PAE): The potential alpha energy of an atom in the decay chain of radon/thoron is the total alpha energy emitted during the decay

Table 1.5: The units related to radiation measurements

Measurement purpose	Quantity measured	Unit	Description
activity of source	radioactive decays or emission	Becquerel (Bq) Curie (Ci)	1 decay/second 3.7×10^{10} decays/second
absorbed dose	energy absorbed per kg of tissue	gray (Gy) rad	1 Gy = 1 J/kg tissue 1 rad = 0.01 J/kg tissue
biologically effective dose	tissue damage	sievert (Sv) roentgen equivalent for man (rem)	Sv = RBE × Gy Rem = ∗ RBE × rad

∗RBE, the relative biological effectiveness is a measure of the relative damage done by the radiation.

Table 1.6: Potential alpha energy concentration (PAEC)(Assuming 3.7 Bq L^{-1} for each ^{222}Rn daughter)(Ph.D thesis, Eappen K.P., 2005)

Daughter Nuclide	Half-life(s)	N_i	E_i(MeV)	$N_iE_i(10^5)$ MeV
^{218}Po	183	976	13.69	0.136
^{214}Pb	1608	8583	7.69	0.660
^{214}Bi	1194	6374	7.69	0.488
^{214}Po	70.0002	0.001	7.69	< 0.001
			TOTAL	1.284

Ni = number of atoms per litre of the i^{th} daughter
Ei= alpha-particle energy released for the i^{th} daughter

of this atom through the decay chain to ^{210}Pb in the case of radon progeny and to ^{208}Pb in the case of thoron progeny.

Potential Alpha Energy Concentration (PAEC): The potential alpha energy concentration of any mixture of short lived radon or thoron decay products is the sum of the total potential alpha energy of all daughter atoms per unit volume of the air. (See Table 1.6).

1.5.1 Equilibrium Factor(F)

Generally steady-state concentration for radon can be established inside a room because of the constant emanation rate from the room surfaces to the ambient atmosphere. The relative concentrations of radon and its progeny inside the rooms are varying due to the difference in ventilation rates, surface deposition activities driven by the internal convective air flow. The influence of electrostatic forces and gravitational settling of the decay products causes the radioactive decay and subsequently the disequilibrium between the radionuclide and its parent is formed. The term equilibrium factor F is the ratio of the total potential alpha energy for the actual daughter concentrations to the total potential alpha energy of the daughter, which would be in equilibrium with the radon concentration.

$$F = \frac{0.136C_a + 0.660C_b + 0.488C_c}{1.284C_{Rn}} = 0.106C_a + 0.514C_b + 0.380C_c \qquad (1.1)$$

where C_a, C_b, C_c are the ^{218}Po, ^{214}Pb and ^{214}Bi concentrations and C_{Rn} is the ^{222}Rn concentration expressed in BqL^{-1}.

1.5.2 Equilibrium Equivalent Concentration (EEC)

The concept of the equilibrium factor defined above gives rise to an alternate unit for the radon concentration in terms of an equilibrium equivalent value with its progeny nuclides. The Equilibrium Equivalent Concentration (EEC) of radon is equal to that quantity of radon concentration which is in secular equilibrium with its progeny nuclides, giving equivalent PAEC for the progeny nuclides actually present

in the atmosphere. If radon concentration is denoted as C_{Rn} and F is the equilibrium factor, then the "Equilibrium Equivalent Concentration"EEC, can be expressed as:

$$EEC = F \times C_{Rn} \tag{1.2}$$

Here C_{Rn} and EEC are expressed in Bq per unit volume.

$$EEC(^{222}Rn) = 0.106(^{218}Po) + 0.514(^{214}Pb) + 0.380(^{214}Bi) \tag{1.3}$$

$$EEC(^{220}Rn) = 0.913(^{212}Pb) + 0.087(^{212}Bi) \tag{1.4}$$

1.5.3 Working Level (WL) and Working Level Month (WLM)

The unit called "working level (WL)"was introduced for the measurement of radon decay products in uranium mining areas. The WL was used to represent the maximum concentration of airborne radon decay products to which uranium miners could safely be exposed. Further, this term has been accepted at the international level to represent the concentration of the daughter activities of radon or thoron. The Working Level is thus defined as that concentration of the short-lived radon decay products in any combination, which would potentially produce 130,000 MeV of alpha particle kinetic energy per liter of air. One WL corresponds to $2.08 \times 10^{-5}\text{Jm}^{-3}$ in SI units.

Consider a working year having 2000 hours. Then a working month has 167 hours that is approximated to 170 hours. The inhalation of air with a concentration of 1 WL of radon or thoron progeny for 170 working hours results in the exposure of one Working Level Month(WLM). 1 WLM is equivalent to 3.54 mJhm^{-3}.

Dose conversion factor (DCF): DCF is defined to establish the relation between effective dose and potential alpha energy concentration of inhaled short-lived radon decay products. The lung dose model with a structure that is consistent with new ICRP respiratory tract model is used for calculating DCF. The inputs used for this calculation are mainly the decay product characteristics and its activity size distributions (attached/unattached). UNSCEAR 2000 estimates a dose conversion factor of 9 nSv $(\mathrm{Bqm}^{-3})^{-1}$ as the effective dose per equilibrium equivalent concentration of radon (EERC) and 40 nSv $(\mathrm{Bqm}^{-3})^{-1}$ as the effective dose per equilibrium equivalent concentration of thoron (EETC).

1.6 Radon monitoring -Applications

Radon is considered as an ideal atmospheric tracer at local, regional and global scales, because: (i) its inert nature, and its synoptic-time scale mean lifetime, (half-life (3.82 d)/ln 2 = 5.51 days), also referred to as e-folding life time and its well-characterized source function and (ii) the residence times of water vapour, aerosols and many important aspects of atmospheric dynamics are comparable to the mean-life of radon (Zahorowski et al. 2004, 2005).

- Radon based studies acts as a sensitive geochemical exploration method because radon is a radioactive noble gas having short half life and it can be detected in low activity levels. Variations in radon activity on earth surface has been extensively studied as it provides a clue to the locations of hydrocarbon deposits, uranium ore, geothermal resources and impending earthquakes and/or volcanic eruptions. The measurements of radon in soil gas above 1 m from earth's surface helps for the identification of these resources or prediction

of the earthquakes or volcanic eruptions.

- Radon-222 and its decay products provide a wealth of information on the sources of air masses and aerosols, the removal rate constants of aerosols, stability and vertical movements of air masses and deposition velocities of aerosols in the planetary boundary layer (Turekian et al., 1977; Turekian and Graustein, 2003; Baskaran, 2011).

- Recently, ^{222}Rn has been utilized widely as a tracer to quantify the submarine groundwater discharge in coastal areas. A multi-detector system that measures ^{222}Rn activities continuously in coastal waters has been developed (Dulaiova et al., 2005).

- The activity of ^{222}Rn in soil gas within 2 m from earth surface indicates how much Radium is present locally and how easily ^{222}Rn can escape from the soil grains that contain radium.

1.7 Objectives of the study

Natural radioactivity exists in various geological formations such as soil, water, rocks, sand and air in the earth's environment. The radionuclides ^{238}U, ^{232}Th and ^{40}K are non-uniformly distributed in earth's crust. There are certain areas in the world where high natural radiations are observed due to the deposits of natural uranium and the presence of minerals like monazites. The coastal lines of Kerala, India, especially the south west region, are well known for the presence of thorium deposits. The indoor radon monitoring has been started globally after the discovery of high radon concentration, of the order of 10^5 Bq m^{-3} in dwellings of eastern

Pennsylvania, USA (Lowder, 1989). Thereafter several studies have been conducted in the natural environment all over the world and reported the indoor radon and thoron levels. In our country, an external gamma ray map was generated by Nambi et al. (Nambi et al., 1986) and a similar profile for terrestrial exposure was constructed by Sankaran et al.(Sankaran et al., 1986). These informations need to be supplemented with inhalation exposures for obtaining a total radiation exposure. In view of this a country wide monitoring program was sponsored by Department of Atomic energy, Govt. of India. This includes the development of passive monitoring devices like dosimeters and progeny sensors based on solid state nuclear track detectors and the deployment of the dosimeters in various places to collect radon and thoron baseline data. In the present study, we are focusing on the deployment of dosimeters in northern side of Kerala because no data has been reported from this area. The proposed research work is aimed at measuring the distribution of radioactive nuclides in sand samples along the entire coast of Kerala to evaluate various parameters including the radiological hazard indices.

The objectives of the present study are as follows:

1. Estimating the distribution of radioactive nuclides ^{238}U, ^{232}Th and ^{40}K in soil samples along the entire cost of Kerala using gamma ray spectrometric technique and hence to evaluate various parameters including the radiological hazard indices.

2. Measurement of indoor radon and thoron concentrations in selected dwellings i) lying around granite quarries ii) lying around two beaches, by deploying twin-cup dosimeters and progeny sensors.

3. Explore the presence of radioactive trace elements uranium, thorium and other heavy metals in soil samples collected as part of objective 1, by using X-Ray Fluorescence technique.

1.8 Relevance of the study

Radon has dual role in human life. It is one of the major contributors to the ionising radiation received by the general population living in the high background radiation areas. At the same time radon is identified as the power tool in geochemical and atmospheric studies. Radon and its decay products are considered as the second most causative factor for lung cancer after smoking (Darby et al., 2005). The International Commission on Radiation Protection (ICRP), a cancer research agency under WHO, recognized radon as a human carcinogen like tobacco. According to WHO 2009 report, the lung cancer cases attributable to radon range from 3 to 14%, depending on the assumptions involved in the risk calculations and the average radon concentrations (WHO, 2009).

Global and national reference levels were set to differentiate the boundary between safer and danger level of radon concentration in residential dwellings. This varies in different countries and the remediation is recommended if the radon level exceeds the action level. It is found from global analysis of data that the indoor radon concentration follows log normal distribution in which majority of the dwellings are in lower radon range.

The radiation risk coefficients are fairly well established at high doses and high dose rates, whereas little is known about the effects of radiation at low dose rates. Several epidemiological study programmes in different countries are in progress to estimate the population exposure due to natural radiation with a view to obtain the radiation risk coefficients at low and prolonged dose rate levels. In this regard, radiation surveys in Kerala will provide necessary input to the nationwide monitoring data. A comprehensive estimate of the inhalation dose received by general

population requires data for both ^{222}Rn and ^{220}Rn levels in the indoor and outdoor atmosphere.

1.9 Organisation of the thesis

Chapter 1 deals with the general introduction about natural radiation sources and radon and thoron. Chapter 2 presents a review of the work carried out within India and the other areas of the world. Chapter 3 includes the methodology adopted including SSNTD based dosimeters, gamma ray spectrometry and X-ray fluorescence analysis (XRF). The results of gamma spectrometric analysis of soil samples are incorporated in chapter 4. Chapter 5 is devoted to the results obtained from passive monitoring studies. The sixth chapter deals with the conclusion of the study and future plans.

1.10 References

1. Bale, W.F. and Shapiro, J. V. (1956) Radiation dosage to lungs from radon and its daughter products. Proc. First.Int. Conf. on peaceful uses of atomic energy, Geneva, United Nations.

2. Baskaran, M. (2011) ^{210}Po and ^{210}Pb as atmospheric tracers and global atmospheric ^{210}Pb fallout: review, J. Environ. Radioact., 102, 500-513.

3. Baskaran, M. (2016) Springer, Radon: A Tracer for Geological, Geophysical

and Geochemical Studies ISBN: 978-3-319-21329-3.

4. Brett F. Thornton and Shawn C. Burdette (2013) Nature Chemistry, Volume 5.

5. Butterweck, G. et al. (2002) Experimental determination rate of unattached radon progeny from respiratory tract to blood. Radiat. Prot. Dosim. 102, 343-348.

6. Darby, S., Hill D., Auvinen A. et al. (2005) Radon in homes and risk of lung cancer: collaborative analysis of individual data from 13 European case-control studies. BMJ 330(7485): 223-226.

7. Dulaiova, H., Peterson, R., Burnett, W.C., Lane-Smith, D. (2005) A multi-detector continuous monitor for assessment of ^{222}Rn in the coastal ocean. J Radioanal. Nucl . Chem 263(2), 361-365

8. Duncan, A., Holiday (1974) Evaluation and control of radon daughter hazards in uranium mines, New Publication (NIOSH), 75-117.

9. Eappen, K.P., (2005) Development of a passive dosimeter for the estimation of inhalation dose due to radon and thoron, Ph.D thesis, University of Mumbai.

10. Gingrich J. E. (1975) Results from a new uranium exploration method: Trans. AIME 258, 61-64.

11. ICRP (1981). Limits for Inhalation of Radon Daughters by Workers. ICRP Publication 32. Ann. ICRP 6 (1).

12. James, L. Marshall and Virginia, R. Marshall (2003) Ernest Rutherford, the "True discoverer"of radon, Bull. Hist. Chem., Volume 28(2), 76-81.

13. Kolthoff, I.M and Philips, J. Elving (1966) Treatise of Analytical Chemistry, 4, part II, 219.

14. Land, H., Parade, L.F., Weinberg, R.A., (1983). Cellular oncogenes and multistep carcinogenesis, Sci. Mag. 222, 771-778.

15. Lowder, W. M. (1989) National environmental radioactivity and radon gas. Il Tommasino, et al. (Eds.), Proceedings of the international workshop on radon monitoring in radioprotection, environmental radioactivity and earth sciences (1-77). New Jersey: World Scientific.

16. Ludewig, P., and Lorenzer, E. (1924) Untersuchungen der Grubenluft in den Schneeberger Gruben auf den Gehalt von Radium-Emanation. Z. Phys. 22,

178-185.

17. Mayya, Y. S., Mishra, R., Prajith, R. (2010) Wire-mesh capped deposition sensors: novel passive tool for coarse fraction flux estimation of radon thoron progeny in indoor environments, Sci. Total Environ, 409, 378-383.

18. Nambi, K.S.V., Bapat, V.N., David, M., Sundaram, V.K., Sunta, C.M., Soman, S.D. (1986) Natural background radiation and population dose distribution in India, Internal Report, Health Physics Division, Bhabha Atomic Research Centre, Mumbai.

19. Nazaroff, W.W., 1988. Chapter 2. In: Nazaroff, W.W., Nero, A.V. (Eds.), Radon and Its Decay Products in Indoor Air. John Wiley Sons, New York, 57-112.

20. Nero, A.V., Gadgil, A.J, Nazaroff W.W., Revzan K.L. (1990) Indoor radon and decay products: concentrations, causes and control strategies, Tech. Rep. DOE/ER-0480P, 138.

21. Richter, S., Eykens, R., Kuhn, H., Aregbea , Y., Verbruggen, A., Weyer S. (2010) New average values for the n(^{238}U)/n(^{235}U) isotope ratios of natural uranium standards, Internat. J of Mass Spect, 295, 94-97.

22. Sankaran, A.V., Jayaswal, B., Nambi, K.S.V., Sunta, C.M. (1986) U, Th and K distributions inferred from regional geology and the terrestrial radiation profiles in India, Technical Report, BARC.

23. Schery, S.D., Gaeddert, D.H., Wilkening, M.H. (1984) Factors affecting exhalation of radon from agravelly sandy loam, J. Geophys Res., 89, 7299-7309.

24. Shapiro, J. V. (1954) An evaluation of the pulmonary radiations dosage from radon and its daughter products, Univ. of Rochester Rep. UR-298.

25. Swakon, J., Kozak, K., Paszkowskib, M., Gradzinskib, R. et al. (2005) Radon concentration in soil gas around local disjunctive tectonic zones in the Krakow area, J. Environ. Radioact. 78 137-149.

26. Turekian, K.K., Graustein, W.C. (2003) Natural radionuclides in the atmosphere, Treatise in Geochemistry, 4, 261-279.

27. Turekian, K.K., Nozaki, Y., Benninger, L.K. (1977) Geochemistry of atmospheric radon and radon products. Ann. Rev. Earth. Planet. Sci. 5, 227-255.

28. UNSCEAR (2000) United nations scientific committee on the effects of atomic radiation, sources and effects of ionizing radiation, New York.

29. World Health Organization (2009). WHO Handbook on Indoor Radon, a Public Health Perspective. World Health Organization, Geneva.

30. Zahorowski, W., Chambers, S.D., Henderson-Sellers, A. (2004) Ground based radon-222 observations and their application to atmospheric studies. J. Environ. Radioact, 76, 3-33.

31. Zahorowski, W., Chambers, S.D., Wang, T. et al. (2005) Radon-222 in boundary layer and free tropospheric continental outflow events at three ACE-Asia sites, Tellus B, 57(2), 124-140.

Chapter 2

Literature Review

2.1 Introduction

It has been found that in the last few years several measurements of radon, thoron and their progenies in the natural environments were reported from all over the world. In the past, researchers were directly measuring decay products from the respective concentration of gases using equilibrium factor approach. With the development of direct progeny sensors, equilibrium factor in various geographical locations are being used for calculating the inhalation dose instead of the UNSCEAR standards (F_R and F_T). In this chapter, indoor radon and thoron measurements, uranium, thorium and potassium measurements carried out globally and in various Indian states is presented.

2.2 Global

Recently, Fawzia Mubarak et al., in 2018, measured the activity of primordial nuclides such as ^{238}U, ^{235}U, ^{232}Th, and ^{40}K in the soil samples collected along the north of Nile Delta, near Rosetta beach in Egypt. External hazard indices (H_{ex})[1] measured ranged between 0.32 - 2.04, radium equivalent activity (Ra_{eq})[2] ranged between 118.67 - 753.91 Bq kg^{-1} and the activity concentration indices (I)[3] varied between 0.42 - 2.61. Both H_{ex} and Ra_{eq} were found to be exceeding the permissible limit in certain locations.

Sami Alharbi and Riaz Akber in the year 2015 measured the indoor radon and thoron at different sites at the Queensland University of Technology (QUT) Gardens Point campus, Australia. The detector used in this study was RAD-7 and the spectrum of alpha energy considered were in the range of 0 - 10 MeV and this was categorized into eight windows (A - H). Windows A and C were used to determine the ^{222}Rn level by collecting alpha energies from ^{218}Po (6.0 MeV) and ^{214}Po (7.69 MeV), respectively. Windows B and D were used to determine ^{220}Rn through ^{216}Po (6.78 MeV) and ^{212}Po (8.78 MeV) levels, respectively. The average radon and thoron concentrations estimated were 10.5 $\pm$ 11.3 and 8.2 $\pm$ 1.4 Bq m^{-3}, respectively. The highest radon concentration was detected in a confined area (86.6 $\pm$ 6.0 Bq m^{-3}), while the maximum thoron level was found in a storage room (78.1$\pm$ 14.0 Bq m^{-3}).

In a study carried out in South Western Cameron in 2015, Saidou et al. mea-

[1]It is obtained from Ra_{eq} expression which indicates that the maximum allowable value (equal to unity) corresponds to the upper limit of Ra_{eq} (370 Bq kg^{-1}). This value must be less than unity in order to minimize the radiation hazard.

[2]See section 4.7

[3]The activity concentration index should be used for identifying materials which might be of concern. The maximum value for activity concentration index is 2 (I $\leq$ 2) to meet 0.3 mSv y^{-1} dose criterion and I $\leq$ 6 to meet 1 mSv y^{-1} criterion

sured indoor radon in the uranium regions of Poli and Lolodorf, using ionization chambers and discriminative RADUET dtectors. The instruments were deployed in 70 houses of the high natural radiation areas. The radon level was found to vary between 27 ± 26 to 937 ± 5 Bq m^{-3} and thoron from 48 ± 40 to 700 ± 128 Bq m^{-3} and these followed lognormal distribution. The arithmetic means of radon and thoron concentrations were found to be 92 ± 3 Bq m^{-3} and 260 ± 13 Bq m^{-3}. The study revealed that less than 2% of houses are having the indoor radon above the reference level of 300 Bq m^{-3} and 30% of houses have thoron concentrations above 300 Bq m^{-3}.

Kudo et al. in 2015 measured indoor radon and thoron levels in HBRAs Yangjiang of China using passive monitoring devices (CR-39 fixed RADUET). Radon, thoron and equilibrium equivalent thoron concentrations were given as 124 ± 78, 1247 ± 1189 and 7.8 ± 9.1 Bq m^{-3}, respectively. The total dose received from radon and thoron is 5.3 ± 3.5 mSv y^{-1} which is 20 times higher than the UNSCEAR 2006 report.

In 2014, the concentrations of radon, thoron and their decay products in indoor environments of the Balkan region were estimated in 43 schools from 5 municipalities of the Republic of Macedonia (Zdenka Stojanovsk et al. 2014). The time-integrated radon and thoron gas concentrations (C_{Rn} and C_{Tn}) were measured by CR-39, whereas the equilibrium equivalent radon and thoron concentrations (EERC and EETC) were measured using direct radon-thoron progeny sensors, consisting of LR-115 nuclear track detectors. The geometric mean (GM) values [and geometric standard deviations (GSDs)] of C_{Rn}, C_{Tn}, EERC and EETC were 76 (1.7), 12 (2.3), 27 (1.4) and 0.75 (2.5) Bq m^{-3}, respectively. The equilibrium factors between radon and its decay products were evaluated: F_{Rn} ranged between 0.10 and 0.84 and F_{Tn}

ranged between 0.003 - 0.998, with GMs (and GSDs) equal to 0.36 (1.7) and 0.07 (3.4), respectively.

In another study carried out in Southern Serbia, the radon (Rn), thoron (Tn) and their progeny concentrations (expressed in terms of equilibrium equivalent concentrations (EERC and EETC), were measured in 40 houses, in four villages of Sokobanja municipality (Zora S et al. 2017). The passive detectors used were : (1) discriminative radon-thoron detector for simultaneous radon and thoron gas measurements (RADUET) and (2) direct Tn and Rn progeny sensors (DRPS/DTPS). Detectors were exposed simultaneously for a single period of 12 months. The radon concentrations varied from 8 - 189 Bq m^{-3} and that of thoron varied from 10 - 412 Bq m^{-3}. Relatively high EETC (0.1 - 3.4 Bq m^{-3}) was reported from there. The EERC concentrations (5 - 22 Bq m^{-3}) showed lower variations.

The natural radioactivity in building materials of plutonic bodies in Greece was studied by Papadopoulos et al. in 2013 using gamma spectroscopy and health hazards were evaluated. They collected 121 samples of various rock-types from gabbro to granite, from all plutonic bodies in Greece. Radioactivity levels ranged from 1 to 315 Bq kg^{-1} for ^{226}Ra, from 2 - 376 Bq kg^{-1} for ^{232}Th and up to 1632 Bq kg^{-1} for ^{40}K, with arithmetic mean values and standard deviations 74 ($\pm$ 51), 85 ($\pm$ 54) and 881 ($\pm$ 331) Bq kg^{-1}, respectively. These are below the international representative values of 78 Bq kg^{-1} for radium and 111 Bq kg^{-1} for thorium for granite stones.

Tsuey-Lin Tsai et al. in 2011 evaluated natural radioactivity in soil samples of Taiwan and the radiological hazard indices were calculated. The average concentrations of uranium, thorium and potassium were 22.53, 33.43 and 406.62 Bq kg^{-1}, respectively. This suggests that the radioactivity levels are within the safe

limit recommended by UNSCEAR 2000. The cluster analysis performed identified three distinct groups of soil variables and Principal Component analysis classified the number of variables into three factors with 87.5% variance.

McLaughlin et al. in 2011 involved in long term indoor radon and thoron measurements using CR-39 based alpha track detectors (RADUET detectors) in Ireland. Their results shows that thoron gas varies from <1 to 174 Bq m^{-3} with an arithmetic mean (AM) of 22 Bq m^{-3}. The radon gas concentration ranged from 4 to 767 Bq m^{-3} with an AM of 75 Bq m^{-3}. Low value of correlation coefficient was found (R^2 =0.31) between indoor radon and thoron due to the different and independent origins of these gases in Irish dwellings.

Celik et al. in 2008 measured indoor radon and radio activity levels in Giresun province located in northern Turkey. The Macrofol SSNTDs were deployed in 70 dwellings for radon measurements and soil samples collected were analysed using HPGe detector. The indoor radon levels varied between 50 - 360 Bq m^{-3} with an average value 130 Bq m^{-3} and radon and radium were correlated with R^2=0.54. BEIR VI empirical model was used to predict the number of lung cancer deaths due to indoor radon exposure and the investigation concludes that indoor radon is responsible for 8% of all lung cancer deaths occurring in this province.

Vasses et al. in 2006 carried out a field survey on the beaches of the Golfe du Lion and Camargue, France to locate the areas enriched with uranium and thorium. The higher activity was recorded along the Camargue coast (where uranium and thorium contributions were greater than 1000 Bq kg^{-1}) due to the sedimentary contribution of the magmatic formations in the River Rhone catchment area. The heavy mineral deposits (especially zircon) are found to be the main contributors to the high levels of radiation (> 1000 nSv h^{-1}) occurring in Camargue beaches.

The uranium, thorium and potassium levels reported in different countries (not included above) are listed in Table 2.1

2.3 India

Punniyakotti and Ponnusamy in 2018 measured natural radioactivity and heavy metal concentration in sand samples using gamma ray spectrometry in the southern region of Tamil Nadu coast. The gamma spectral analysis showed that the average radioactivity contents of radium, thorium and potassium in the intertidal zone sand samples are 12.13 ± 4.21, 59.03 ± 4.26, and 197.03 ± 26.24 Bq kg^{-1}, respectively. The average radioactivity content of ^{232}Th alone is higher than the world average value.

Sankaran Pillai in 2017 reviewed more than 40 research papers dealing with radioactivity levels in south east coast of Tamil Nadu reported during the past four decades (1974-2016). The review shows that mean activity concentrations of ^{238}U, ^{232}Th, and ^{40}K were 58.8 ± 28.7, 465.2 ± 147.3 and 311.2 ± 27.8 Bq kg^{-1}, respectively. The annual exposure rate was found to vary from 0.29 to 12.8 mSv y^{-1} with the mean value of 3.7 mSv y^{-1}, which is above the global average of 2.4 mSv y^{-1} as reported by UNSCEAR 2008. The review concluded with the finding that there is appreciable elevation in radioactivity levels along the coastal areas and therefore it recommends for new radiological surveys using improved methodology along the coastal stretch.

Table 2.1: Uranium, thorium and potassium levels in soils reported in various countries

S.No	Country	^{238}U Bq kg^{-1}	^{232}Th Bq kg^{-1}	^{40}K Bq kg^{-1}	Reference
1	Turkey	37±18	40 ±18	667 ±281	Taskin et al., 2008
2	Kuwait	36	6	227	Saad and Al-Azmi, 2002
3	Xiamen Island, China	14.6	10.9	364.4	Yingnan Huang, 2015
4	Dois Rios beach, Brazil	6-78	12-87	269-587	Freitas and Alencar, 2004
5	East coast, Thailand	3.2 - 18.6	5.1-34.5	182.4 - 559.7	Malain et al., 2010
6	Corbu beach,Romania	12.2	8.5	233.3	Margineanu et al., 2013
7	Guangdong, China	134±41	187± 80	680 ± 203	Gang Song et al., 2012

Paraminder Singh et al. in 2016 made measurements of indoor radon and thoron concentration in 96 dwellings from 22 different villages in Hamirpur district, Himachal pradesh, using twin cup dosimeters and deposition based progeny sensors. The annual average indoor radon and thoron was 63.82 and 89.59 Bq m^{-3}. The average value of equilibrium factor for radon and thoron are 0.50 and 0.05 respectively. The annual effective inhalation dose obtained from their study was within the safe limit recomended by ICRP.

Ramola et al. in 2016 engaged in time integrated passive measurements of indoor radon and thoron in Garhwal Himalaya with the aim of investigating the health risk due to exposure of radon, thoron and their decay products. The study pointed out that the total annual inhalation dose received by the public do not cause health risk, however the contribution of thoron to the total inhalation dose cannot be negleted. They also made few attempts to measure progeny concentrations contrary to the traditionally used equilibrium factor approach to calculate progeny concentrations from the gas concentrations. The study reveals the fact that contribution of indoor thoron and its progeny was 13 - 52% of the total inhalation dose.

Ravisankar et al. in 2015 assessed the radioactivity concentration and radiological hazard indices in coastal sediments from Pattipulam to Devanampattinam from the East coast of Tamilnadu using a NaI(Tl) detector based gamma-spectrometry. The mean activity concentration of uranium, thorium and potassium was reported as 62.21, 14.29 and 360.23 Bq kg^{-1}, respectively and the radiological parameters are well below the internationally approved safety limits. This study concludes that coastal sediments do not to pose any significant radiological health risk to the people living in nearby areas along the east coast of Tamilnadu.

Inigo Valan et al. in 2015 carried out the activity concentration analysis of

radionuclides and estimated the radiological parameters in the sand sediments collected at Krusadai Island in Gulf of Mannar near Rameswaram, Tamil Nadu. The Activity concentration of uranium was found to be below the detectable limit (BDL) for all the sites and thorium had the range between BDL to 27.81 ± 8.9 Bq kg^{-1} while ^{40}K had the range from BDL to 413.13 ± 49.6 Bq kg^{-1}. This study concludes that Krusadai Island is safe and is naturally background radiation area and the locations are unpolluted with respect to radioactivity.

Suresh et al. in 2011 reported the results of radioactivity measurements in sediment samples of the Ponnaiyar River, Tamil Nadu state, India. They studied the influence of mineralogical and heavy metal composition on radioactivity levels. The activity concentration ranges for ^{238}U, ^{232}Th, and ^{40}K are BDL - 11.60 ± 6.13 Bq kg^{-1} with an average 7.31 ± 3.41 Bq kg^{-1}, BDL - 106.11 ± 9.20 Bq kg^{-1} with an average 46.85 ± 5.25 Bq kg^{-1} and 201.23 ± 19.90 - 467.71 ± 34.34 Bq kg^{-1} with an average 384.03 ± 26.82 Bq kg^{-1}, respectively. This shows that the average activity concentrations are within the world and Indian average values. The mineralogical analysis using IR spectroscopy indicates that the influence of mineralogical characterization on level of radioactivity is significant, whereas the influence of the heavy metal composition on level of radioactivity should be limited.

Sivakumar estimated the indoor radiation dose, and radon - thoron progeny concentrations in Coonoor (Tamilnadu) - the hilly areas located on the Eastern side of Western ghat of peninsular India. The indoor gamma radiation dose were measured by $CaSO_4$ Dy based luminescent dosimeters and the indoor gamma dose rate was found to vary between 71 - 327 nGy h^{-1}. The indoor gamma dose rate was found to vary with the building materials used and the type of houses. The highest gamma dose was observed in summer and the lowest in winter. But the highest

average radon content was shown in winter and it also depends on the type of house and the building materials used.

Prabhjot Singh et al., in 2015 carried out measurements in 90 dwellings in 13 different villages situated around Tosham region, Haryana. The equilibrium factor for radon and thoron in this region varies between 0.20 - 0.71 and 0.03 - 0.13. The total annual inhalation dose due to radon and thoron varies from 1.33 - 2.44 mSv y^{-1} and it lies within the safe limit recommended by UNSCEAR 2000.

Rangaswamy et al., in 2015 measured the activity concentrations of radium, thorium and potassium in rock samples of Ramnagara and Tumkar districts, Karnataka using HPGe detector. The radium, thorium and potassium activities in the samples were 41.08 ± 2.12, 86.26 ± 2.94, 869.29 ± 3.78 Bq kg^{-1} respectively. The average radium equilent actvity in the study area is 225.29 Bq kg^{-1} which is within the recommended limit of 370 Bq kg^{-1}. The external and internal hazard index were less than unity.

Avinash et al., determined the radon, thoron and their progeny concentrations in the dwellings of Gogi region, Yadgir district, Karnataka using passive detector systems. The equilibrium factor for radon was found to be varying from 0.32 - 0.37 with a mean of 0.35. The equilibrium factor for thoron varied from 0.03 - 0.04 with a mean of 0.04. The arithmetic mean of annual inhalation dose in the Gogi region is 1 ± 0.03 mSv y^{-1}, which was found to be within the UNSCEAR limit.

Ashok et al., in 2012 measured the residential radon and thoron levels in Banglore city using twin cup based dosimter designed and developed by BARC. The highest radon and thoron concentration was found in dwellings with mud flooring and the lowest in dwellings havng mosaic flooring. The geometric mean value of radon and thoron concentrations were 24.1 ± 8 and 24.5 ± 10 Bq m^{-3} respectively.

Shakir Khan and Ameer Azam in 2010 carried out the measurements of indoor radon, thoron, and their progeny concentration in four villages in rural areas of district Kanshiram Nagar (Kasganj) in Uttar Pradesh using twin cup dosimeters. There the concentration of indoor radon and thoron was found to vary from 10.32 to 72.24 and 11.61 to 84.49 Bq m^{-3} with a geometric mean (GM) of 29.49 and 31.20 Bq m^{-3}, respectively. The concentration of radon and thoron daughters was found to vary from 1.11 to 7.80 and 0.31 to 2.28 mWL, respectively.

Deepak Verma and Shakir Khan in 2013 studied the levels of radon, thoron and their progeny in the dwellings of Bareilly in U.P using twin chamber dosimeter cups. The concentrations of radon and thoron were found to vary from 16.62 - 155.12 Bq m^{-3} and 4.16 - 24.93 Bq m^{-3}, respectively. Their progeny concentrations were found to vary from 1.80 - 16.77 mWL and 0.112 - 0.674 mWL, respectively. The values of life time fatality risk and annual effective dose were found to vary from 0.24×10^{-4} - 1.21×10^{-4} and 0.31 - 2.78 mSv y^{-1} respectively. The study indicated that the variation in the above parameters are strongly influenced by the type of dwelling construction and their ventilation conditions.

Satheeshkumar et al. measured the activity concentrations of primordial nuclides along the south east coast of India, from Pondichery to Velanganni. The activity was measured using high purity germanium detector and 10 sampling stations were identified along the 290 km coast. It was found that the distribution of nuclides was non-uniform along the coastal strech and elevated level of thorium deposits were recorded in Karaikal coast. The effective inhalation dose varied from 0.04 - 0.38 mSv y^{-1} indicating that the Bay of Bengal falls under normal background area.

Ramachandran and Sathish in 2011 involved in a country wide large scale moni-

toring program and they surveyed 1500 dwellings across the country with more than 5000 measurements. The geometric mean of estimated annual inhalation dose rate due to indoor ^{222}Rn, ^{220}Rn and their progeny in the dwellings was 0.94 mSv y^{-1} (geometric standard deviation 2.5). It was observed that the major contribution to the indoor inhalation dose was due to indoor ^{222}Rn and its progeny. However, the contribution due to indoor ^{220}Rn and its progeny was not significant and it contributes only to 20% of the total indoor inhalation dose rates.

Kannan et al. in 2002 studied the distribution of natural and anthropogenic radionuclides in soil and beach sand samples in coastal environments of of Kalpakkam, India using HPGe detector. The activity concentrations of ^{238}U, ^{232}Th, and ^{40}K in dry soil samples were 5 - 71, 15 - 776 and 200 - 854 Bq kg^{-1} respectively. In beach sand samples, ^{238}U, ^{232}Th, and ^{40}K contents varied in the range of 36 - 258, 352 - 3872 and 324 - 405 Bq kg^{-1}, respectively. Significantly higher levels of uranium and thorium activities were found at four locations very close to the beach, namely Devneri, Meyyur, Kokkilimedu and Sadras.

Table 2.2: Indoor radon and thoron concentrations in different states of India

S.No	Area (State)	Indoor radon (Average)Bq m^{-3}	Indoor thoron (Average)(Bq m^{-3})	Reference
1	Gogi,Yadgir (Karnataka)	25.3 - 38.7 (31.4)	21.0-33.7 (26.7)	Avinash et al., 2016
2	Hamirpur district (Himachal Pradesh)	25.5-208.5 (63.8)	6.7-290.0 (89.6)	Paraminder Singh et al., 2016
3	Yamuna,Tons valleys Garhwal Himalaya	27-148 (54)	5-174 (43)	Ramola et al., 2016
4	Kanshinram Nagar (UttarPradesh)	10.32-72.24	11.61-84.49	Shakir Khan Ameer Azam 2013
5	Bareilly city (Uttarakhand)	16.62-155.12	41.6-24.93	Deepak Verma Shakhir Khan, 2014
6	Ambala distrct (Hariyana)	4.8-29.1(13) (13)	1.2-69.2(14.4) (14.4)	Vimal Mehtha et al., 2014
7	Hamirpur Una (Himachal pradesh)	19.7-146.3(55.1) (55.1)	9.1-70.7(25.5) (25.5)	Virk, Navajeeth Sharma 2000
8	Madhya predesh	21.7-31.9	10.9-30.1	Kher et al., 2008
9	Faizabad city (Uttar Pradesh)	11.57-104.10 (60.57)	5.78-43.74 (26.12)	Deepak Verma and Shakhir Khan 2013

The seasonal variation of indoor radon and thoron were measured in 132 dwellings from 10 different villages selected from the central part of India by Kher et al. They also measured the uranium, thorium and potassium in the soil samples belonging to this area. No significant correlations were found between uranium/thorium content of the soil and indoor radon/thoron. The study shows that flooring material strongly determines the indoor radon level.

The results from the above mentioned studies are summarised in Table 2.2

2.4 Kerala

Monica et al. in 2016 evaluated the indoor and outdoor gamma dose rates along the coastal region of Kollam district, Kerala using portable gamma survey meter and analysis of soil samples were carried out using gamma spectroscopic system. The mean indoor annual effective dose (AED) due to background gamma rays along the coastal region was found to vary between 1.32 - 7.12 mSv y^{-1}, which is larger as compared with the worldwide average of the AED of 0.48 mSv y^{-1} and the outdoor mean effective dose of 4.83 mSv y^{-1}. The excess life time cancer risk estimated in this region was also higher than the world average value.

Reshma et al. in 2016 measured radium, thorium and potassium concentrations in the rocky areas of Wayanad district, located in Western Ghats. The study shows that the potassium, radium and thorium levels are 265 $\pm$ 334, 21 $\pm$ 15, 39 $\pm$ 38 Bq m^{-3} respectively. The radon and thoron concentrations were also studied by deploying the pin hole dosimeters and progeny sensors. The average radon and thoron concentrations were found to be 31 Bq m^{-3} and 96 Bq m^{-3} .

Venunathan et al. in 2016 determined the activity concentrations of ^{232}Th, ^{226}Ra

and ^{40}K in the sediments and river bank soil samples collected from the Kallada river sides of coastal Kerala. The radiological risk coefficients associated with these radionuclides were calculated. The activity of the processed samples were counted using a high efficiency 5″×5″NaI (Tl) detector coupled to GSPEC gamma spectroscopy system. The mean values of measured activities of ^{232}Th, ^{226}Ra and ^{40}K in soil samples were found to be 98.1 ± 0.4, 60.3 ± 1.1 and 343.4 ± 1.8 Bq kg^{-1}, respectively, which results in an average absorbed dose rate of 103 ± 95 nGy h^{-1}. The corresponding values for sediment samples were found to be 88.0 ± 0.4, 48.6 ± 0.9 and 423.2 ± 2.0 Bq kg^{-1}, respectively, with a resulting absorbed dose rate of 95 nGy h^{-1}.

Ramaswamy et al. in 2015 calculated the activity concentrations of uranium, thorium and potassium in sediment samples of coastal areas of Kerala. Mineralogical characterization of different layers of the sediments were done to find the relation between the radioactivity content, specific minerals and their distributions in spatial and depth wise manner. The radioactivity analysis suggests that the average activity concentrations of radionuclides are higher than the world average values suggested by the regulatory bodies and the radiological parameters in all layer samples are more than the recommended safety levels. The mineralogical characterization of sediments were done using FTIR and XRD. Statistical analyses including cluster and factor analysis were done to assess the relation between the radioisotopes and minerals. The results show that (1) the total level of the radioactivity in all layers mainly depends on the activity concentrations of uranium and thorium (2) the concentration of ^{40}K may have a strong association with the light mineral calcite and spatial distributions of ^{40}K and calcite are almost similar in every layer (3) The minerals like quartz, microcline feldspar and kaolinite are completely un-associated

with any measured radioisotopes.

Ramaswamy et al, in 2013 estimated the distribution of radionuclides in 39 locations along the HBRA of Kerala using NaI(Tl) detector. The activity concentrations of the ^{238}U, ^{232}Th, and ^{40}K are BDL - 1187 $\pm$ 21.7 Bq kg^{-1}, BDL - 5328$\pm$ 23.2 Bq kg^{-1} and BDL - 693 $\pm$ 31.2 Bq kg^{-1} respectively. The radiological parameters calculated were higher than the recommended level and the study indicates that thorium is the main contributor over the others to the total radioactivity.

Mary Thomas Derin et al. in 2012 studied the distribution of radionuclides in the Chavara - Neendakakara belt, along the south west coast of Kerala, using HPGe detector. Out of the 22 km coastal area featured in this study, the highest activity of uranium and thorium was recorded in Puthenthura while the lowest was in Chavara. SEM-EDAX anlyses reveal that titanium (Ti) and zircon (Zr) are the major trace elements in the sand samples, followed by aluminum, iron, copper, magnesium, ruthenium, calcium, lead and sulphur. The study pointed out that annual effective external dose in Chavara-Neendakara region varied from 1.19 mSv y^{-1} to 9.33 mSv y^{-1} with an average of 1.2 mSv y^{-1} which are considerably higher than the other known HBRAs.

Christa E Pereira in 2012 investigated the level of radon and thoron concentrations in Neendakara and Chavara, a well known high background radiation area in the south west coast of India, using twin cup dosimeters. In Neendakara Panchayath the radon concentration was found to be between 7 - 100 Bq m^{-3} and thoron concentration between 4 - 66 Bq m^{-3}. In Chavara, the radon showed the variation from 7 - 83 Bq m^{-3} and thoron between 4 - 86 Bq m^{-3}. The investigation carried out in 110 dwellings indicated that the bed rooms and dining rooms have high radon concentration due to poor ventilation conditions. Also, the radon and thoron

concentrations in the study area are of a wide range indicating the heterogeneity of primordial soil radioactivity.

Ben Byju et al., in 2012 measured the radon and thoron levels in Karunagappally, Chavara and Thevalakkara in the mineral rich area of south west coast. Around 500 dwellings with 10 years after construction were randomly selected for the study. The dwellings in Thevalakkara village showed lower radon and thoron concentrations when compared to Chavara and Karunagappally. The radon and thoron concentrations in Chavara village were found to be varying between 5 - 73 Bq m^{-3} (for radon) and 5 - 94 Bq m^{-3} (for thoron). In the case of Thevalakkara, the values for radon and thoron levels varied between 7 to 36 Bq m^{-3} and between 4 to 47 Bq m^{-3} , respectively. This wide variation in the concentrations of both radon and thoron was attributed to the variation in the concentration of the primordial radioactivity in the region.

Mathew et al. in 2011 measured the soil radioactivity in Chellanam, suburbs of Cochin, with the Arabian Sea in the west, using a $5'' \times 4''$NaI(Tl) gamma-ray spectrometer. It was seen that the activity concentration of thorium varies from 76 to 267 Bq kg^{-1}, with a mean value of 163 Bq kg^{-1}, that of ^{238}U varies from 12 to 34 Bq kg^{-1} with a mean value of 26.1 Bq kg^{-1} and that of ^{40}K varies from 307 Bq kg^{-1} to 557 Bq kg^{-1}, with a mean of 420.3 Bq kg^{-1} .

Shetty et al.in 2005 had undertaken a detailed study in the coastal areas of Karunagapalli, Chavara, Neendakara and Kollam to find the distribution and enrichment of the radionuclides. The sand samples collected at different distances from the sea waterline and at different depths were analysed using NaI(Tl) gamma ray spectrometer. The minimum thorium activity was 9.4 Bq kg^{-1} , found in Kollam at a depth of 10 - 20 cm, 40 m away from waterline in 500 - 250 μ m particle size

fraction and maximum activity of 136 - 811.2 Bq kg^{-1} was observed in Chavara in grains of size 125 - 63 μ m at a depth of 0 - 10 cm for a sample collected 20 m away from the waterline. Calculations show that there exists strong correlation between ^{226}Ra and ^{232}Th, for the samples in all sampling locations with a correlation coefficient of 0.91.

2.5 References

1. Alzoubi, F.Y., Al-Azzam, K.M., Alqadi, M.K., Al-Khateeb, H.M., Ababneh,Z.Q., (2013). Radon concentration levels in the historical city of Jerash, Jordan, Radiat. Meas. 49, 35-38.

2. Ashok, G.V., Nagaiah, N., Shiva Prasad, N.G., Ambika, M.R., Sathish, L.A., Karunakara N. (2012) Residential radon exposure in some areas of Bangalore city, India, Radiat. Prot. Environ. 35, 59-63.

3. Avinash, P. R., Rajesh, S., Kerur, B.R., Mishra, R., (2014). Determination of radon, thoron and their progeny concentrations in dwellings of Gogi region, Yadgir District, Karnataka, India, Radiat. Prot. Environ, 37, 157-160.

4. Ben, Byju S., Koya, P. K. M., Sahoo, B. K., Jojo, P. J., Chougaonkar, M. P., Mayya, Y. S. (2012). Inhalation and external doses in coastal villages of high background radiation area in Kollam India, Radiat. Protect. Dosim., 152, 154-158.

5. Celik N, Cevik U., Celik A., Kucukomeroglu B., (2008) Determination of indoor radon and soil radioactivity levels in Giresun, Turkey, J. Environ. Radioact. 99, 1349-1354.

6. Christa, E. Pereira, Vaidyan, V. K., Chougaonkar, M. P., Mayya, Y. S., Sahoo, B. K., Jojo, P. J. (2012). Indoor radon and thoron levels in Neendakara and Chavara regions of southern coastal Kerala, India. Radiat. Protect. Dosim. 150, 385-390.

7. Deepak Verma, Shakir khan, M, (2014). Assessment of indoor radon, thoron and their progeny in dwellings of Bareilly city of northern India using track etch detectors, Rom. Journ. Phys. 59 (1-2), 172- 182.

8. Fawzia Mubarak, Fayez-Hassan M., Mansour N.A, Talaat Salah Ahmed, Abdallah Ali. (2018) Radiological Investigation of High Background Radiation Areas, Scientific reports, 7, 15223.

9. Freitas, A.C., Alencar, A.S., (2004). Gamma dose rates and distribution of natural radionuclides in sand beaches- Ilha Grande, South eastern Brazil, J. Environ. Radioact. 75, 211-223.

10. Gang Song, Diyun Chen, Zeping Tang, Zhiqiang Zhang, Wenbiao Xie, (2012). Natural radioactivity levels in topsoil from the Pearl River Delta Zone, Guang-

dong, China, J. Environ. Radioact. 103, 48-53.

11. Inigo Valan, I., Mathiyarasu, R., Sridhar, S. G. D., Narayanan, V. Stephen, V., (2015). Investigation of background radiation level in Krusadai Island Mangrove, Gulf of Mannar, India, J. Radioanal. Nucl. Chem. 304,735-744.

12. Kannan, V., Rajan, M.P., Iyengar, M.A.R., Ramesh, R., (2002). Distribution of natural and anthropogenic radionuclides in soil and beach sand samples of Kalpakkam (India) using hyper pure germanium (HPGe) gamma ray spectrometry, Appl. Radiat. Isotop. 57, 109-119.

13. Kher, R.S., Khokhar, M.S.K., Rathore, V.B., Ramachandran, T.V. (2008) Measurement of indoor radon and thoron levels in dwellings and estimation of uranium, thorium and potassium in soil samples from central part of India, Radiat. Meas. 43, S414 - S417.

14. Kudo H., Tokonami S., Omori Y., Ishikawa T., Iwaoka K., Sahoo S. K., Akata N., Hosoda M. , Wanabongse P., Pornnumpa C., Sun Q. , Li X. and Akiba S. (2015) Comparitive dosimetry for radon and thoron inhigh background radiation areas in China, Radiat. Protect. Dosim. 6, 1-5.

15. Mary Thomas Derin, Perumal Vijayagopal, Balasubramaniam Venkatraman, Ramesh Chandra Chaubey, Anilkumar Gopinathan (2012). Radionuclides and Radiation Indices of High Background Radiation Area in Chavara-Neendakara

Placer Deposits (Kerala, India), PLOS ONE, 7(11), e50468.

16. Mathew, S., Rajagopalan, M., Abraham, J. P., Balakrishnan, D., Umadevi, A. G. (2012). Natural radioactivity content in soil and indoor air of Chellanam. Radiat. Protect. Dosim. 152, 1-4.

17. Malain, D., Regan, P.H., Bradley, D.A., Matthews, M., Santawamaitre, T., Al-Sulaiti, H.A., (2010). Measurements of NORM in beach sand samples along the Andaman coast of Thailand after the 2004 tsunami. Nucl. Instrum. Methods Phys. Res. A 619, 441-445.

18. Margineanu, R.M., Duliu, O.G., Blebea-Apostu, A.M., Gomoiu, C., Bercea, S., (2013). Environmental dose rate distribution along the Romanian Black Sea Shore. J. Radioanal. Nucl. Chem. 298, 1191-1196.

19. McLaughlin J., Murray M., Currivan L., Pollard D., V. Smith V., Tokonami S., Sorimachi A., and Janik M.,(2011) Long term measurements of thoron , its air born progeny and radon 205 dwellings in Ireland, Radiat. Protect. Dosim. 145(2-3), 189-193

20. Monica, S., Visnuprasad, A.K., Soniya, S.R., Jojo P.J., (2016). Estimation of indoor and outdoor effective doses and lifetime cancer risk from gamma dose rates along the coastal regions of Kollam district, Kerala. Radiat. Prot.

Environ. 39, 38-43.

21. Papadopoulos, A., Christofides, G., Koroneos, A., Papadopoulo,L., Papastefanou,C., Stoulos, S. (2013) Natural radioactivity and radiation index of the major plutonic bodies in Greece, J Environ. Radioact. 124, 227-238.

22. Paraminder Singh, Komal Saini, Rosaline Mishra, Bijay Kumar Sahoo, Bikramjith Singh Bajwa, (2016). Attached, unattached fraction of progeny concentrations and equilibrium factor for dose assessments from ^{222}Rn, and ^{220}Rn Radiat. Environ. Biophys. 55, 401-410.

23. Punniyakotti, J., Ponnusamy, V. (2018) Environmental radiation and potential ecological risk levels in the intertidal zone of southern region of Tamil Nadu coast (HBRAs), India, Marine Pollution Bulletin 127, 377-386.

24. Ramasamy, V., Sundarrajan, M., Paramasivam, K., Suresh, G., (2015). Spatial and depth wise characterization of radionuclides and minerals in various beach sediments from high background radiation area, Kerala, India., Appl. Radiat. Isotop. 95, 159-168.

25. Rangaswamy, D.R., Srilatha, M.C., Ningappa, C., Srinivasa E., Sannappa J. (2015) Measurement of natural radioactivity and radiation hazard assesment in rock samples of Ramanagara and Tumkar districts of Karanataka, India. Environ Earth Sci, 75, 373-384.

26. Ramasamy, V., Sundarrajan, M., Paramasivam, K., Meenakshisundaram, V., Suresh, G. (2013). Assessment of spatial distribution and radiological hazardous nature of radionuclides in high background radiation area, Kerala, India, Appl. Radiat. Isotop. 73, 21-31.

27. Ravisankar, R., Chandramohan, J., Chandrasekaran, A., Prince Prakash Jebakumar, J., Vijayalakshmi, I., Vijayagopal, P., Venkatraman, B., (2015). Assessment of radio activity concentration of natural radionuclides and radiological hazard indices in sediment samples from the east coast of Tamilnadu, India, Statistical approach. Mar. Pollut. Bull. 97, 419-430.

28. Ramola, R.C, Mukesh prasad, Tushar Kandri, Preeti Pant, Peter Bossow, Rosaline Mishra, Tokonomi, S., (2016). Dose estimation derived from the exposure to radon, thoron and their progeny in the indoor environment. Sci.Rep 6, 31061

29. Reshma Bhaskaran, Ravikumar C. D, Vinodkumar A. M, Vijayalakshmi I, et al. Hazard indices and annual effective dose due to terrestrial radioactivity in Northern Kerala, India, J. Radioanal. Nucl. Chem. 314(3), 2171-2179

30. Saad, H.R., Al-Azmi, D.(2002) Radioactivity concentrations in sediments and their correlation to the coastal structure in Kuwait, Appl. Radiat. Isotop. 56, 991-997

31. Sami, H. Alharbi, Riaz, A. Akber (2015) Radon and thoron concentrations in public workplaces in Brisbane, Australia, J Environ. Radioact. 144, 69-76.

32. Sankaran Pillai,G., S. Chandrasekaran, S., Sivasubramanian, K., Baskaran R., and Venkatraman, B., (2017). A review on variation of natural radioactivity along the south east coast of Tamil nadu for the past 4 decades (1974-2016) Radiat. Protect. Dosim. 1-11.

33. Saidou, Shinji Tokonami, c., Miroslaw Janik, Bineng Guillaume Samuel, Abdourahimi, Ndjana Nkoulou II Joseph Emmanuel (2015). Radon-thoron discriminative measurements in the high natural radiation areas of southwestern Cameroon, J. Environ. Radioact. 150, 242-246.

34. Satheeshkumar, G., Shahul Hameed, P., Sankaran Pilla,i G., Anbusaravanan, N. (2012) Environmental radioactivity evaluation in the coastal stretch of Bay of Bengal from Pondycherry to Velanganni (South East coast of India). Radiat. Prot. Environ. 35, 90-5.

35. Shakir Khan, M., Ameer Azam (2013). Measurements of indoor radon, thoron, and their progeny using twin cup dosimeters in rural areas of northern India, Environ Earth Sci, DOI 10.1007/s12665-013-2538-1

36. Shetty , P.K., Narayana, Y. , Siddappa, K. (2006) Vertical profiles and enrichment pattern of natural radionuclides in monazite areas of coastal Kerala, Journal of Environmental Radioactivity, 86, 132-142.

37. Shuaibu, H.K., et al., (2017) Assessment of natural radioactivity and gamma-ray dose in monazite rich black Sand Beach of Penang Island, Malaysia, Mar. Pollut. Bull., http://dx.doi.org/10.1016/j.marpolbul.2017.03.026

38. Sivakumar, R., (2016). A study of indoor radiation dose, radon, thoron and progeny concentrations in hilly area, Envi.Earth.Science 75, 393.

39. Suresh, G., Ramasamy, V., Meenakshisundaram, V., Venkatachalapathy, R., Ponnusamy, V., (2011). Influence of mineralogical and heavy metal composition on natural radionuclide concentrations in the river sediments. Appl. Radiat. Isotop. 69, 1466-1474.

40. Taskin, H., Karavus, M., Ay P., Topuzoglu, A., Hidiroglu, S., Karahan, G., (2009). Radionuclide concentrations in soil and lifetime cancer risk due to gamma radioactivity in Kirklareli, Turkey, J. Environ. Radioact. 100, 49-53.

41. Tsuey-Lin Tsai, Chi-Chang Liu, Chun-Yu Chuang, Hwa-Jou Wei, Lee-Chung Men (2011) The effects of physico-chemical properties on natural radioactivity levels, associated dose rate and evaluation of radiation hazard in the soil of

Taiwan using statistical analysis. J Radioanal Nucl Chem, 288, 927-936.

42. Vassas C., Pourcelot L., Vella C., Carpe'na J., Pupin J.P., Bouisset P., Guillot L.(2006) Mechanisms of enrichment of natural radioactivity along the beaches of the Camargue, France J Environment. Radioact. 91, 146-159.

43. Venunathan, N., Kaliprasad, C.S, and Narayana, Y., (2016). Natural radioactivity in sediments and river bank soil of Kallada river of Kerala, south India and associated radiological risk Radiat Protect Dosim. 171(2), 271-276

44. Vimal Mehta, singh, S. P., chauhan R.P., Mudahar G.S. (2014). Measurement of indoor radon, thoron and their progeny levels in dwellings of Ambala district, Haryana, northern India using solid state nuclear track detectors, Rom. journ. phys., vol. 59 (7-8), 834-845

45. Virk, H.S., and Sharma Navjeet (2000) Indoor radon/thoron survey report from Hamirpur and Una districts, Himachal Pradesh, India, Appl. Rad. Isotop. 52, 137 -141.

46. Yingnan Huang, Xinwei Lu, Xiang Ding, Tingting Feng, (2015). Natural radioactivity level in beach sand along the coast of Xiamen Island, China, Mar. Pollut. Bullet. 91, 357-361.

47. Zdenka Stojanovsk, Zora S. Zunic, Peter Bossew, Francesco Bochicchio, Carmela Carpentieri, Gennaro Venoso, Rosaline Mishra, Rout R.P., Sapra B.K., Bety D. Burghele, Cucos-Dinu A., Blazo Boev and Cosma C., (2014) Results from time integrated measurements of indoor radon, thoron and their decay product concentrations in scools in the republic of Macedonia, Radiation Protection Dosimetry, 162(1-2), 152-156.

48. Zora S. Zunic, Stojanovska Z., Veselinovic N., Mishra R., Yarmoshenko I. V., Sapra B. K., Ishikawa T., Omori Y., Curguz Z., Bossew P., Udovicic V., Ramola R. C., (2017), Indoor radon, thoron and their progeny concentrations in high thoron rural Serbia environments, Radiation Protection Dosimetry, pp. 1-4.

Chapter 3

Materials and Methods

3.1 Introduction

There are many methods based on different principles which are available for the measurement of radon concentration in the environment. Each specific analytical method depends on the concentration of the radon in the sample and the precision required for the measurement. The radon measurement techniques are broadly classified into three categories, depending on the type of results expected from the measurements:

(i) Measurement for radon alone or radon + progeny nuclides

(ii) Active or passive mode of measurement

(iii) Measurement principle based on alpha or beta particles or gamma radiation.

The most common method for the estimation of radon and thoron is the Lucas cell method where the alpha particles emitted from radon and progeny nuclides are used for the computation of radon/thoron gas collected in the known volume of the Lucas cell. A continuous measurement method is used in Alpha Guard and RAD7

instruments, based on the detection of alpha particles from the progeny nuclides produced in the detector volume during the sampling period. Some methods are based on the detection of gamma-rays emitted by the progeny radionuclides during the radioactive decay of ^{222}Rn (^{214}Bi, ^{214}Pb).

There are three modes of samplings used in the measurement of radon/thoron, depending on the utility of the results for various applications or computations.

(a) Grab sampling or spot sample measurement for immediate assessment of the radon/thoron values.

(b) Continuous measurements to provide time-series concentrations of radon in samples (soil gas, air, water). Instruments like Alpha Guard, RAD7, Barasol (ALGADE) etc. are used for continuous measurement of radon in environment and environmental samples. Recently developed instruments such as Smart Radon Duo and Scintillation Radon Monitors (www.eeipl.in) based on Lucas cell techniques are also used for continuous monitoring of radon as well as thoron in air, soil or gas.

(c) Passive techniques based on Solid State Nuclear Track Detectors, commonly used for integrated measurement of radon/thoron in atmosphere. Such measurements are useful to determine monthly or annual average ^{222}Rn concentration in houses for the assessment of inhalation dose to humans. Such devices are useful to assess the effectiveness of remedial techniques to alleviate indoor radon problems.

3.2 Integrated techniques

This method gives the time integrated radon concentration for a period of sampling, ranging from few days to few months. The technique uses the number of alpha incidences occurring during the period of exposure and calculates the radon values

based on the calibration factors obtained for the system. The solid state nuclear track detectors are satisfying these criteria by recording the radioactive signature of radon-alpha particles. These detectors are inexpensive and easy to use. For the measurements of indoor radon levels, LR -115 based track detectors are exposed for a known period. Following the exposure, the film is etched in an appropriate etchant to enhance the size of the tracks so that the track density (number of tracks per unit area) can be easily determined to calculate radon concentration. Annual average values of radon levels in dwellings are obtained from quarterly measurements and the average of the measurements is computed for a year to obtain the desirable precision at relatively low analytical cost. The unique advantages of this technique include: (i) the alpha particles produced from the decay of ^{222}Rn and its progeny (alpha particles from the decay of ^{218}Po and ^{214}Po) produce etchable damage tracks in a variety of polymeric solids (ii) other lightly ionizing radiation such β and γ rays from other natural sources and from cosmic-rays are not recorded.

3.3 Theory of SSNTDs

SSNTDs are dielectric materials that produce damages within the materials when heavy ions pass through them. The damaged zones are called latent or hidden tracks and it can be treated with chemically aggressive solutions such as NaOH, KOH etc., called etchants. The damaged zones react with the etchants faster as compared to undamaged regions and tracks become visible under ordinary microscope. This process is called chemical etching.

The field of Solid State Nuclear Track Detectos (SSNTD) had its origin in 1958 when the first etch pit was observed in a crystal of LiF by D.A Young (Young, 1958).

Later Silk and Barnes noticed the damaged regions produced by fission fragments in thin sheets of mica (Silk and Barnes, 1959). Subsequently a wide range of materials have been used by Fleischer et al., in 1965 for track related applications. The materials like Mica, Apatite and Olivine also showed track forming capability. They mostly find applications in fission track studies. The commonly used detectors in SSNTD family are CR-39, Macrofol (Poly carbonate group) and LR-115 (cellulose nitrate group). CR-39 is chemically Polyallyl diglycol carbonate and was discovered by Cartwright et al. in 1978.

3.3.1 Track formation mechanisms in dielectric media

Ion explosion spike model

This model was put forward by Fleischer and Price in 1965 (Fleischer and Price, 1965) to explain the track formation mechanism in inorganic solids. According to this model, charged particles interact with the atomic electrons via Columbic interaction and ionisation is produced along the path of the particles. These primary ionisations take place in less than a femto second and create an electrostatically unstable array of positive ions which repel one another from their normal sites to interstitial sites. After this, electron relaxation takes place which diminishes the actual stress by spreading the strain more widely. Such long range strains makes possible the observation of hidden tracks in crystals by transmission electron microscopy. The secondary effects of delta rays and excitation process are unimportant in the case of inorganic solids.

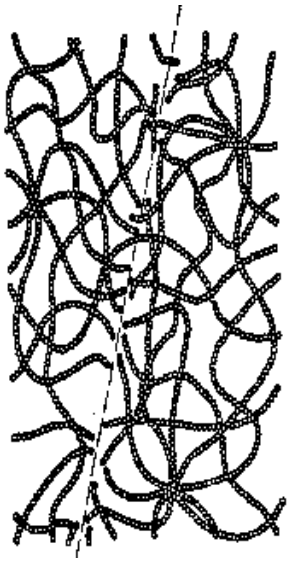

Figure 3.1: Radiochemical damage mechanism in polymer chains.

Radiochemical damage mechanism

In the case of organic solids (polymers), electrons ejected by ionisation (primary electrons) as well as secondary electrons (delta rays) may break the polymer chains. According to this model, the etchable tracks are formed by the radioanalytic scission of polymer chains into shorter fragments and the production of reactive, low molecular weight polymers, which are easily dissolved in etchants than the surrounding undamaged regions. Figure 3.1 shows the mechanism of radiochemical damage in polymer chains.

3.3.2 Requirement for Latent track formation

Inorganic solids

- In order for the ion explosion to take place, the Coulomb repulsive force inside the ionised channel must be greater than the coherent attractive force due to

lattice bonding. This condition is satisfied in materials having low mechanical strength, low dielectric constant and close inter atomic spacing.

- The positive ions produced in the channel should not get neutralized within 100 femto seconds (lattice vibration time) because that much time is required for the ions to be displaced from their lattice sites. This indicates that tracks are formed in solids having conduction electron density less the 10^{20} /cm^3 and hence metals will not record latent tracks.

- There must be at least one ionization per atomic plane crossed by incident particle. If they are discontinuous, the etch pit profile would be rough and irregular. This is the criterion mostly imposed for tracks which are revealed by chemical etching.

- To preserve the latent track formed in the detector material permanently, the hole mobility must be low (less than 0.1m/s for a field strength of 100 V/m). This condition is not satisfied by the semiconductors and hence semiconductors will not create tracks.

Organic solids

Systems that are highly unstable chemically, such as cellulose nitrate, tend to be more sensitive than radiation resistant polymers. Thermoset plastics like CR-39 that do not cross link upon irradiation and are susceptible to interfacial degradation by convenient etchant constitute ideal polymer detector. Their amorphous nature and radiation sensitivity will further enhance the track detection property.

3.4 Track visualization techniques

Latent tracks are damaged zones produced along the path of particles, which can be enlarged to sizes that can be seen under an optical microscope. Since they are usually less than 10 nm in diameter, special techniques are needed for the visualization of latent tracks. Most widely used methods for this purpose are 1) chemical etching, 2) electrochemical etching

3.4.1 Chemical etching

In this method, detectors containing latent tracks are immersed in a suitable chemical solution. The damaged trails which intersect the surface get preferentially dissolved in the etching solution than the bulk material. The rate of these two etching process are designated as track etch rate (V_T) and bulk etch rate (V_G) respectively. The track etch rate must be greater than the bulk etch rate for the formation of tracks by chemical action. V_T depends on specific ionisation. The shape of etched track surface is conical for constant V_T and curved inward or outward for varying V_T. V_T and V_G depend on etchant, concentration and temperature of etching. The track length and diameter increase as the etching time is increased. Figure 3.2 shows a standard chemical etching set up. Different computer codes are also being used for analysing the track profile.

3.4.2 Electrochemical etching

In this technique, chemical etching of tracks is combined with an electrical breakdown process called treeing. When electric field strength exceeds a certain threshold value, discharge takes place along the branched paths in the form of a tree. The

Figure 3.2: Chemical etching set up

electric field strength can be enhanced by forming pointed etch pits, filled with surrounding etchant or another electrolyte. The branches of tree are susceptible to accelerated chemical attack, similar to that along latent tracks. The treeing phenomenon can be employed for large track counting by chemical means. The resulting large, high contrast blobs can be easily observed. The inherent tendency of discharge process prevents merging between neighbouring trees. Therefore even very large trees form closely spaced latent tracks as distinct and can be counted separately. Using this method tracks in plastic can be enlarged to a size where they can be observed even with naked eye.

3.5 Track counting

Nuclear tracks can be counted manually under an optical microscope or automatically with the help of a spark counter.

3.5.1 Spark counter

In a spark counter, the etched detector is placed between two electrodes forming a capacitor. The thin detector is placed on the top of a thick conductive electrode,

Figure 3.3: Spark counter

made of brass and covered with an aluminized mylar. A heavy weight is placed on top of aluminised mylar to have an intimate contact between the thin detector and the electrodes. When a high voltage is applied across the capacitor, an electric discharge or spark takes place through the track hole. The voltage pulse produced across the load resistor is counted by a counter. The spark passing through a track hole has enough energy to evaporate the aluminium coating on the aluminised mylar and produces a circular spot. After short circuit, the spark is stopped and the capacitor is charged again, but a second spark cannot occur in the same track hole, because of the evaporation on the aluminium electrode. Thus the spark jumps from one track hole to another till the whole area is scanned. The number of evaporated aluminium spot (diameter 100 micrometer) is equal to the number of sparks produced and hence the number of track holes. The operating voltage of spark counter lies between 400 V to 600 V. The prespark voltage (900 V) is set higher than the operating voltage in order to punch out those tracks which have not been completely etched through.

3.6 SSNTDs for radon monitoring

Radon measurements are routinely performed in different laborataries in the world and developed various alpha detectors. The selection of detectors depends on the sensitivity, coast, study purpose etc. LR-115 and CR-39 are the widely used detectors for indoor radon measurements.

3.6.1 LR-115 detector

Original formation of the alpha particle tracks were observed in cellulosic materials such as cellulose nitrate and cellulose acetate butyrate. Subsequently, alpha particle tracks were also seen in polycarbonates such as bisphenol-A polycarbonate, i.e., Lexan and allyl diglycol carbonate, CR-39. Due to good ionization sensitivity and stability against various environmental factors, the LR-115 (Cellulose nitrate) film has been used for environmental radon measurements. Studies indicate that detector time efficiency is larger for LR-115 than for CR-39 detector and this shows that LR-115 is more sensitive and efficient than CR-39 (Nidal Dwaikat et al., 2007). It is a deep red coloured cellulose nitrate film coated on 100 micrometer polyester backing. The LR-115 type 2 film (Kodak pathe type manufactured by DOSIRAD) has thickness of 12 micrometers. The film is insensitive to electromagnetic radiation and is to be handled with care to avoid aberrations. Kodalpha film type (LR-115) has several characteristics: (1) very sensitive to alpha particles only; (2) insensitive to environmental changes such as humidity, water and temperature up to 60^0 C; (3) can be used for short term measurement at minimum 10-30 days of exposure and also for long-term measurements (3 months up to 1 year); (4) suitable to use for radon measurements in stagnant or flowing water and in oil.

3.6.2 CR-39

CR-39 detectors require calibration, pre used preparation and is less sensitive and efficient when compared to LR-115 films. Also, detector time efficiency is smaller than that of LR-115. This indicates that the response of CR-39 detector is small for radiation detection compared to LR-115 (Nidal Dwaikat et al., 2007).

The SSNTD based instruments designed for radon monitoring are described below.

3.7 Twin cup dosimeter

Indoor levels of radon, thoron and their progeny concentrations were estimated using twin - cup based dosimeter, developed at BARC, India (Eappen and Mayya, 2004). It consists of two chambers working in two modes, namely the filter mode and the membrane mode, as shown in Figure 3.4. Each chamber has an inner volume of 135 cm^3 and a length of 4.5 cm. LR -115 type 2 strippable films were fixed inside the cup to register tracks due to radon, thoron and their progenies. The entry of the filter mode chamber was covered with glass fiber filter paper to allow the entry of both radon and thoron gases. The other side of chamber is operating in the membrane mode and this entry was covered with a semi permeable membrane (permeability constant in the range of 10^{-8} to 10^{-7} cm^2s^{-1}), between two glass fiber filter papers. The semi permeable membrane blocks thoron gas almost completely and allows more than 95% of radon gas to enter inside the chamber. The dosimeter is usually placed at a height of 2.5 m above the ground and exposed for a period of three months.

After the exposure, the detector films will be removed from the dosimeters and subjected to chemical etching for the revelation of alpha tracks. Films are etched

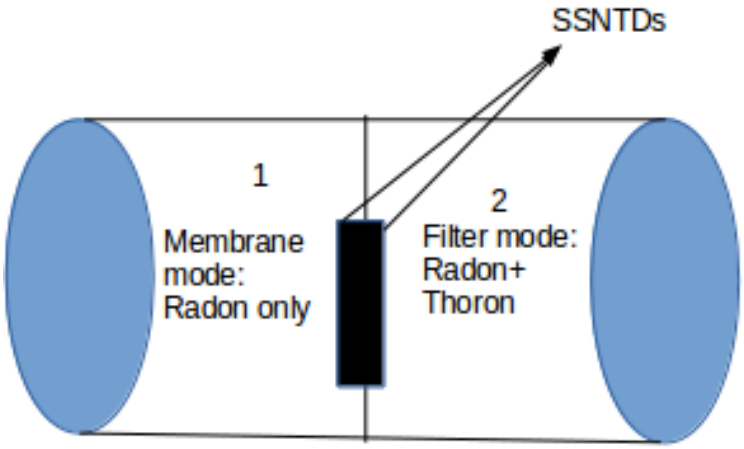

Figure 3.4: Schematic diagram of Twin cup dosimeter

with 2.5 N NaOH solution in a constant temperature bath at 60^0 C for 90 min. 4 μm bulk etch removal of the films will be ascertained in order to use the calibration factors obtained by Eappen and Mayya in their calibration experiment (Eappen and Mayya, 2004). Alpha tracks developed in the films will be counted using a spark counter at an operating voltage fixed at midway of the plateau region determined from the counter. Pre-sparking of the films is to be done at twice the operating voltage for developing the undeveloped holes in the films.

3.7.1 Calibration of the twin cup dosimeter

The calibration of the twin- cup dosimeter was done at BARC, Mumbai. The calibration chamber used in this experiment is cubical in shape, made of stainless steel having a capacity of 0.5 m^3 as shown in Figure 3.5. The dosimeters are suspended inside the chamber by means of a rod with arm. Radon/thoron gas and aerosols are

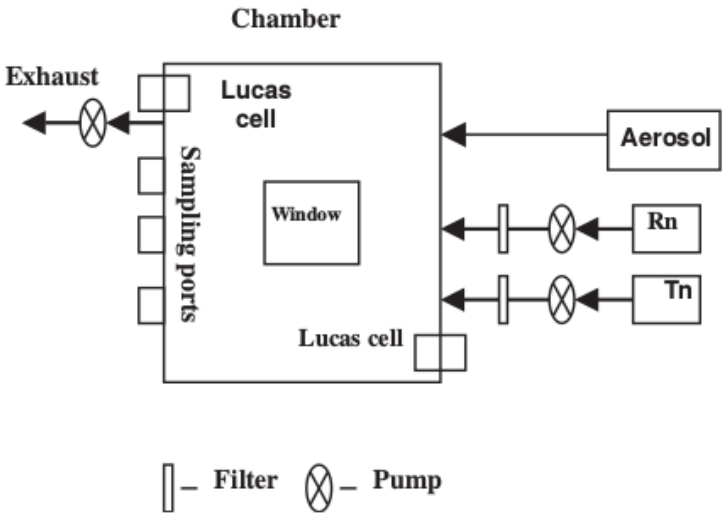

Figure 3.5: Block diagram of the calibration chamber

injected into the chamber through inlets provided and the fans fitted at the bottom and the top of the chamber helps to attain the spatial uniformity of gas concentrations. Standard sources (Pylon Electronics Inc., Canada) of radon and thoron gases were used throughout the calibration experiments. Radon was periodically injected whereas thoron was continuously injected at a steady rate. Also, aerosols inside the chamber were maintained at a constant level. Radon gas was measured online using a scintillation cell connected to an alpha counting system after introducing the dosimeters inside the chamber for 3 hours. The filter paper samples collected were used to find out the progeny concentrations. The circulation of air through the source was continued in a close-circuit manner to maintain the thoron concentration inside the chamber. Thoron gas was measured by using the Lucas cell technique.

3.7.2 Calibration factors-theoretical assumptions

Calibration factors are used to convert the observed track density to activity concentration of radon or thoron gases. In cup mode, the progeny species are filtered out and only gases enter inside the cup. It is assumed that the progeny species produced inside the cup will be in equilibrium with the respective parents. Since the exposure times are of the order of few months, the contribution inside the cups is due to the gases only. The corresponding calibration factors are given by

$$K_{R,(M/F)} = \frac{T_{R,(M/F)}}{tC_{R,(M/F)}} \tag{3.1}$$

$$K_{T,(M/F)} = \frac{T_{T,(M/F)}}{tC_{T,(M/F)}} \tag{3.2}$$

The subscripts R and T stands for the gas species and M and F denotes the membrane and filter compartments. Since the cup geometries are the same,

$K_{R,M}$ =$K_{R,F}$ and $K_{T,M} = 0$, because thoron in the membrane cup is negligible.

The following assumptions are used for modeling the development of tracks during the etching process (Eappen and Mayya, 2004). (i) The etching of paths traced by the alpha particles in the SSNTD takes place only in regions wherein the alpha-particle energy has fallen below a certain value E_c. E_c is generally assumed to be about 4 MeV. (ii) The track etching rates are distinctly higher than the bulk etching rate. (iii) A track is counted when a through hole is formed along the damaged region of the track.

A theoretical model has been developed based on the above assumptions to characterize the response of these detectors to alpha particles of different energies incident at different angles on the detector surfaces. This involves the estimation of

the total time required for track formation that incorporates both bulk etch rates and the track etch rates. Using this information, the region of influence for the given geometry of the dosimeter is determined. The radon and thoron concentrations in the respective cup is given by the equations

$$C_R = \frac{\rho_M}{K_{RM}.T} \tag{3.3}$$

$$C_T = \frac{\rho_F}{K_{TF}.T} - \frac{K_{RF}.C_R}{K_{TF}} \tag{3.4}$$

where ρ_M and ρ_F are the track densities (tr.cm^{-2}) in membrane mode and filter mode respectively. T represents the exposure period in days. The calibration factors K_{RM}, K_{RF} and K_{TF} were determined experimentally by exposing the dosimeters to known concentrations of radon, thoron and their progenies using standard sources. These were compared with the theoretically computed values. The calibration factors used in this experiment are shown below.

$K_{RM} = 0.019 \pm 0.003$ tracks $cm^{-2}d^{-1}/Bqm^{-3}$

$K_{RF} = 0.020 \pm 0.004$ tracks $cm^{-2}d^{-1}/Bqm^{-3}$

$K_{TF} = 0.016 \pm 0.005$ tracks $cm^{-2}d^{-1}/Bqm^{-3}$

The progeny working levels (Potential Alpha Energy Concentration-PAEC) were calculated using the formula.

$$C_p = \frac{C \times F}{3.7} \tag{3.5}$$

where F is the equilibrium factor and it is 0.4 for radon and 0.1 for thoron (UNSCEAR, 2000) and C stands for radon or thoron concentration.

The annual Effective Inhalation Dose (EID) was calculated using the formula

$$EID(Rn) = EEC(Rn) \times DCF(Rn) \times OF \tag{3.6}$$

$$EID(Tn) = EEC(Tn) \times DCF(Tn) \times OF \tag{3.7}$$

where EEC(Rn) and EEC(Tn) are the equilibrium equivalent concentration of radon and thoron respectively. Now

$$EEC(Rn) = F \times C_{Rn} \tag{3.8}$$

$$EEC(Tn) = F \times C_{Tn} \tag{3.9}$$

DCF(Rn) (9 nSv h^{-1} Bq^{-1} m^3) and DCF(Tn) (40 nSv h^{-1} Bq^{-1} m^3) are the radon and thoron dose conversion factors and OF (7000 h) is the occupancy factor, i.e. hours of indoor air exposure per year.

3.8 DTPS and DRPS

One of the shortcomings of the cup based dosimeter system is that it will respond only to gas concentrations and the decay products are calculated from the equilibrium factor approach. On the other hand, if one deploys air irradiation based bare card solid state nuclear track detectors, it suffers interference from gas concentrations. To overcome this difficulty, direct progeny sensors were developed which are deposition based systems and hence responds only to progenies, not to gas concentrations (Mishra et al., 2009a and 2009b, Mishra et al., 2008). DTPSs consists of an absorber (aluminized mylar of 50 micrometer thickness) mounted on LR-115 type

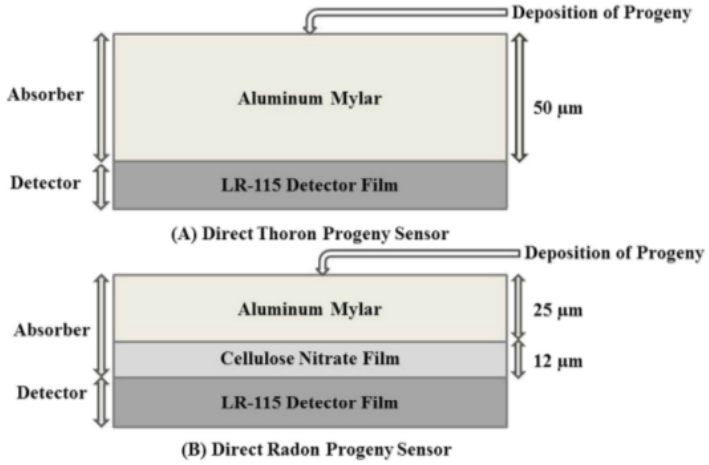

Figure 3.6: Schematic diagrams of (A) DTPS and (B) DRPS

nuclear track detectors, which exclusively detect 8.78 MeV alpha particles originating from ^{212}Po atoms, which are formed from the radioactive decay of ^{212}Pb and ^{212}Bi atoms deposited on the absorber surface. The schematic diagrams of DTPS and DRPS are shown Figure 3.6. Generally, LR-115 detects alpha particle's tracks having energy 1-4 MeV. In order to degrade the alpha particle energy below 4 MeV, an absorber is placed on the surface of LR-115 without any intervening air gap and these are fixed to a metal base. The calibration experiments and actual field situations indicate that the contribution from ^{212}Pb is higher than that of ^{212}Bi.

Similarly, the direct radon progeny sensor (DRPS) are made up of LR -115 detector with an absorber having an effective thickness of 37 micrometer. It detects mainly the alpha particles emitted from ^{214}Po (7.69 MeV) formed from the deposited activity of ^{218}Po, ^{214}Pb and ^{214}Bi on the surface. Alternatively, they are designed to yield the time averaged equilibrium equivalent thoron/radon concentration (EETC/EERC).

The sensitivity factor of the detector combination is expressed as track density

registered for 1 day exposure to an environment containing 1 Bq m^{-3} of EETC or EERC. The sensitivity factor depends on the track registration efficiency and the deposition velocity of progeny atom on the absorber surface (Mishra et al., 2014). Through this method, the total decay products, both in attached and unattached fractions are recorded in deposition based DTPS/DRPS. The minimum detection limit for DTPS is 0.1 Bq m^{-3} whereas that for DRPS is 1 Bq m^{-3}. It was found from the theoretical prediction and experiment that the sensitivity factor is nearly constant with 0.94 tracks/cm^2/d/EETC(Bqm^{-3}) for DTPS and 0.09 tracks/cm^2/d/EERC(Bq m^{-3}) for DRPS in natural environment (Mishra et al., 2010a; Mishra et al., 2009a) as shown in Table 3.1. Hence it is considered as the promising technique for measuring time averaged progeny concentrations.

For calculation of EERC, the tracks obtained from DTPS were eliminated from DRPS, to obtain the exact track density from radon progeny in DRPS. The EERC is calculated from the tracks recorded in the DRPS by eliminating the tracks obtained in the DTPS.

$$Tracks_{Rn\ progeny} = Tracks_{DRPS} - (\eta_{RT}/\eta_{TT})Tracks_{DTPS} \tag{3.10}$$

where η_{RT} and η_{TT} are explained in Table 3.1

The equilibrium equivalent radon concentration and equilibrium equivalent thoron concentration are given by the follwing formulae.

$$EERC(Bqm^{-3}) = \frac{Tracks_{only\ due\ to\ Rn\ progeny}}{K_R \times Exposure\ days(d)} \tag{3.11}$$

$$EETC(Bqm^{-3}) = \frac{Tracks_{DTPS}}{K_T \times Exposure\ days(d)} \tag{3.12}$$

The dose conversion factor reported by UNSCEAR 2000 has been used to estimate the inhalation dose due to radon,thoron and their progenies.

$$D(mSvy^{-1}) = 8760 \times 0.8 \times 10^{-6}[(0.17 + 9 \times F_R)C_R + (0.11 + 40 \times F_T)C_T] \quad (3.13)$$

Table 3.1: The parameters associated with DTPS and DRPS (Mishra et al., 2010a; Mishra et al., 2009a)

Track registration efficiency in DTPS	η_{TT} = 0.083 ± 0.004 η_{TR} = 0.002 ± 0.001
Track registration efficiency in DRPS	η_{RR}= 0.07 ± 0.005 η_{RT} = 0.01±0.0004
Sensitivity factor of DRPS	K_R = 0.09±0.0036 tr/cm^2/d/ EERC (Bq/m^3)
Sensitivity factor of DTPS	K_T=0.94±0.027tr/cm^2/d/EETC (Bq/m^3)

3.9 Gamma-ray spectrometry

Gamma spectrometry is the most commonly used radio-analytic method to estimate the radionuclides in various environmental samples. It is one of the non destructive methods to allow the simultaneous determination of various nuclides in bulk samples by applying basic sample preparation method (drying, ashing and sieving). Typical gamma ray spectroscopic system generates an electric pulse proportional to the magnitude of energy emitted by the radioactive materials being measured. Nowadays two types of gamma ray spectrometers are widely used, namely Scintillation detectors and High Purity Germanium (HPGe) detectors. Thallium doped sodium iodide detectors are still used as an industrial standard gamma ray spectrometer having better efficiency and poor resolution. The great superiority of HPGe detectors is their energy resolution which allows the separation of close photo peaks that remain unresolved in scintillation detectors.

3.9.1 Germanium detectors -theory

Germanium detectors are semiconductor diodes in which the intrinsic region is sensitive to X-rays and gamma rays. Under reverse biased condition, the electric field extends over the depleted region. When photons interact with the active volume of the detector, the electron - hole pairs are formed. The applied electric field separate these charge carriers into p and n electrodes. The voltage pulse produced by the pre-amplifier is proportional to the energy of the incident photon in the detector material. Because of the relatively small energy gap of Germanium (0.7 eV), the room temperature operation of the detector destroys the resolution due to thermally induced leakage current. Normally the detector is cooled to 77K through the use of insulated dewar in which the detector is put in thermal contact with the liquid nitrogen, the common cooling medium. The detector is then mounted in a vacuum chamber inserted in the dewar to protect from moisture and condensable contaminants. The block diagram of the data acquisition system used in HPGe detector is shown in Fig 3.7.

3.10 X-Ray Fluorescence method

X-Ray Fluorescence (XRF) method is a widely used analytical method to determine the elemental composition of the samples. It is one of the non-destructive methods which require minimum sample preparation. In XRF, the X-rays produced by the source (X-ray tube, radioactive source or synchrotron) irradiate the samples. The elements present in the sample will emit characteristic radiations with discrete energies corresponding to each element. In other words, it is possible to identify the elements by measuring the energy of the emitted radiations. The intensity of emitted

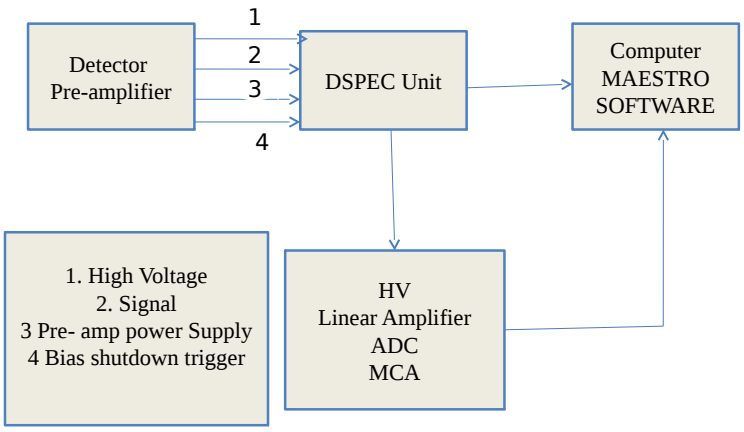

Figure 3.7: Block diagram of the data acquisition system with HPGe detector.

radiation determines how much of each element is present in the analysed samples. When X-rays interact with the material, a fraction will be transmitted, a fraction will be scattered and the other fraction will be absorbed (reemit via fluorescence). The fluorescence and scattering generally depend on the density of the material, energy of the X-rays, composition of the material and its thickness. In energy dispersive XRF, the detector measures different energies coming from the samples. Then it converts the radiation from the samples into its constituent elements. Generally, in ED-XRF, the elements from sodium to uranium can be detected and is good for identifying heavy elements.

3.11 References

1. Cartwright, B.G., Shirk, E.K., Price, P.B., (1978) A nuclear-track-recording polymer of unique sensitivity and resolution. Nucl. Instrum. Methods 153, 457-460.

2. Eappen K.P., Mayya Y.S., (2004). Calibration factors for LR-115 (type-II) based radon thoron discriminating dosimeter, Radiat. Meas. 38, 5-17.

3. Fleischer, R.L., Price, P.B., Walker, R.M., (1965) Solid-State Track Detectors: Applications to Nuclear Science and Geophysics, Annu. Rev. Nucl. Sci. 15, 1-28.

4. Fleischer, R.L., Price, P.B., Walker, R.M., (1975) Nuclear Tracks in Solids. University of California Press, Berkley.

5. ICRP-65 (1993). Protection against Radon-222 at home and at work. Ann International Commission on Radiological Protection, 23(2), 1-48 (Pergamon Press, Oxford).

6. Mishra, R., Mayya, Y. S., and Kushwaha, H. S.(2009a) Measurement of ^{220}Rn/ ^{222}Rn progeny deposition velocities on surfaces and their comparison with theoretical models, J. Aerosol Sci. 40, 1-15.

7. Mishra, R., Sapra, B. K., and Mayya, Y. S.(2009b) Development of an integrated sampler based on direct ^{220}Rn/ ^{222}Rn progeny sensors in flow-mode for estimating unattached/attached progeny concentration, Nucl. Instrum. Methods Phys. Res. B 267, 3574-3579.

8. Mishra, R., Prajith, R., Sapra, B. K., and Mayya, Y. S.(2010a) Response of Direct Thoron Progeny sensors (DTPS) to various aerosol concentrations and ventilation rates, Nucl. Instrum. Methods Phys. Res. B 268, 671-675.

9. Nidal Dwaikat, Ghassan Safarini, Mousa El-hasan, Toshiyuki Iida (2007) CR-39 detector compared with Kodalpha film type (LR-115) in terms of radon concentration, Nucl. Instrum. Methods Phys. Res. A, 57, 289-291.

10. Ramachandan, T. V., Sathish, L. A. (2011) Nationwide indoor ^{222}Rn and ^{220}Rn map for India: A review. J. Environ. Radioact 102, 975-976.

11. Rosaline Mishra, Sapra B. K., and Mayya Y. S. (2014) Multi-parametric approach towards the assessment of radon and thoron progeny exposures, Review of Scientific Instruments 85, 022105

12. Rosaline Mishra, Mayya, Y.S. (2008) Study of a deposition-based direct thoron progeny sensor (DTPS) technique for estimating equilibrium equivalent thoron concentration (EETC) in indoor environment, Radiat. Meas. 43, 1408 - 1416.

13. Silk, E.C.H., Barnes, R.S. (1959). Examination of fission fragment tracks with an electron microscope, Philos. Mag. 4, 970-972.

14. UNSCEAR,(1999) United Nation Scientific Committee on the Effects of Atomic Radiation, Sources and Effects of Ionizing Radiation, United Nations: New York.

15. UNSCEAR 2000. United Nations Scientific Committee on the Effects of Atomic Radiation, Sources and Effects of Ionizing Radiation, UNSCEAR 2000 Report Vol.1 to the General Assembly, with Scientific annexes, United Nations Sales Publication, United Nations, New York.

16. Young, D. A., (1958). Etching of Radiation damage in Lithium Flouride Nature 182, 375-377.

Chapter 4

External Dose

4.1 Introduction

Our country is having a coastal line of 7516 kms. The coastal sand in the southern part of Kerala consists of monazite ores having uranium oxide (~0.35%) and thorium oxide (~9%) with other minor rare earth compounds. In addition to this, the beach sand along Chavara-Neendakara in Kollam district is rich in ilmenite, rutile, zircon and garnet, which offer potential scope of exploitation for industrial purposes (District Survey Report of Minor Minerals, 2016). Natural radiation is largely caused by the presence of primordial radionuclides and their decay products present in nature. South west coastal belt of Kerala being an HBRA region, assessment of the primordial radionuclides is imperative and data from marine coastal monitoring of radioactivity acts as a baseline for the assessment of radioactive pollution experienced by the biota. The terrestrial radioactivity in soil is measured through the concentrations of primordial radionuclides such as ^{238}U,^{232}Th and ^{40}K. The radionuclides ^{238}U, ^{232}Th and ^{40}K are aberrantly distributed in earth's crust and

the geographical variation of the radionuclides are due to soil erosion, weathering of rocks, selective leaching of elements etc. Most of the studies reported related to this are confined to Neendakara-Chavara coastal region. The main objective of the following work is to carry out an extensive estimation of the primordial radionuclides like uranium, thorium and potassium in the entire coastal areas of Kerala and to evaluate their radiological parameters.

4.2 Region of the study

Surface soil samples weighing from 1.5 to 2 kg were collected from 17 locations along the coastal area of Kerala having 590 km length, with Arabian sea on the west. Kerala constitutes 10% of India's coastal zone, with an exclusive economic zone (EEZ) of 2,18,536 Sq km. Fisheries have prominent contribution to the Kerala economy and fishermen population is around 10 lakhs, living in the 222 marine villages (Kerala Marine Fisheries Statistics, 2015). The density of population in the coastal area of Kerala is 2168 persons per km^2, whereas that of the state average is 859. Among the 14 districts of Kerala, 9 districts are sharing the coastal zone. Kerala's coastal belt is almost flat and mostly utilized as paddy fields, interconnected by canals and rivers. The natural hazards like landslides, coastal erosion, flooding and tsunami happen in coastal zones. The sampling areas selected for the present study are from the coastal regions of Thiruvananthapuram (Th), Alappuzha (Al), Kollam (Ko), Ernakulam (Ek), Thrissur (Tr), Malappuram (Ma), Kozhikode (Kz), Kannur (Kn), and Kasaragod (Ks) districts. Figure 4.1 gives the sampling areas covered for the study.

An average of 5 to 10 samples were collected from each sampling location. Sam-

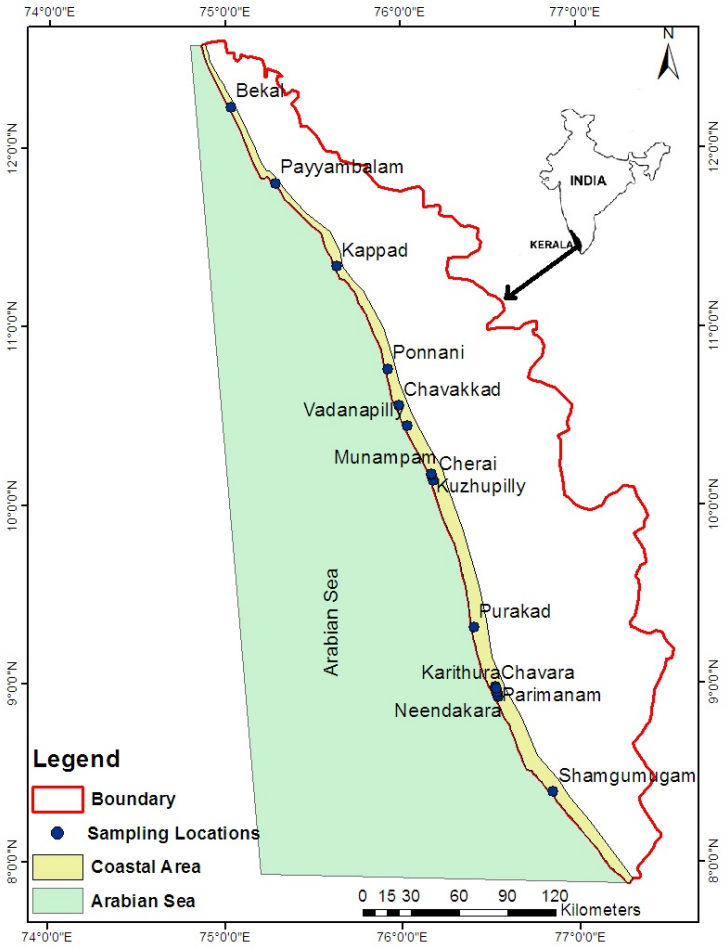

Figure 4.1: Sampling locations

ples were collected at 10 m interval at the sampling area, depending on the contour and layout. Individual sample was collected from 1 m^2 area. After removing the upper layer of the soil, the area is divided into 16 equal squares. Soil from top 5 cm depth was scrapped from the middle of each square and combined to make a gross sample of approximately 1.5 to 2 kg from each sampling location. The samples collected were then dried in an oven at 110 ^{0}C for 24 hours to remove the moisture content. It was homogenized and sieved through 0.5 mm size mesh. The samples were then hermetically sealed, weighed and stored in air tight plastic containers of diameter 6.5 cm and height 8.4 cm for a period of 4-6 weeks to attain secular equilibrium between parent and daughters of the uranium and thorium series. The samples were then counted for gamma ray activity using an HPGe detector for a period of 36000 seconds to get a reasonable area under the photo-peaks, corresponding to various gamma energies.

4.3 Energy calibration

Prior to the acquisition of the actual data from the samples, the energy calibration (Gamma ray energy as a function of channel number) of the HPGe detector was performed using standard gamma ray sources (^{60}Co, ^{137}Cs, ^{22}Na, and ^{133}Ba). The HPGe detector was connected to the DSPEC hardware unit. This unit provides High Voltage (HV) to the detector, working voltage for the preamplifier and multi channel analyser (MCA). MCA is working according to the instructions from the MAESTRO-32 software installed on the PC. Figure 4.2 depicts the energy calibration graph obtained.

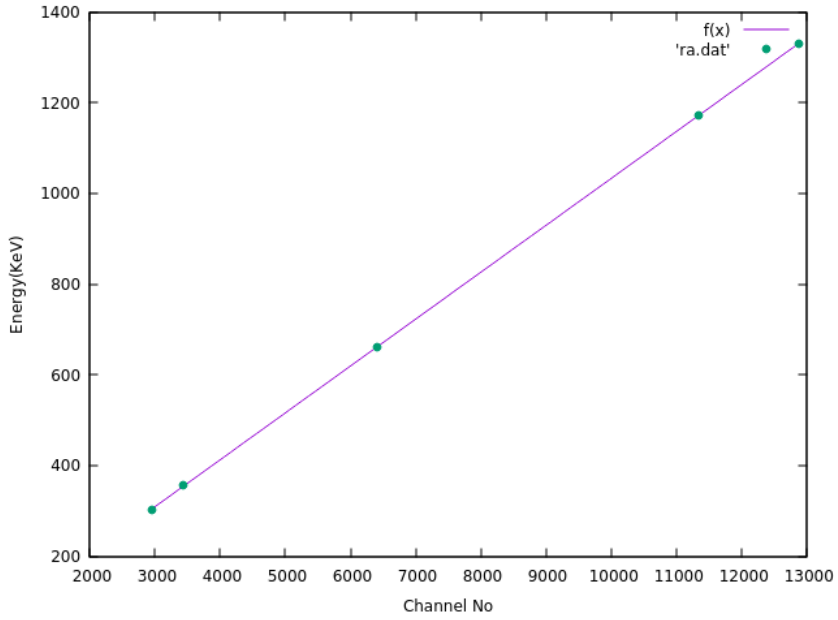

Figure 4.2: The energy calibration graph HPGe detector.

4.4 Efficiency Calibration

In gamma ray spectrometry, we come across two types of full energy peak efficiencies (FEP) (Pablo, 2015). They are:

1. Absolute FEP efficiency (ϵ_{abs})

$$\epsilon_{abs} = \frac{No\ of\ photons\ recorded\ in\ the\ FEP}{No\ of\ photons\ emitted\ by\ source.} \tag{4.1}$$

2. Intrinsic FEP efficiency (ϵ_{int})

$$\epsilon_{int} = \frac{No\ of\ photons\ recorded\ in\ the\ FEP}{No\ of\ photons\ incident\ on\ the\ detector} \tag{4.2}$$

ϵ_{abs} depends upon the detector characteristics and the material between source and detector while ϵ_{int} depends only on the physical and chemical characteristics of

the detector.

$$\epsilon_{abs} = \epsilon_{int} \times F \tag{4.3}$$

where F is called the geometric efficiency and it represents the fraction of photons emitted by the source that reach the detector. F depends upon the source-detector position and the attenuation of photons.

For analyzing the environmental samples, the quantification of the radiation emitted is a difficult task. Among all the photons emitted by the source, only a fraction will be detected because of the limitations due to the geometry (solid angle), intrinsic characteristics of the detector (intrinsic efficiency) and the matrix effects (self-attenuation). Due to the complications to determine these factors independently, it is convenient to use the absolute efficiency, because this considers all effects simultaneously (Guembou et al., 2017). Once the absolute efficiency of the detector is known, the specific activity of the sample can be easily found out for large volume samples.

For efficiency calibration, standard sources were prepared using IAEA reference materials RGTh-1, RGU-1, and RGK-1. The standard sources were filled in plastic containers of 6.5 cm diameter and 8.4 cm height. This geometry was maintained throughout the experiment for the spectrum analysis of the samples. The efficiency calibration graph of HPGe detector is shown in Figure 4.3

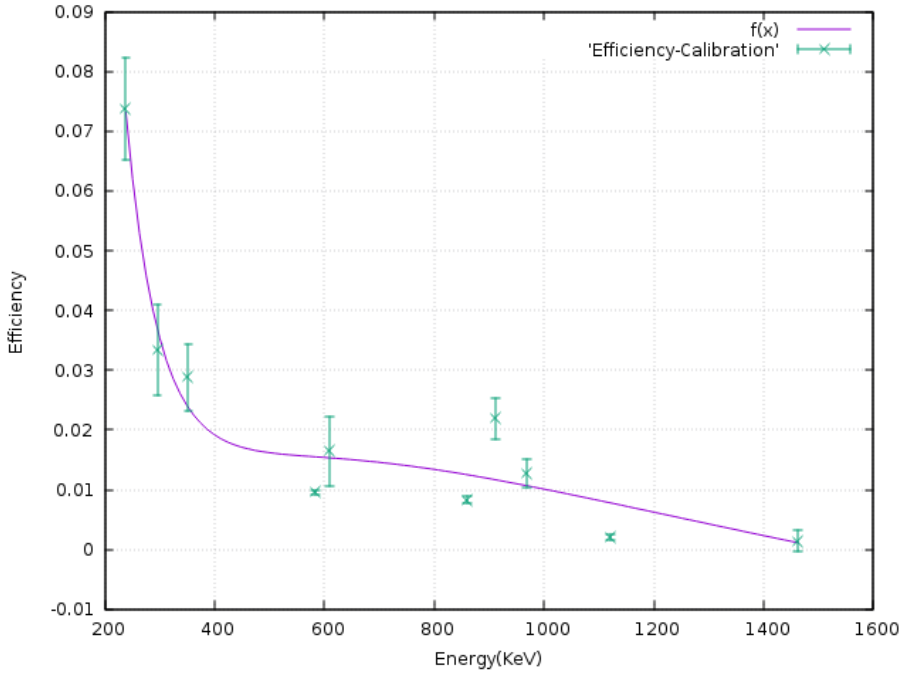

Figure 4.3: Efficiency calibration graph of HPGe detector.

4.5 Data aquisition system

The spectrum of gamma rays emitted by the samples was generated using a HPGe detector having a relative efficiency of 21%, with an energy resolution of 1.7 keV at 1.33 MeV peak of ^{60}Co. As mentioned earlier, the detector was coupled with DSPEC digital signal processing unit that includes high voltage filter, preamplifier and 32K display memory.

4.6 The activity concentration

The activity of the primordial radionuclides were calculated using the equation

$$A(Bqkg^{-1}) = \frac{C}{\gamma \epsilon t m} \tag{4.4}$$

where C is the counts above background, γ is the absolute gamma ray transition probability, t is the exposure time and m is the mass in kg.

MAESTRO-32 spectrum analysis software was used for the data acquisition and spectrum analysis. The standard reference materials and samples were taken in containers of same size and type so that the detector geometry remained the same. The samples were counted for 36000 seconds to reduce the counting error. Also, the background spectrum (taken for 36000 seconds) was subtracted from the measured spectrum of each sample. ^{238}U was estimated through the photo peaks of ^{214}Pb(351.9 keV, 37.1%) and ^{214}Bi(609.3 keV, 46.1%). ^{232}Th was estimated through ^{228}Ac(911.2 keV, 29%), ^{212}Pb(238.6 keV, 43.1%) and ^{208}Tl(583.2 keV, 86%) photo peaks. The estimation of ^{40}K was directly done by measuring the 1460.8 keV full energy peak. Typical sample spectra are given in the Appendix as figures A1 and A2.

Table 4.1: Activity concentrations of ^{238}U, ^{232}Th and ^{40}K expressed in (Bq kg^{-1}) in various sampling locations

Location	**S. No**	**Uranium**	**Thorium**	**Potassium**
Thiruvananthapuram	1	18.25±4.77	30.76±2.37	173.83±5.30
	2	20.74±5.39	33.84±2.61	150.54±6.45

Continued on next page

Table 4.1 – continued from previous page

Location	S. No	Uranium	Thorium	Potassium
	3	21.02±5.62	39.32±3.07	160.23±5.71
Neendakara jyothi	4	481.27±75.10	1267.83±112.41	172.79±7.74
	5	362.05±56.49	870.11±64.98	145.37±7.05
	6	516.09±80.49	1327.55±96.78	154.33±8.22
	7	250.27±39.05	568.26±53.52	164.90±5.47
	8	767.55±119.59	2232.88±191.82	78.54±10.10
	9	569.74±88.61	1233.89±104.82	154.67±8.40
	10	763.39±101.21	2141.67±162.34	156.34±6.81
	11	351.36±49.39	851.60±73.09	189.63±7.55
Neendakara	12	569.74±88.61	1233.89±104.82	158.07±8.40
	13	927.72±144.94	2614.90±184.95	176.55±11.30
	14	376.08±58.02	990.96±76.56	161.21±7.70
	15	65.21±10.51	103.41±8.76	151.60±7.92
	16	827.68±130.32	2349.39±188.82	205.38±9.98
	17	437±67.59	1075.12±88.28	168.68±7.59
	18	401±62.27	905.60±74.27	155.27±6.94
	19	431.25±67.59	1167.83±88.13	160.55±7.59
	20	530.26±83.28	1573.57±92.21	186.74±12.07
	21	568.89±86.78	1636.10±135.26	145.36±6.25
Parimanam	22	508.15±99.12	2683.33±113.17	134.41±8.00
	23	557.86±86.91	1571.54±137.91	155.80±9.01

Continued on next page

Table 4.1 – continued from previous page

Location	S. No	Uranium	Thorium	Potassium
	24	523.26±66.67	1502.23± 123.61	139.61±5.33
	25	566.67±71.24	1096.46±76.77	148.56±5.61
	26	570.12±71.41	999.37±76.51	163.58±7.11
Chavara	27	749.49±116.09	2291.61±200.43	221.62±10.05
	28	535.70±83.28	1636.10±128.81	187.66±10.30
	29	179.15±27.80	273.11±23.91	170.06±5.74
	30	223.06±34.83	516.21±50.64	184.07±6.03
	31	241.46±37.59	663.43±55.39	186.13±6.65
	32	361.74±55.74	991.86±84.97	190.14±7.25
	33	315.66±49.05	923.76±86.56	193.77±7.25
	34	170.38±27.18	390.59±35.71	181.09±5.41
	35	193.67±30.38	535.70±39.32	164.77±5.36
	36	296.30±41.96	663.43±58.62	130.26±6.40
Chavara IRE	37	117.78±18.43	299.22±25.97	167.80±4.83
	38	85.55±13.26	186.42±18.50	174.07±4.54
	39	147.84± 22.81	322.84±27.79	164.96±5.03
	40	345.28±51.24	999.16± 70.12	169.35±7.1
	41	325.62±46.51	512.36±48.41	203.23±8.49
Karithura	42	1172.75±178.50	2308.17±289.05	431.08±11.64
	43	967.71±150.56	1142.33±86.12	335.11±6.49
	44	1121.21±125.67	1256.25±83.17	336.21±9.65

Continued on next page

Table 4.1 – continued from previous page

Location	S. No	Uranium	Thorium	Potassium
	45	1101.32±98.75	1365.62±87.93	296.33±6.88
	46	997.32±162.41	1355.11±85.42	346.13±9.86
	47	1176.75±188.16	3485.46±284.64	436.52±13.69
Ek.Kuzhupilly	48	13.89±2.76	51.14±4.07	190.46±4.36
	49	17.04±3.00	59.53±5.35	228.29±4.17
	50	14.25±3.67	41.33± 4.53	251.34±7.98
	51	13.51±3.31	58.67±6.01	242.51±6.56
	52	13.28±2.71	46.44±5.01	235.54±5.54
Munampam	53	11.54±2.19	32.13±2.72	218.13±5.23
	54	11.22±2.25	29.86±2.61	254.03±4.27
	55	10.11±1.81	15.13±1.78	262.14±5.61
	56	10.31±1.98	28.44±2.11	216.16±5.11
Charai	57	5.70±1.40	9.00±0.74	108.46±8.93
	58	6.28±1.43	9.77±0.89	285.85±4.52
	59	6.21±1.76	8.51±0.82	262.13±8.34
	60	5.24±1.43	7.54±0.68	264.22±4.55
	61	6.15±1.37	9.41±0.96	248.55±7.61
Tr vadanapilly	62	4.96±1.32	8.89±0.80	292.03±4.55
	63	4.94±1.43	8.59±0.82	313.41±4.46
	64	3.31±1.05	5.54±0.62	281.31±8.56
	65	4.24±1.25	7.51±0.72	279.14±7.44

Continued on next page

Table 4.1 – continued from previous page

Location	S. No	Uranium	Thorium	Potassium
	66	5.21±1.71	9.11±0.91	283.21±8.12
Chavakkad	67	4.44±1.21	6.96±1.21	296.03±6.51
	68	4.46±1.43	6.90±0.64	385.04±5.32
	69	4.12±1.81	7.31±0.69	364.88±12.01
	70	4.11±1.56	5.22±0.51	286.14±9.54
	71	3.17±1.12	6.24±0.71	292.55±10.92
Ma-Ponnai	72	18.91±3.63	67.07±6.12	214.14±4.37
	73	17.04±3.39	43.68±6.32	281.29±4.68
	74	19.61±4.22	52.96±7.11	267.19±6.71
	75	16.71±3.56	55.64±6.55	271.18±7.21
Kappad	76	5.51±1.48	8.52±0.64	248.81±5.11
	77	5.21±1.47	9.39±0.83	191.03±3.62
	78	4.21±1.01	11.07±1.10	225.12±7.8
	79	6.14±2.10	10.29±0.87	217.16±8.5
Alapuzha	80	28.60±5.89	24.76±5.32	138.83±5.28
	81	48.60±8.42	71.65±7.44	150.41±4.46
	82	34.71±6.21	42.73±6.32	179.32±7.32
Ks-Bekal	83	2.12±0.57	9.42±0.81	140.82±7.72
	84	1.19±0.42	7.83±0.61	122.39±5.61
	85	1.77±0.61	10.91±0.91	130.72±5.61
	86	2.62±0.71	11.31±1.02	152.61±6.77

Continued on next page

Table 4.1 – continued from previous page

Location	S. No	Uranium	Thorium	Potassium
	87	2.51±0.62	12.43±1.41	159.11±6.71
Kn-Payyambalam	88	5.62±1.56	16.81±1.72	179.21±7.61
	89	4.36±0.96	10.19±0.81	156.87±8.52
	90	3.95±1.01	10.11±0.84	187.76±9.17
	91	3.11±0.81	12.76±1.51	132.98±6.34
	92	4.36±0.87	19.07±1.98	147.71±7.12

4.7 Radiation Hazard Indices

The absorbed dose rates (D) due to gamma radiation in air at 1 meter above the ground surface, was calculated based on the guidelines provided by UNSCEAR, 2000 (Eq. 4.5). Uniform distribution of the naturally occurring radionuclides (^{238}U, ^{232}Th and ^{40}K) was assumed in the calculation.

$$D(nGyh^{-1}) = 0.461A_U + 0.623A_{Th} + 0.043A_K \tag{4.5}$$

where A_U, A_{Th} and A_K are the the activities of ^{238}U, ^{232}Th and ^{40}K expressed in Bq kg^{-1}.

To assess the health effects caused by the radionuclides, the annual effective dose (AED) received by the population was estimated using the conversion coefficients 0.70 Sv y^{-1} and outdoor occupancy of 0.2, as suggested by UNSCEAR 2000

(Chougaonkar et al., 2004). Accordingly,

$$AED(mSvy^{-1}) = D \times 8760 \times 0.2 \times 0.7(SvGy^{-1}) \times 10^{-6} \tag{4.6}$$

where D (nG h^{-1}) is the absorbed dose rate in the outdoor air and 8760 h is the number of hours in one year. Radium equivalent activity (Ra_{eq}), a widely used hazard index, is calculated using Eq. 4.7 (Sroor et al. 2002; Yingnan Huang et al., 2015)

$$Ra_{eq}(Bqkg^{-1}) = A_U + 1.43A_{Th} + 0.07A_K \tag{4.7}$$

The radiological suitability of a material is usually expressed in terms of the external hazard index H_{ex}. If H index is greater than unity, then the exposure recieved by the individual, exceeds the recommended limits and remedial action is required (Veiga et al., 2006). It was evaluated using Eq. 4.8 where ^{232}Th and ^{40}K activities are normalised to that of ^{238}U values considering the radiological effect from these elements.

$$H_{ex} = A_U/370(Bqkg^{-1}) + A_{Th}/259(Bqkg^{-1}) + A_K/4810(Bqkg^{-1}) \tag{4.8}$$

4.8 Results and discussion

The actvity concentrations of ^{238}U, ^{232}Th and ^{40}K in each of the 92 samples collected from the 17 locations are listed in Table 4.1. In Kollam district, the samples were collected from Neendakara, Neendakara-Jyothi, Parimanam, Chavara, Chavara -IRE and Karithura. The results indicate that all of these beaches show elevated radioac-

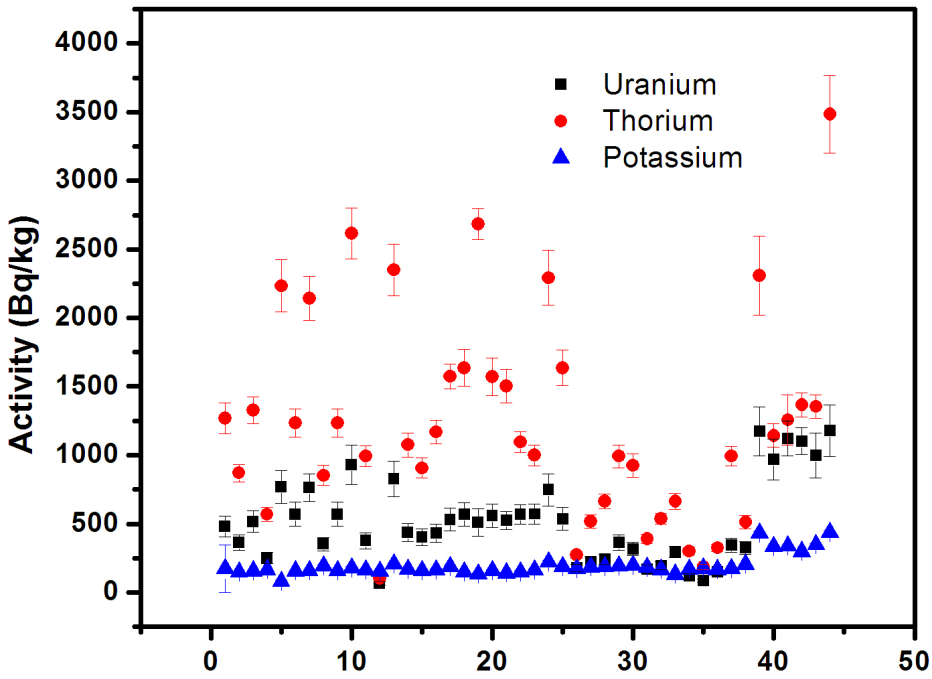

Figure 4.4: Activity of radionuclides in soil samples from different beaches of Kollam district.

Table 4.2: Average Activity Concentration (Bq kg^{-1}) in the surface beach samples collected from the coastal areas of Kerala.

S. No	Sampling area	No of samples - Code	N/E	Uranium (Bq/kg) A.M S.D	Uranium (Bq/kg) Min Max	Thorium (Bq/kg) A.M S.D	Thorium (Bq/kg) Min Max	Pottasium (Bq/kg) A.M S.D	Pottasium (Bq/kg) Min Max
1	Thiruvananthapuram	3	8.40	20.00	18.25	34.64	30.76	161.53	150.54
	Shangumugam	SH1-SH3	76.98	1.52	21.02	4.34	39.32	11.70	173.83
2	Neendakara	8	8.88	507.72	250.27	1311.72	568.26	151.93	78.54
	Jyothi	NJ1-NJ8	76.59	188.77	767.55	598.22	2232.88	32.65	189.63
3	Neendakara	10	8.94	513.48	65.21	1365.08	103.41	166.94	145.36
		N1-N10	76.54	228.46	927.72	687.82	2614.90	17.19	205.38
4	Parimanam	5	8.95	545.21	508.15	1570.59	999.37	148.39	134.41
		P1-P5	76.53	24.88	570.12	598.99	2683.33	10.57	163.58
5	Karithura	6	8.97	1089.51	967.71	1818.82	1142.33	363.56	296.33
		K1-K6	76.52	80.64	1176.75	837.82	3485.46	52.06	436.52
6	Chavara	5	8.98	204.41	85.55	933.76	186.42	175.88	164.96
	IRE	CHI1-CHI5	76.52	108.97	345.28	343.37	991.16	13.99	203.23
7	Chavara	10	8.99	326.46	170.38	888.58	273.11	180.96	130.26
		CH1-CH10	76.54	174.62	747.49	594.18	2291.61	22.21	221.62
8	Alapuzha	3	9.35	37.30	28.60	49.71	34.76	156.14	138.68
	Porakad	A1-A3	76.36	10.25	48.60	19.41	71.65	20.92	179.32
8	Eranakulam	5	10.14	5.92	5.24	8.85	7.54	233.84	108.46
	Cherai	CHR1-CHR5	76.17	0.44	6.28	0.87	9.77	71.35	285.85
10	Kuzhuppilly	5	10.16	14.39	13.28	51.42	41.33	229.63	190.46
		KU1-KU5	76.17	1.36	17.04	7.00	59.53	21.02	251.34
11	Munampam	4	10.18	10.80	10.11	26.39	15.13	237.62	216.16
		M1-M5	76.17	0.60	11.54	76.63	32.13	20.68	262.14
12	Thrissur	5	10.43	4.53	3.31	7.93	5.54	289.82	279.14
	Vadanapilly	V1-V5	76.07	0.77	5.21	1.47	9.11	14.07	313.41
13	Chavakkad	5	10.56	4.06	3.17	6.53	5.22	324.93	286.14
		CHV1-CHV5	76.09	0.53	4.46	0.83	7.31	46.36	385.04
14	Ponnani	4	10.77	18.07	16.71	54.84	43.68	258.45	214.14
		PO1-PO4	75.93	1.41	19.61	9.63	67.07	30.13	281.29
15	Kappad	4	11.38	5.27	4.21	9.80	8.52	220.43	191.03
		KP1-KP4	75.73	0.80	6.14	1.08	11.01	23.66	248.41
16	Payyambalam	5	11.86	4.28	3.11	13.78	10.11	160.90	132.98
		PY1-PY5	75.35	0.81	5.62	3.59	19.07	20.13	187.76
17	Bekal	5	12.42	2.04	1.19	10.38	7.83	141.13	122.39
		B1-B5	75.023	0.58	2.62	1.78	12.43	15.12	159.11

N/E-Latitude/Longitude
AM- Arithmetic mean and S.D -Standard deviation

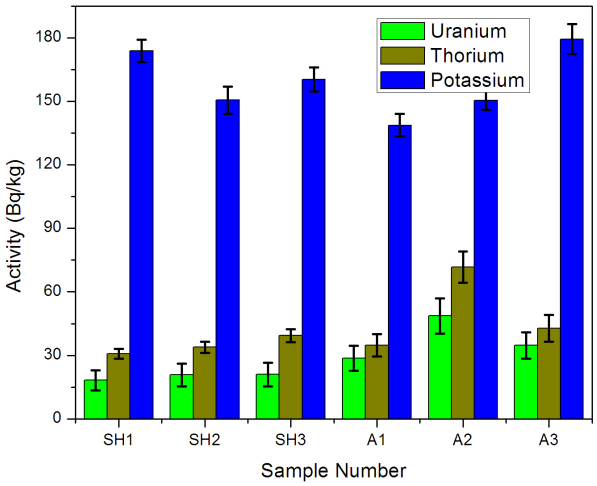

Figure 4.5: Uranium, thorium and potassium distribution in coastal areas of Thiruvananthapuram and Alapuzha(Shanghumugham and Porakad)

tivity and come under the high background radiation area. Also thorium activity dominated the uranium acitivity in all the analysed samples as shown in Figure 4.4. This is due to the fact that thorium has only one oxidation state Th(+4), and this is insoluble in water (Aswathanarayana, 1985) whereas uranium has two states (+4 and +6) and +6 is more reactive and highly soluble compared to +4. The activity of ^{238}U and ^{232}Th in the analysed samples are higher than the UNSCEAR 2008 reference limit of 33 Bq kg^{-1} for uranium and 45 Bq kg^{-1} for thorium (UNSCEAR, 2008). Except in two samples from Karithura beach, all other samples showed the potassium activity less than the UNSCEAR 2008 reference limit of 420 Bq kg^{-1}.

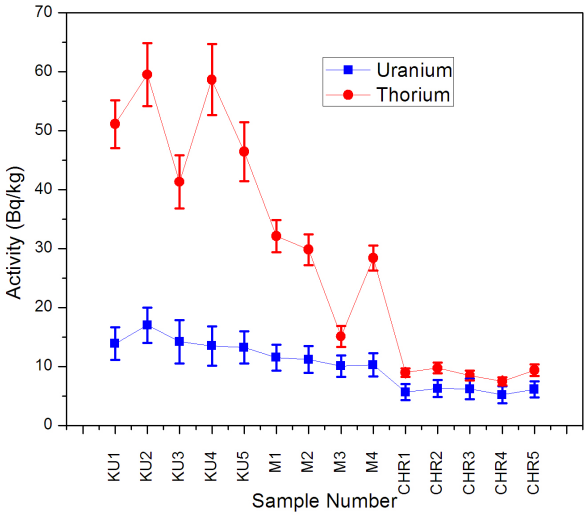

Figure 4.6: Uranium, thorium distribution in coastal areas of Eranakulum district

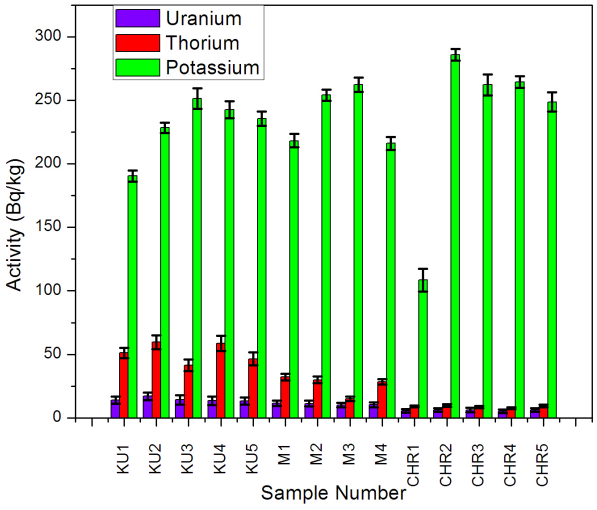

Figure 4.7: Uranium, thorium and potassium distribution in coastal areas of Eranakulum district

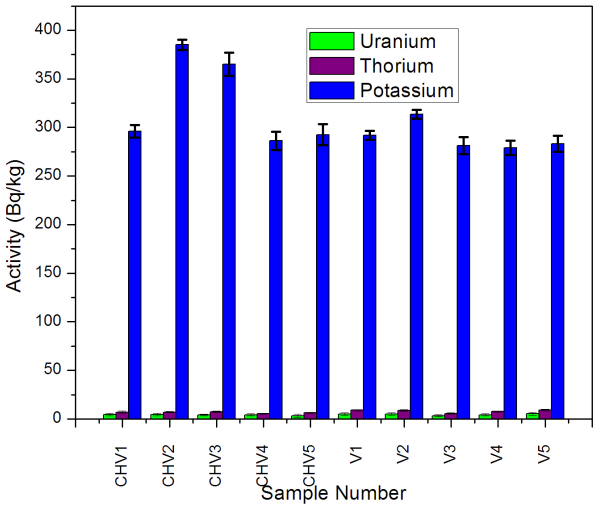

Figure 4.8: Uranium, thorium and potassium distribution in coastal areas of Thrissur district

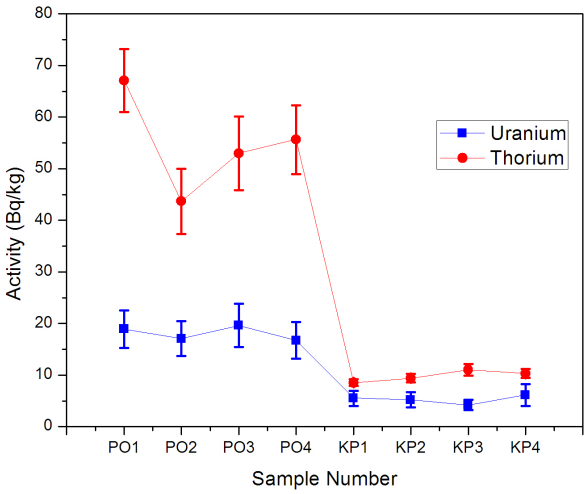

Figure 4.9: Uranium, thorium distribution in coastal areas of Ponnani and Kappd.

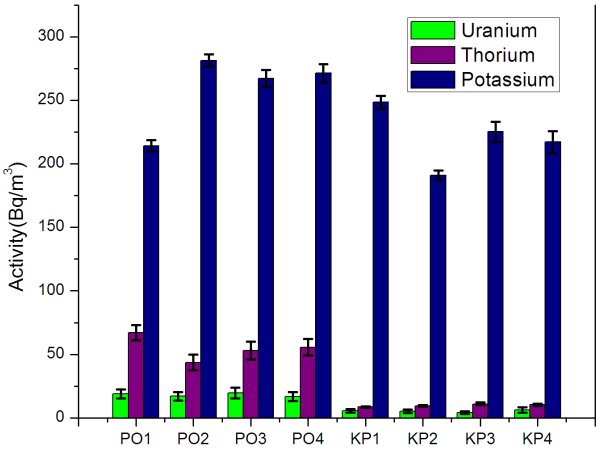

Figure 4.10: Distribution of Uranium, thorium and potassium in Ponnani and Kappad

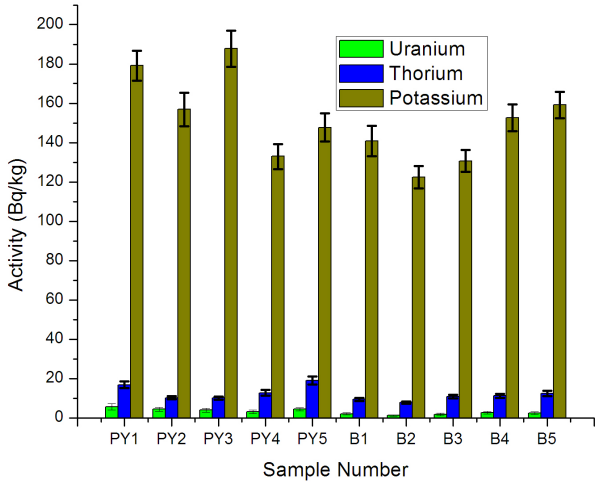

Figure 4.11: Distribution of Uranium, thorium and potassium in Payyambalam and Bekal

Table 4.3: Dose, Annual effective dose (AED) and External Hazard Index (H_{ex})

S. No	Location	Absorbed Dose (nGy/h)		(AED) (mSv/y)		H_{ex}	
		A.M	S.D	A.M	S.D	AM	S.D
1	Thiruvananthapuram	37.75	3.06	0.046	0.004	0.22	0.02
2	Neendakara Jyothi	1058.20	457.63	1.298	0.561	6.47	2.81
3	Neendakara	1094.75	533.08	1.343	0.654	6.69	3.27
4	Parimanam	1236.63	362.99	1.517	0.445	7.57	2.25
5	Karithura	1651.02	550.95	2.025	0.676	9.98	3.51
6	Chavara	712.13	450.95	0.873	0.553	4.35	2.77
7	Chavara IRE	390.04	222.59	0.478	0.273	2.37	1.36
8	Alapuzha	54.88	17.72	0.067	0.022	0.33	0.11
9	Cherai	18.29	3.18	0.022	0.004	0.10	0.02
10	Kuzhuppilly	48.55	4.59	0.060	0.006	0.29	0.03
11	Munampam	31.63	3.82	0.039	0.005	0.18	0.02
12	Vadanapilly	19.49	1.62	0.024	0.002	0.10	0.01
13	Chavakkad	19.49	2.48	0.024	0.003	0.10	0.01
14	Ponnani	53.61	5.13	0.066	0.006	0.31	0.03
15	Kappad	18.01	1.03	0.022	0.001	0.10	0.01
16	Payyambalam	17.48	2.50	0.021	0.003	0.09	0.01
17	Bekal	13.47	1.94	0.016	0.002	0.07	0.01

The uranium, thorium and potassium levels in the coastal areas of Eranakulam (Kuzhupilly, Cherai and Munampam), Thiruvanthapuram (Shanghumugham), Alapuzha (Porakad) Thrissur (Vadanapilly and Chavakkad), Kozhikode (Kappad), Kannur (Payyambalam) and Kasaragod (Bekal) districts show that at these locations the radioactivity levels are less than the UNSCEAR 2008 reference limit(see Figures 4.5, 4.7, 4.8, 4.10, 4.11). However, the potassium activity is much higher than the uranium and thorium activities in the coastal areas of Eranakulam, Thrissur, Malappuaram, Kozhikode, Kannur and Kasaragod districts. Among the various beaches in these districts, the average thorium level in Ponnani (54.84 Bq kg^{-1}) and Porakad (49.71 Bq kg^{-1})) are higher than the UNSCEAR 2008 reference limit (45 Bq kg^{-1}). These coastal areas come under the normal background radiation areas (NBRA) where the presence of monozite sands are negligible. Table 4.2 shows the average activity concentration of uranium, thorium and potassium in each of the 17 locations.

Table 4.3 shows the summary of radiological hazard indices estimated and the

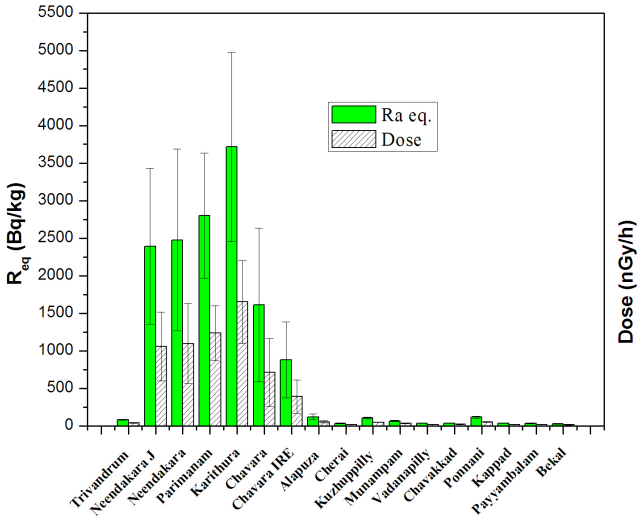

Figure 4.12: Ra_{eq} and Absorbed dose to population

details are included in Appendix A (Table A.1). Except at Chavara-IRE, the annual effective dose received by the population in the coastal areas of Kollam district are higher than the world wide average value of 0.5 mSv y^{-1} (UNSCEAR, 2000). The fishermen communities who live in coastal areas and spend their time for livelihood receive the radiation dose caused by the radionuclides. The annual effective dose received by the population in normal background areas (Thiruvananthapuram, Alapuzha, Eranakulam, Malappuram, Kozhikode, Kannur and Kasaragod districts) varies from 0.013 to 0.090 and hence it can be considered as negligible.

In the present study, covering the entire coastal areas of Kerala, the absorbed dose rate (D) in beach sands of Kollam and Malappuram districts are found to be higher than the global mean value of 60 nGy h^{-1} (UNSCEAR, 2000). The highest value of the absorbed dose(D) (1651 $\pm$ 550 nGy h^{-1}) was found at Karithura in Kollam district and the lowest value was found at Bekal (13.47 $\pm$ 1.94 nGy h^{-1})

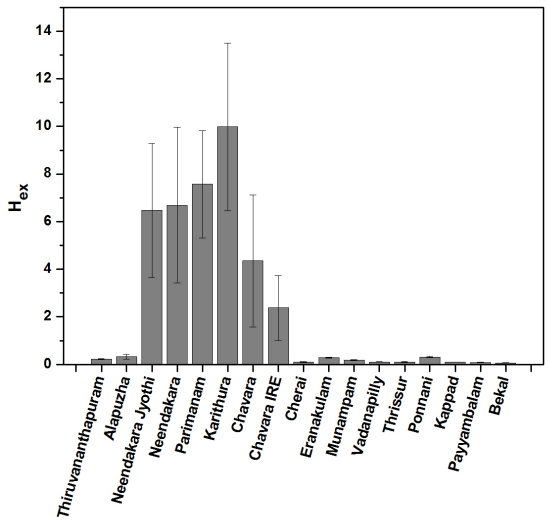

Figure 4.13: The external hazard index

in Kasaragod district as shown in Figure 4.12. The radium equivalent activities in the beach sands of Kollam district varies from 877 Bq kg^{-1} to 3715 Bq kg^{-1}), which is higher than the reference limit of 370 Bq kg^{-1} (UNSCEAR, 2000). The external hazard index (H_{ex}) in the beaches of Kollam varies from 2.37 - 9.98, which is greater than the value 1, that is recommended for external exposure index (see Figure 4.13). This indicates that the hazardous effect caused by the surface beach sand is high. The H_{ex} in the normal background areas of Kerala (i.e., except Kollam district) varies from 0.07 to 0.33, which is within the value recommended.

To draw a valid conclusion regarding the nature and distribution of the radioactive elements, a correlation matrix analyis was done using SPSS- 20 software package. The Pearson correlation matrix for the activity concentration of radionuclides and the corresponding radiological parameters obtained for HBRA and NBRA is presented in Table 4.4 and Table 4.5. The correlation matrices obtained shows that

Table 4.4: Pearson correlation matrix for HBRA

	^{238}U	^{232}Th	^{40}K	D	AED	R_{eq}	H_{ex}
^{238}U	1						
^{232}Th	0.775**	1					
^{40}K	0.687**	0.352*	1				
D	0.864**	0.988**	0.452**	1.00**	1		
AED	0.864**	0.989**	0.452**	1.00**	1.00**		
R_{eq}	0.860**	0.989**	0.447**	1.00**	1.00**	1	
H_{ex}	0.859**	0.989**	0.446**	1.00**	1.00**	1.00**	1

** Correlation is significant at the 0.01 level (2 tailed).
* Correlation is significant at the 0.05 level (2 tailed).

Table 4.5: Pearson correlation matrix for NBRA

	^{238}U	^{232}Th	^{40}K	D	AED	R_{eq}	H_{ex}
^{238}U	1						
^{232}Th	0.804**	1					
^{40}K	-2.44	-1.78	1				
D	0.869**	0.974**	-0.031	1			
AED	0.869**	0.974**	-0.031	1**	1		
R_{eq}	0.876**	0.982**	-0.079	0.999**	0.999**	1	
H_{ex}	0.874**	0.981**	-0.061	0.999**	0.0999**	1.00**	1

** Correlation is significant at the 0.01 level (2 tailed).

all radiological parameters have strong depence on dose rate (0.999, 1). It is confirmed that activity of thorium and uranium contribute much to the dose rate. The ^{40}K is weakly correlated with uranium and thorium in HBRA while it is negatively correlated with uranium and thorium in NBRAs. It is expected naturally because ^{40}K is singly occuring and is indepenent of the radioactive series.

In view of the present study, the radioactivity levels in soil along different coastal beaches of India and the other countries are listed in Table 4.6. The uranium activity in the HBRA (Kollam district) is comparable to the well known HBRA like Ullal in Karnataka, whereas the thorium activity is less than that of Ullal. The uranium

levels in coastal areas (NBRA) of Kerala are comparable to the nearby coastal parts of Tamilnadu (Punniyakotti, J. and Ponnusamy, V., 2018; Kannan et al., 2002) but thorium level is less than that at the other studied NBRAs within India. Like the coastal areas of Kerala, the neighbouring state Tamilnadu also is having high background (Suresh Gandhi et al., 2014) and normal background radiation areas (Punniyakotti, J. and Ponnusamy, V., 2018). The potassium activity in China, Brazil, Turkey and Thailand are higher than that at the coastal areas of Kerala. Table 4.6 shows that Indian coastal areas are thorium rich with less potassium content, compared to other countries.

Table 4.6: Uranium, thorium and potassium levels in soils, observed in various coastal areas of other countries.

S No	Country	^{238}U Bq kg^{-1}	^{232}Th Bq kg^{-1}	^{40}K Bq kg^{-1}	Reference
1	Kollam-HBRA, Kerala, India	516	1229	194	Present study
2	Coastal areas of Kerala-NBRA	11.91	26.07	241.94	Present study
3	Southern region of Tamil Nadu coast (HBRAs), India	12.13	59.03	197.03	Punniyakotti Ponnusamy 2018
4	North East coast of Tamilnadu, India	349	713	35	Suresh Gandhi et al., 2014
5	Odisha, Eastern India	274	249	-	Ghosal et al., 2017
6	Ullal, Karnataka, India	546	2971	268	Ramasamy et al.,2013
7	Kalpakkam, Tamilnadu, India	16	119	406	Kannan et al., 2003
7	Xiamen Island, China	14	11	40	Yingnan et al., 2015
9	Red sea coast Safaga Hurguda	25 20	21 22	122 548	El-Arabi, 2005
10	Guangdong, China	134	187	680	Gang et al., 2012
11	Kirklareli, Turkey	37	40	667	Taskin et al., 2009
12	East coast, Thailand	3-18	5-34	182-559	Malain et al. 2010
13	Dois Rios beach, Brazil	6-78	12-87	269-587	Freitas et al., 2004

4.9 XRF analysis

To check the presence of heavy mineral deposits along the coastal ares of Kerala, the soil samples were subjected to XRF analysis. The presence of radioactive elements like uranium, thorium, heavy metals (Cr, Ni, Pb, Cu, Zn) and other trace elements in the sampling locations were determined for the purpose of evaluating the potential ecological risks.

The representative samples from each sampling location were subjected to Energy Dispersive -XRF analysis using Xenometric EX-3600 ED-XRF spectrometer. The powdered samples taken in the specto-membrane cups were bombarded with the X-rays emitted from X-ray tube (50 kV) with Rh anode. The X-rays emitted by the atoms were measured by Si(Li) detector having resolution of 1.43 eV at 5.9 keV. These equipments were connected to the multichannel analyser and EXWIN software package which display the raw spectrum. The elements having concentrations ranging from few parts per million (ppm) to 100% can be analysed using XRF spectrometer.

XRF analysis reveals the significant contribution of thorium, uranium and lead in all the analysed samples (see Figures 4.14, 4.15). The thorium concentration varies between 0.735 to 1071 ppm. The highest value is shown in the sample collected from Neendakara, as can be seen in Figure 4.14. Thorium is the main component of monazite and the XRF analysis confirms the presence of monazites in these areas. The uranium concentration varies between 0.085 to 86.93 ppm. Soil samples collected from HBRA shows uranium concentration ($>$ 19 ppm) and thorium concentration($>$ 60 ppm) while that for NBRA is less than 4ppm (except in one sample from Munampam).

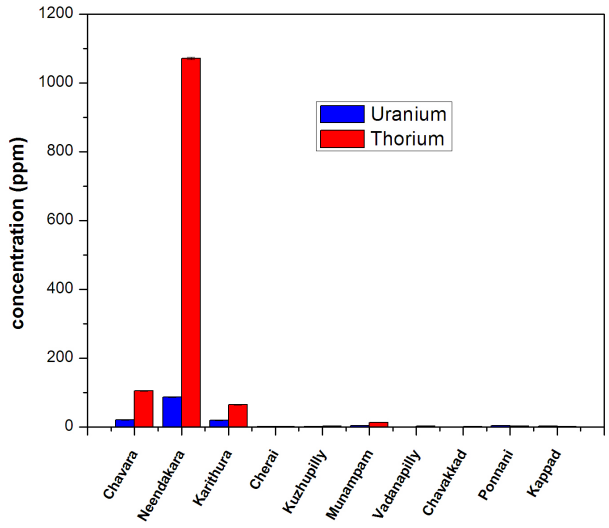

Figure 4.14: Uranium and throrium concentration in soil samples collected from the coastal areas of Kerala from XRF data

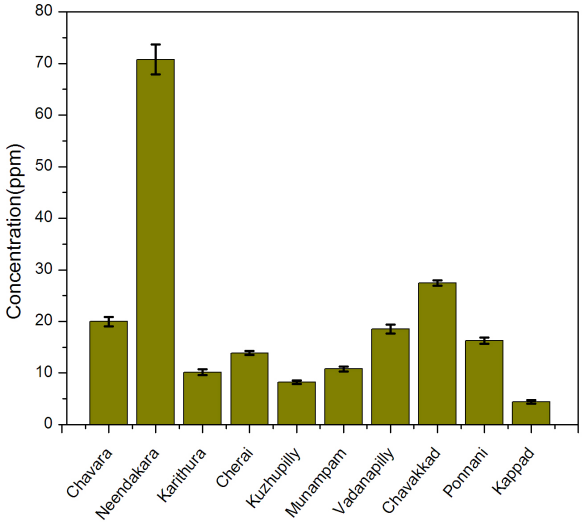

Figure 4.15: Lead concentration in soil samples collected from the coastal areas of Kerala

The presence of heavy metals like Cr, Cu, Zn, Ni and Pb is also identified in the XRF analysis. To understand the concentrations of heavy metals and to predict their toxicity, a comparative study was made with background reference values such as toxicological reference values, the world surface rock average (WSA), the effect range low (ERL) and the effect range medium (ERM) (Suresh et al., 2012). ERL values represent the minimal-effect range in which the biological effects are rarely observed (Gao and Chen, 2014; Long et al., 1995). The ERM values correspond to the range in which the biological effects happen occasionally and the concentrations above ERM cause portable effects, which results in adverse biological effects. The results are presented in Table 4.7.

It is observed that the concentration of heavy metals in Neendakara beach is higher than the toxicity reference value (TRV) and Effect Range Low (ERL). Among the heavy metals analysed, concentrations of chromium level dominated that of the other heavy metals such as Ni, Zn, Pb and Cu at all locations and was higher than the toxicity reference value (TRV). Generally chromium exhibit two oxidation states +3 and +4, and the +4 oxidation states is more harmful and toxic (WHO, 1990). The higher concentrations of chromium in all beaches are due to the effect of effluences from harbours (Suresh G et al., 2015).

Table 4.7: The summary of the heavy metal concentrations in the coastal region of Kerala.

S.No	Sampling locations	Cr	Ni	Pb	Cu	Zn
	(ppm)	(ppm)	(ppm)	(ppm)	(ppm)	(ppm)
1	Chavara	220.70±1.60	15.29±1.3	19.99±0.91	6.52±1.70	94.79±1.40
2	Neendakara	624.10±4.70	48.90±3.30	70.76±2.9	28.93±6.10	311.00±4.00
3	Karithura	168.10±1.20	9.34±0.93	10.16±0.55	4.92±0.99	36.19±0.80
4	Cherai	27.27±0.67	13.03±0.78	13.91±0.39	3.66±0.49	14.05±0.48
5	Kuzhupilly	58.90±0.79	23.17±0.98	8.254±0.36	4.54±0.76	40.36±0.76
6	Munampam	99.91±1.10	32.21±1.20	10.83±0.47	4.78±0.82	53.92±0.97
7	Vadanapilly	49.5±0.8	15.58±0.88	18.50±0.87	4.36±0.57	16.97±0.55
8	Chavakkad	27.72±0.78	11.28±0.94	27.47±0.55	4.24±0.59	13.10±0.61
9	Ponnani	117.70±1.40	36.10±1.40	16.27±0.61	7.62±0.86	70.72±1.20
10	Kappad	73.74±0.93	16.24±0.90	4.41±0.36	0.09±0.00	14.54±0.52
	WSA	97	49	20	32	129
	TRV	26	16	31	16	110
	ERL	81	20.9	47	34	150
	ERM	370	51.6	218	270	410

Except at Neendakara, the Cu and Ni concentrations in all other beaches are less than the background reference values like ERL, TRV and WSA. The excessive concentration of heavy metals in marine environment affects the living organisms and poses risk to human beings through the intake of sea foods. The presence of radioactive elements and other trace elements in Neendakara, crossing the safety levels, had been pointed out earlier also.

Table 4.8: Pearson correlation matrix for trace elements

	Cr	Cu	Ni	Pb	Zn	U	Th	Fe
Cr	1							
Cu	0.951**	1						
Ni	0.696*	0.777**	1					
Pb	0.874**	0.949**	0.636*	1				
Zn	0.980**	0.978**	0.795**	0.903**	1			
U	0.991**	0.957**	0.650*	0.900**	0.967**	1		
Th	0.966**	0.974**	0.702*	0.937**	0.969**	0.983**	1	
Fe	0.574	0.658*	0.927**	0.510	0.671**	0.506	0.527	1

** Correlation is significant at the 0.01 level (2 tailed).
* Correlation is significant at the 0.05 level (2 tailed).

To understand the correlation of radioactive elements with the other trace elements, a Pearson correlation matrix is generated using SPSS -20 software package as shown in Table 4.8. It is seen that uranium and thorium are strongly correlated with Cr, Cu, Pb and Zn. It indicates that the concentration of these heavy metals are high in the areas where the presence of heavy mineral deposits were identified.

4.10 References

1. Aswathanarayana., U. (1985) Principles of Nuclear Geology. Oxonian Press Pvt. Ltd, New Delhi, 88-90.

2. Chougaonkar, M.P., Eappen, K.P., Ramachandran, T.V., Shetty, P.G., Mayya, Y.S., Sadasivan, S., Venkat Raj, V. (2004) Profiles of doses to the population living in the high background radiation areas in Kerala, India. J. Environ. Radioact. 71, 275-297 .

3. District Survey Report of Minor Minerals, Prepared as per Environment Impact Assessment (EIA) Notifcation, (2006) issued under Environment Protection Act 1986, Department of Mining and Geology, November, 2016, Thiruvananthapuram, www.dmg.kerala.gov.in

4. El-Arabi, A.M. (2005) Natural radioactivity in sand used in thermal therapy at the Red Sea Coast. J. Environ. Radioact. 81, 11-19.

5. Freitas, A.C., Alencar, A.S. (2004) Gamma dose rates and distribution of natural radionuclides in sand beaches-Ilha Grande, South eastern Brazil. J. Environ. Radioact. 75, 211-223.

6. Gang Song., Diyun Chen., Zeping Tang., Zhiqiang Zhang., Wenbiao Xie. (2012). Natural radioactivity levels in topsoil from the Pearl River Delta Zone, Guangdong, China. J. Environ. Radioact. 103, 48-53.

7. Gao, X., Chen, C.T.A. (2014) Heavy metal pollution status in surface sediments of the coastal Bohai Bay. Water Res. 46, 1901-1911.

8. Ghosal S., Agrahari S., Guin R., Sengupta D (2017) Implications of modelled radioactivity measurements along coastal Odisha, Eastern India for heavy mineral resources. Estuar. Coast. Shelf. Sci. 184, 83-89

9. Guembou Shouop Cebastien Joel, Samafou Penabei, Moyo Maurice Ndontchueng, Gregoire Chene, Eric Jilbert Nguelem Mekontso, Alexandre Ngwa Ebongue, Motapon Ousmanou, Strivay David.(2017) Precision measurement of radioactivity in gamma-rays spectrometry using two HPGe detectors (BEGe-6530 and GC0818-7600SL models) comparison techniques: Application to the soil measurement, MethodsX 4, 42-54.

10. Inigo Valan I., Mathiyarasu R., Sridhar S.G.D, Narayanan V., Stephen A. (2015) Investigation of background radiation level in Krusadai Island Mangrove, Gulf of Mannar, India, J. Radioanal. Nucl. Chem 304, 735-744.

11. Kannan, V., Rajan, M.P., Iyengar, M.A.R., Ramesh, R. (2003) Distribution of natural and anthropogenic radionuclides in soil and beach sand samples of Kalpakkam (India) using hyper pure germanium (HPGe) gamma ray spectrometry. Appl. Radiat. Isot. 57, 109-119.

12. Kerala Marine Fisheries Statistics (2015) Director of Fisheries, Government of Kerala, India. http: www.fisheries.kerala.gov.in.

13. Long, E.R., MacDonald, D.D., Smith, S.C., Calder, F.D. (1995). Incidence of adverse biological effects within ranges of chemical concentrations in marine and estuarine sediments. Environ. Manage. 19, 81-97.

14. Malain, D., Regan, P.H., Bradley, D.A., Matthews, M., Santawamaitre, T., Al-Sulaiti, H.A., (2010). Measurements of NORM in beach sand samples along the Andaman coast of Thailand after the 2004 tsunami. Nucl. Instrum. Methods Phys. Res. A 619, 441-445.

15. Pablo C. Ortiz - Ramirez (2015) Development of an absolute method for efficiency calibration of a coaxial HPGe detector for large volume sources, Nucl. Instrum. Methods Phys. Res. A 793, 49-56.

16. Punniyakotti, J., and Ponnusamy, V. (2018) Environmental radiation and potential ecological risk levels in the intertidal zone of southern region of Tamilnadu coast (HBRAs), India, Mar. Pollut. Bull. 127, 377-386.

17. Ramasamy, V., Sundarrajan, M., Paramasivam, K., Meenakshisundaram, V., Suresh, G. (2013). Assessment of spatial distribution and radiological hazardous nature of radionuclides in high background radiation area, Kerala, India, Appl. Radiat. Isotop. 73, 21-31.

18. Sroor, A., Abdel-Haleem, S.Y., Salman, A.B., Abdel-Sammad, M. (2002) En-

vironmental pollutant isotope measurements and natural radioactivity assessment for North Tushki area, South Western desert, Egypt. Appl. Radiat. Isot. 57, 427-436.

19. Suresh, G., Sutharsan, P., Ramasamy, V., Venkatachalapathy, R. (2012). Assessment of spatial distribution and potential ecological risk of the heavy metals in relation to granulometric contents of Veeranam lake sediments, India. Ecotox. Environ. Saf. 84, 117-124.

20. Suresh, G., Ramasamy V, Sundarrajan M, Paramasivam, K. (2015) Spatial and vertical distributions of heavy metals and their potential toxicity levels in various beach sediments from high-background-radiation area, Kerala, India. Mar. Pollut. Bull, 91 (1), 389-400.

21. Suresh Gandi M., Ravisankar R., Rajalakshmi A., Sivakumar S., Chandrasekaran A, Anand D.P. (2014) Measurements of natural gamma radiation in beach sediments of north east coast of Tamilnadu, India by gamma ray spectrometry with multivariate statistical approach. J. Radiat. Res. Appl. Sci. 7, 7-17.

22. Taskin, H., Karavus, M., Ay, P., Topuzoglu, A., Hidiroglu, S., Karahan, G. (2009) Radionuclide concentrations in soil and lifetime cancer risk due to gamma radioactivity in Kirklareli, Turkey. J. Environ. Radioact. 100, 49-53.

23. UNSCEAR 2000. United Nations Scientic Committee on the Effects of Atomic Radiation, Sources and Effects of Ionizing Radiation, UNSCEAR 2000 Report Vol.1 to the General Assembly, with scientic annexes, United Nations Sales Publication, United Nations, New York.

24. UNSCEAR 2008. Sources and efects of ionising radiation, Vol1. United Nations Scientic Committee on the Effect of Atomic Radiation, report to the general assembly with scientic annexe, New York.

25. Veiga, R., Sanches, N., Anjos, R.M., Macario, K., Bastos, J., Iguatemy, M., Aguiar, J.G., Santos A.M.A, Mosquera, B., Carvalho, C., Baptista Filho, M., Umisedo, N.K. (2006) Measurement of natural radioactivity in Brazilian beach sands. Radiat. Meas. 41, 189-196.

26. WHO, 1990. Chromium (Environmental Health Criteria 61) International Programme on Chemical Safety. World Health Organization, Geneva, Switzerlands.

27. Yingnan Huang., Xinwei Lu., Xiang Ding., Tingting Feng. (2015) Natural radioactivity level in beach sand along the coast of Xiamen Island, China. Mar. Pollut. Bull. 91, 357-361.

Chapter 5

Inhalation Dose

5.1 Introduction

Humans are continuously getting exposed to ionizing radiations, emitted by radon, thoron, and their corresponding progenies. The radiation exposure to humans due to these sources occur mainly in three ways 1) external gamma rays 2) inhalation of radon and thoron gases, their progenies, and other radioactive nuclides 3) ingestion of radioactive materials through food and water. It is well known that about 50% of the natural radiation exposure results from inhalation mode (UNSCEAR, 2000), the major contributors being radon, thoron and their short lived radioactive decay products. The indoor radon monitoring had been started globally after the discovery of high radon concentration of the order of 10^5 Bq m^{-3} in the dwellings of Pennsylvania USA (Lowder, 1989). In view of this, a country wide radon monitoring program had been started in India for estimating radiation risk coefficients at places of high and low level doses. Several studies have been conducted in south west coast of Kerala, especially at Neendakara, Chavara, Kollam and Chellanam

and reported a high level of radioactivity at these places (Christa et al., 2012; Ben et al., 2012; Mathew et al., 2012). In the present study, we have included locations in the northern districts of Kerala, where no studies were reported earlier.

5.2 Region of the study

5.3 Areas selected for indoor radon monitoring

Since only few indoor radon studies were reported from northern side of Kerala, we have chosen three highly populated regions from three northern districts of Kerala, namely Pirayiri-Palakkad, Ponnani-Malappuram and Kappad-Kozhikode. The first location is a quarry region and the others are coastal areas. The dwellings in coastal areas have high ventilation rates. The detailed description of the region selected is given below.

5.3.1 Pirayiri - Palakkad district

The geological area selected for the present study is situated in the middle zone of Kerala state, specifically in Pirayiri, Palakkad district. Since the area contains more than five quarries, the surrounding dwellings are mainly populated by mining workers of these quarries. Most of the dwellings selected are made up of rock salt bricks and concrete roof, with tiled floors. Dosimeters were deployed in 25 nearby dwellings. According to the Indian census 2011, the population in Pirayiri is 41,359. This census indicates that 24% of the district is urbanized and the population density is 627/km^2. The site is located at 10.46 N latitude and 76.37 E longitude.

5.3.2 Ponnani - Malappuram district

This study area is the coastal town of Ponnani, where Kerala's second largest river Bharatapuzha comes to end and joins the Arabian sea. Thus, the land is bordered by the estuary on the northern side, backwaters in the south and the Arabian Sea on the West. It is located at an altitude of 5m from sea level and is one of the famous fishing centres in Kerala. The area of study is located at the latitude: 10. 46 N and longitude 75. 54 E in Malappuram district, Kerala. Here, most of the dwellings are highly ventilated and are having concrete roof with cemented floor.

5.3.3 Kappad - Kozhikkode district

Kappad is one of the the most charming beaches of Kerala and is the gateway to the Malabar Coast. Kappad coast has the historical importance because it was here that Vasco da Gamma sailed in and stepped into the land of India. Its latitude is 11.38 N and longitude is 75.71 E. It is one of the highly populated areas with the majority of dwellings made up of concrete roof and tiled/cemented floor with good ventilation condition.

5.4 Experimental technique

Indoor radon, thoron and the progeny concentrations were estimated out by installing the twin cup dosimeters and progeny sensors (DTPS and DRPS) in the respective study area. The dosimeters were calibrated in Bhabha Atomic Research Centre (BARC), Mumbai, India. The dosimeters were suspended for a period of 3 months at a height of 2.5 m from the floor in each dwelling. Care was taken to keep

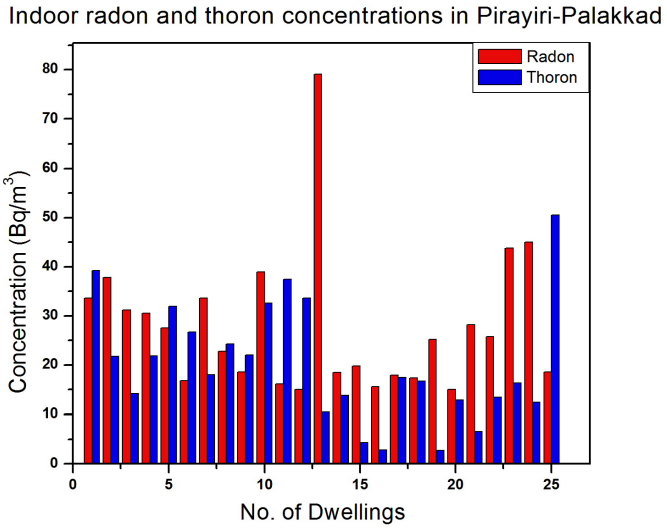

Figure 5.1: Indoor radon and thoron concentration in different dwellings of Pirayiri-Palakkad.

the dosimeters away from fan and walls. After the exposure period, the dosimeters were retrieved back and the detector films were chemically etched in 2.5 N NaOH solution in a constant temperature bath at 60 ^{0} C for 90 min. Then the films were dried, pealed off from its base and subjected to track counting by means of a spark counter (model PSI-SC 1)(Details are included in chapter 3).

5.5 Results and discussions

5.5.1 Pirayiri

Indoor radon and thoron concentrations, potential alpha energy concentrations and annual effective inhalation dose in Pirayiri-Palakkad are listed in Table 5.1. The variation of radon and thoron concentration in different dwellings of the Pirayiri-

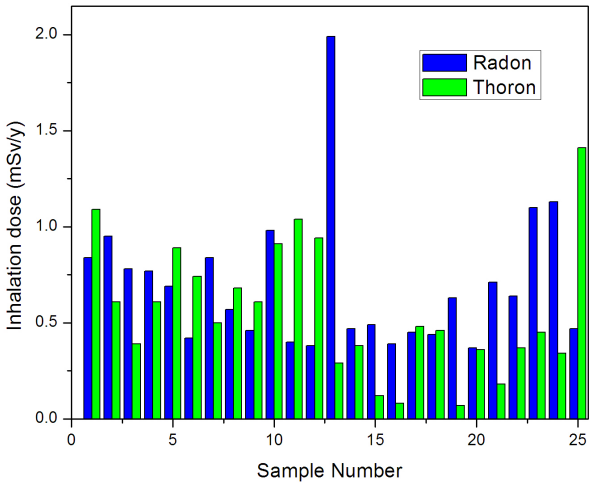

Figure 5.2: Inhalation dose due to radon and thoron in different dwellings of Pirayiri-Palakkad.

Palakkad is shown in Figure 5.1. The indoor radon (25.52 Bq m^{-3}) and thoron (14.58 Bq m^{-3}) concentrations in Pirayiri region are higher than the nation-wide geometric mean (GM) value of 23 Bq m^{-3} (GSD 2.6) for radon and 12 Bq m^{-3} (GSD 3.2) for thoron (Ramachandran and Sathish, 2011). This may be due to the increase in the emanation rate of radioactive elements from the building materials and the atmosphere around the granite quarries. However, the range of radon concentrations in the study area is within the limit of 10-60 Bq m^{-3}, presented by UNSCEAR, 2008 for East Asia (UNSCEAR, 2008). The inhalation dose received by the public in the study area is shown in Figure 5.2. The annual effective inhalation dose due to radon and thoron in Pirayiri-Palakkad is less than the action level limit (3-10 mSv y^{-1}) suggested by the ICRP (ICRP-65 1993).

Table 5.1: Indoor radon and thoron concentrations, potential alpha energy concentrations and Annual effective inhalation dose in Pirayiri-Palakkad, Kerala, India.

S No	ρ_m	ρ_f	C_R	C_T	$PAEC_R$	$PAEC_T$	EID_R	EID_T
	Tr.cm^{-2}	Tr.cm^{-2}	Bq m^{-3}	Bq m^{-3}	mWL	mWL	mSv/y	mSv/y
1	56	87	33.59	39.18	3.63	1.06	0.84	1.09
2	63	92	37.79	21.81	4.08	0.59	0.95	0.61
3	52	71	31.19	14.20	3.37	0.38	0.78	0.39
4	51	80	30.59	21.91	3.30	0.59	0.77	0.61
5	46	88	27.59	31.95	2.98	0.86	0.69	0.89
6	28	63	16.79	26.72	1.81	0.72	0.42	0.74
7	56	80	33.59	18.02	3.63	0.49	0.84	0.50
8	38	70	22.79	24.32	2.46	0.66	0.57	0.68
9	31	60	18.60	22.06	1.06	0.60	0.46	0.61
10	65	108	38.99	32.57	2.01	0.88	0.98	0.91
11	27	76	16.20	37.49	1.75	1.01	0.40	1.04
12	25	69	15.00	33.65	1.62	0.91	0.38	0.94
13	132	147	79.14	10.49	8.55	0.28	1.99	0.29
14	31	53	18.51	13.88	2.01	0.37	0.47	0.38
15	33	39	19.80	4.34	2.14	0.12	0.49	0.12
16	26	30	15.60	2.86	1.68	0.08	0.39	0.08
17	30	53	17.99	17.46	1.94	0.47	0.45	0.48
18	29	51	17.40	16.69	1.88	0.45	0.44	0.46
19	42	46	25.19	2.74	2.72	0.07	0.63	0.07
20	25	42	15.00	12.88	1.62	0.35	0.37	0.36
21	47	56	28.19	6.55	3.04	0.18	0.71	0.18
22	43	61	25.79	13.51	2.78	0.37	0.64	0.37
23	73	95	43.78	16.35	4.73	0.44	1.10	0.45
24	75	92	44.98	12.49	4.86	0.34	1.13	0.34
25	21	97	18.60	50.54	2.01	1.37	0.47	1.41
AM	-	-	28.09	19.79	2.90	0.55	0.71	0.57
SD	-	-	14.30	12.31	1.57	0.33	0.36	0.34
GM	-	-	25.52	14.58	2.60	0.44	0.64	0.45
GSD	-	-	1.52	2.15	1.58	2.15	1.52	2.17

5.5.2 Ponnani

The indoor radon, thoron and potential alpha energy concentrations and annual effective inhalation dose in Ponnani is listed in Table 5.2. The variation of radon

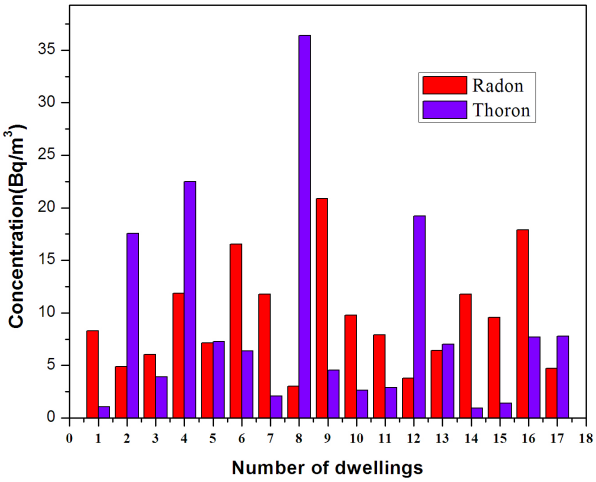

Figure 5.3: Indoor radon and thoron concentration in different dwellings of Ponnani coastal area.

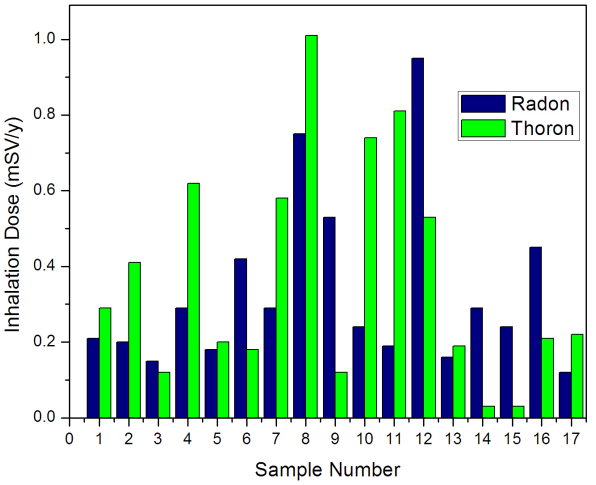

Figure 5.4: Inhalation dose due to radon and thoron in different dwellings of Ponnani coastal area

Table 5.2: Indoor radon and thoron concentrations, potential alpha energy concentrations and Annual effective inhalation dose in Ponnani -Malappuram, Kerala, India.

S No	ρ_m	ρ_f	C_R	C_T	$PAEC_R$	$PAEC_T$	EID_R	EID_T
	Tr.cm^{-2}	Tr.cm^{-2}	Bq m^{-3}	Bq m^{-3}	mWL	mWL	mSv/y	mSv/y
1	22	25.5	8.27	1.05	0.89	0.03	0.21	0.29
2	13	53	4.88	17.55	0.53	0.47	0.2	0.41
3	16	25	6.02	3.91	0.65	0.11	0.15	0.12
4	31	83	11.84	22.47	1.28	0.61	0.29	0.62
5	19	36	7.14	7.27	0.77	0.19	0.18	0.20
6	44	60	16.54	6.37	1.78	0.17	0.42	0.18
7	31	37	11.76	2.07	1.27	0.05	0.29	0.58
8	8	90	3.01	36.4	0.33	0.98	0.75	1.01
10	26	33	9.77	2.64	1.06	0.07	0.24	0.74
11	21	28	7.89	2.89	0.85	0.08	0.19	0.81
12	10	53	3.76	19.22	0.42	0.52	0.95	0.53
13	17	33	6.39	7.01	0.69	0.18	0.16	0.19
14	31	35	11.76	0.91	1.27	0.02	0.29	0.03
15	25	30	9.58	1.41	1.03	0.03	0.24	0.03
16	47	67	17.89	7.67	1.93	0.21	0.45	0.21
17	12	30	4.69	7.78	0.50	0.21	0.12	0.22
AM			9.53	8.89	1.02	0.23	0.33	0.37
SD			5.09	9.63	0.54	0.26	0.22	0.29
GM			8.32	5.29	0.90	0.13	0.2	0.24
GSD			1.73	2.94	1.72	3.06	1.77	2.82

and thoron concentration in different dwellings of the Ponnani is shown in Figure 5.3. The radon concentration in Ponnani coastal area varies from 3.01 to 20.86 Bq m^{-3} with an arithmetic mean of 9.53 Bq m^{-3}. It is less than the world average value of 40 Bq m^{-3}, reported for dwellings and lies within the limit of (10-60 Bq m^{-3}), UNSCEAR prediction for East Asia (UNSCEAR, 2008). The studies carried out in Ponnani also shows that the inhalation dose (see Figure 5.4) due to radon and thoron are well below the limit (3-10 mSv/y) recommended by the ICRP (ICRP-65, 1993). This again indicates that hazardous radionuclides present in the indoor

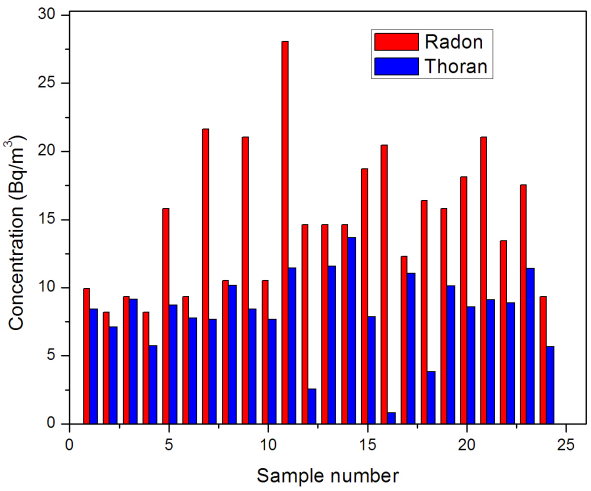

Figure 5.5: Indoor radon and thoron concentration in different dwellings of Kappad coastal area.

atmosphere are very low. The higher ventilation rate in the coastal belt prevents the radon build up inside the dwellings. This study brings out the fact that radon and thoron concentrations are negligible in the coastal belt of Ponnani, Malappuram district, when compared to the south west coast of Kerala.

5.5.3 Kappad

The summary of indoor radon and thoron concentrations, EERC and EETC, equilibrium factors and annual effective inhalation dose in Kappad coastal area are listed in Table 5.3. The variation of radon and thoron concentration in different dwellings of the Kappad is shown in Figure 5.5. The average Radon concentration measured at Kappad (14.98 Bq m^{-3}) is less than the world average value of 40 Bq m^{-3}, reported for dwellings. The average value of thoron concentration (8.22 Bq m^{-3}) was

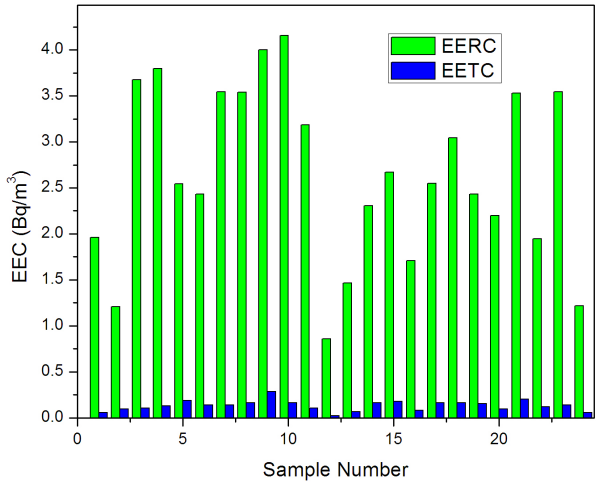

Figure 5.6: EERC and EETC in Kappad

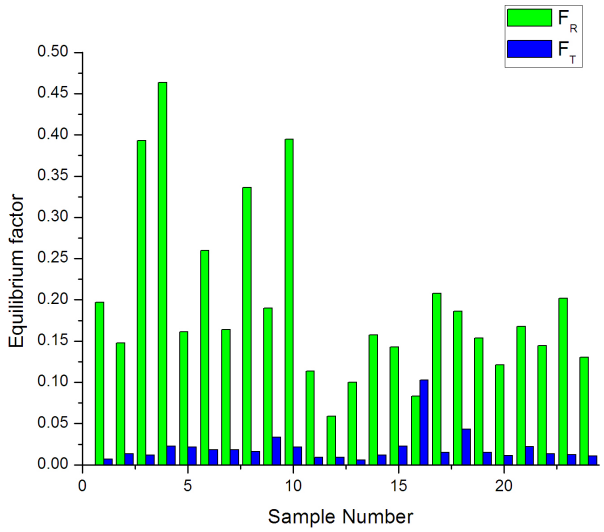

Figure 5.7: Equilibrium factor distribution in Kappad

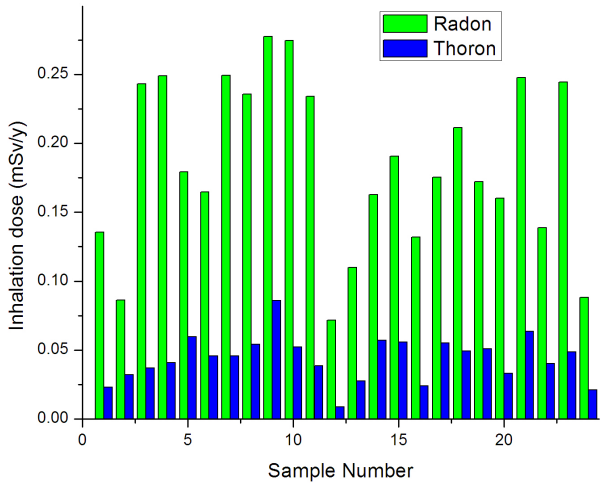

Figure 5.8: Inhalation dose due to radon and thoron in different dwellings of Kappad coastal area

found to be less than the national average of 12.2 Bq m^{-3} (Ramola et al., 2016). The variation of EERC and EETC in different dwellings are shown in Figure 5.6. The average value of EERC and EETC in the study area has been found to be 2.64 and 0.13 Bq m^{-3}, respectively. The equilibrium factor for radon (0.19) in the study area is less than the globally assumed value (0.4) recommended by UNSCEAR 2008 (UNSCEAR, 2008). The variation of equilibrium factors in different dwellings of kappad is shown in Figure 5.7. The equilibrium factor of thoron and its progeny for the region (0.02±0.01) has been found to be in good agreement with its globally assumed value (0.02)(UNSCEAR, 2008). This results indicate that the equilibrium factors vary from place to place and it is important to calculate the equilibrium factor in each study area for actual dose estimation. The inhalation dose received by the public in the study area is shown in Figure 5.8. The estimated inhalation dose in the monitored areas are within the safe level limit (3 - 10 mSv/y) as prescribed

Table 5.3: Indoor radon and thoron concentrations, EERC, EETC, F_R, F_T and annual effective inhalation dose due to radon and thoron and total dose in Kappad -Kozhikode, Kerala, India.

S No	C_R	C_T	EERC	EETC	F_R	F_T	EID_R	EID_{Tn}	EID_T
	Bq m^{-3}	Bq m^{-3}	Bq m^{-3}	Bq m^{-3}			mSv/y	mSv/y	mSv/y
1	9.94	8.40	1.96	0.05	0.19	0.01	0.13	0.02	0.15
2	8.18	7.12	1.21	0.09	0.14	0.01	0.08	0.03	0.11
3	9.35	9.13	3.67	0.10	0.39	0.01	0.24	0.03	0.27
4	8.18	5.73	3.79	0.13	0.46	0.02	0.24	0.04	0.28
5	15.78	8.73	2.54	0.18	0.16	0.021	0.17	0.06	0.23
6	9.35	7.74	2.43	0.14	0.26	0.02	0.16	0.04	0.21
7	21.63	7.67	3.54	0.14	0.16	0.01	0.24	0.04	0.29
8	10.52	10.17	3.53	0.16	0.33	0.02	0.23	0.05	0.28
9	21.05	8.40	4.00	0.28	0.19	0.03	0.27	0.08	0.36
10	10.52	7.67	4.15	0.16	0.39	0.02	0.27	0.05	0.32
11	28.07	11.44	3.18	0.10	0.11	0.01	0.23	0.04	0.27
12	14.61	2.55	0.85	0.02	0.05	0.01	0.07	0.01	0.08
13	14.61	11.58	1.46	0.06	0.10	0.01	0.10	0.03	0.13
14	14.61	13.66	2.30	0.16	0.15	0.01	0.16	0.05	0.21
15	18.71	7.85	2.67	0.17	0.14	0.02	0.19	0.05	0.24
16	20.46	0.80	1.70	0.08	0.08	0.10	0.13	0.02	0.15
17	12.28	11.038	2.55	0.16	0.20	0.01	0.17	0.05	0.23
18	16.37	3.83	3.04	0.16	0.18	0.04	0.21	0.04	0.26
19	15.78	10.12	2.43	0.15	0.15	0.01	0.17	0.05	0.22
20	18.12	8.58	2.19	0.09	0.12	0.01	0.16	0.03	0.19
21	21.05	9.10	3.52	0.20	0.16	0.02	0.24	0.06	0.31
22	13.45	8.88	1.94	0.11	0.14	0.01	0.13	0.04	0.17
23	17.54	11.40	3.54	0.14	0.20	0.01	0.24	0.04	0.29
24	9.35	5.66	1.21	0.05	0.13	0.01	0.08	0.02	0.10
AM	14.98	8.22	2.64	0.13	0.19	0.02	0.18	0.04	0.22
SD	5.17	2.95	0.95	0.05	0.10	0.01	0.06	0.01	0.07
GM	14.15	7.34	2.45	0.11	0.17	0.01	0.17	0.03	0.21
GSD	1.41	1.81	1.52	1.68	1.63	1.83	1.47	1.61	1.46

by ICRP (ICRP-65, 1993).

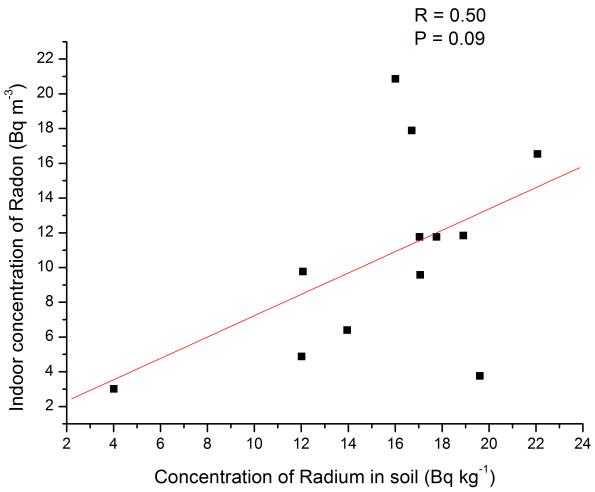

Figure 5.9: Correlation between radon and radium content in the soil in Ponnani.

5.5.4 Correlation studies in coastal areas

To carry out correlation studies, the soil samples were collected from the vicinity of the houses where the dosimeters were deployed in Ponnani and Kappad coastal areas. These soil samples were subjected to the gamma spectrometric analysis as described in section 4.6. Correlation graphs were plotted between radon concentration and the radium content in the soil and thoron concentration and thorium content as shown in Figures 5.9, 5.10, 5.11, 5.12.

No significant correlation was observed, and this indicates the radon/thoron emanating from the building materials do not get build up in the dwellings due to higher ventilation rate in these areas. The indoor radon concentration varies significantly with ventilation conditions of the houses. Even with the houses located in places having radium and thorium, the indoor radon may not be very high or may be even low if it is well ventilated. Besides the variation in the type of building materials, the flooring and roofing may also affect the indoor radon concentrations

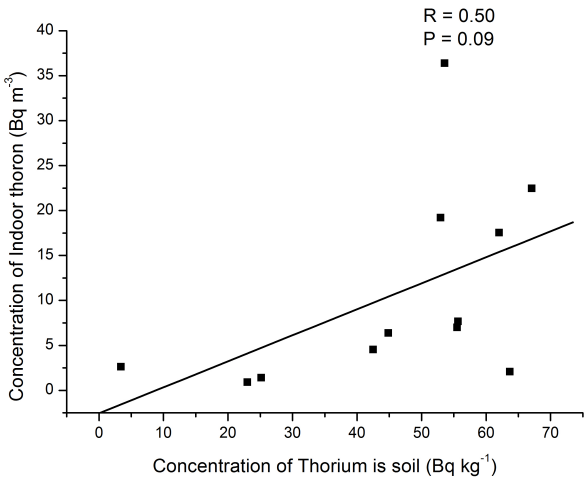

Figure 5.10: Correlation between thoron and thorium content in the soil in Ponnani.

and the correlation may be lost. In the case of thoron, these factors mentioned for radon along with its short half life influences the indoor thoron concentrations.

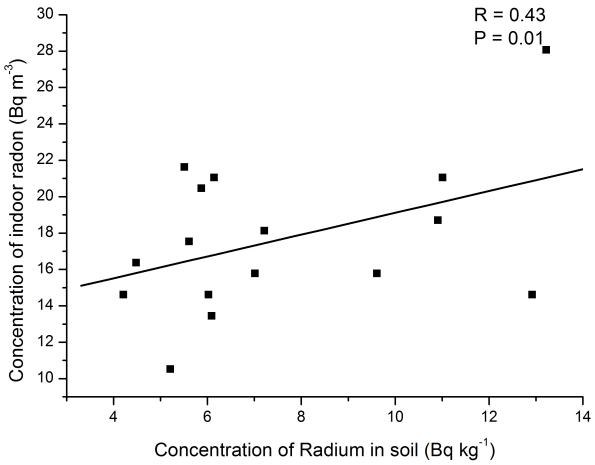

Figure 5.11: Correlation between radon and radium content in soil samples of Kappad coastal area

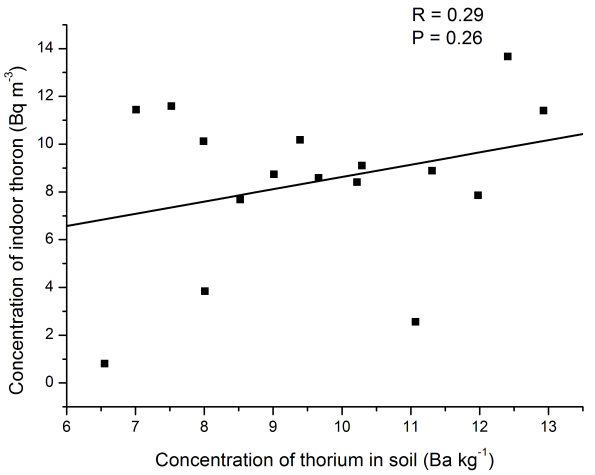

Figure 5.12: Correlation between thoron and thorium content in soil samples of Kappad coastal area

5.6 Comparison of indoor radon levels in various countries

We also compared the indoor radon level with the data reported in other countries and is listed in Table 5.4 .

Table 5.4: Comparison of indoor radon levels in the study area with that in other countries.

S.No	Country	C_R(GM)	References
1	Mexico city	55	(Martinez et al., 2004)
2	Spain	45	(Quindos et al., 2004)
3	China (Gansu Province)	81	(Yuji et al., 2006)
4	Bulgeria	99	(Kremena et al., 2013)
5	Hungary	58	(Krisztian et al., 2006)
6	India(Nationwide)	23	(Ramachandran and Sathish, 2011)
7	Pirayiri	25	(Present study)
8	Ponnani	8.30	(Present study)
9	Kappad	14.15	(Present study)

5.7 References

1. Ben, Byju S., Koya, P. K. M., Sahoo, B. K., Jojo, P. J., Chougaonkar, M. P., Mayya, Y. S.(2012). Inhalation and external doses in coastal villages of high background radiation area in Kollam India. Radiat. Protect. Dosim. 152, 154-158.

2. Christa, E. Pereira, Vaidyan, V. K., Chougaonkar, M. P., Mayya, Y. S., Sahoo, B. K., Jojo, P. J. (2012). Indoor radon and thoron levels in Neendakara and Chavara regions of southern coastal Kerala, India. Radiat. Protect. Dosim. 150, 385-390.

3. ICRP-65. (1993). Protection against Radon-222 at home and at work. An International Commission on Radiological Protection, 23(2), 1-48 (Pergamon Press, Oxford).

4. Kremena, I., Zdenka, S., Viktor, B., Bistra, K. (2013). Pilot survey of indoor radon in the dwellings of Bulgaria. Radiat. Protect. Dosim. 157(4), 594-599.

5. Krisztian, Hamori, Eszter, Toth, Lenard, Pal, George, Koteles, Andras, Losonci, Mihaly, Minda (2006). Evaluation of indoor radon measurements in Hungary, J. Environ. Radioact. 88, 189-198.

6. Lowder, W. M. (1989) National environmental radioactivity and radon gas. Il Tommasino, et al. (Eds.), Proceedings of the international workshop on radon monitoring in radioprotection, environmental radioactivity and earth sciences (1-77). New Jersey: World Scientific.

7. Mathew, S., Rajagopalan, M., Abraham, J. P., Balakrishnan, D., Umadevi, A. G. (2012) Natural radioactivity content in soil and indoor air of Chellanam. Radiat. Protect. Dosim. 152, 1-4.

8. Martinez, T., Navarrte, M., Gonzalez, P., Ramrez. (2004). Variation in indoor thoron levels in Mexico city dwellings. Radiat. Protect. Dosim. 11, 111-115.

9. Quindos, Poncela L. S., Fernandez, P. L., Gomez Arozamena, J., Sainz, C., Fernandez, J. A., Suarez Mahou, E., et al. (2004). Natural gamma radiation map (MARNA) and indoor radon levels in Spain. Environment International 29, 1091-1096.

10. Ramachandan, T. V., Sathish, L. A. (2011). Nationwide indoor ^{222}Rn and ^{220}Rn map for India: A review. J. Environ. Radioact. 102, 975-986.

11. Ramola, R. C. et al. (2016), Dose Estimation Derived from the Exposure to Radon, Thoron and their Progeny in the Indoor Environment. Sci. Rep. 6, 31061.

12. UNSCEAR. (2008). United nations scientific committee on the effect of atomic radiation. ANNEXURE-E.

13. UNSCEAR. (2000) United nations scientific committee on the effects of atomic radiation, sources and effects of ionizing radiation, New York.

14. Yuji, Y., Quanfu, S., Shinji, T., Suminori, A., Weihai, Z., Changsog, H., et al. (2006). Radon-thoron discriminative measurements in Gansu province, China, and their implications for dose estimates. J. Toxicol. Environ. Health Part A 69, 723-734.

Chapter 6

CONCLUSION AND FUTURE SCOPE

The primary objective of this thesis work is to study the presence of naturally occuring radionuclides along the coastal areas of Kerala and evaluate the radiation hazard indices. It is well known that about 50% of the natural radiation exposure results from inhalation pathway and the major contributors are radon and thoron gases and their short lived radioactive decay products. Radon and thoron are the decay products from the decay series of uranium (^{238}U) and thorium (^{232}Th) respectively. We have estimated the inhaltion dose due to radon, thoron and their progenies in the highly populated areas (Pirayiri, Ponnani and Kappad) in the northern part of Kerala. The evaluation of external dose received by the public due to the presence of naturally occuring radionuclides along the coastal areas of Kerala was also done . The conclusions of the present study is summarized as given below.

6.1 External dose

- The present study is carried out along the coastal region of Kerala, India to evaluate the distribution of radium, thorium and potassium concentrations in surface sand samples, using High Purity Germanium detector.

- The coastal regions of Kerala being a monazite deposit area, the study is envisaged to determine the background radiation levels in the area and the findings can be used as a baseline data for future doismetric or epidemiological studies.

- A total of 92 samples were collected from various locations along the coastal line of Kerala, by the side of the Arabian sea. The highest value of uranium (1176.75 Bq kg^{-1}) and thorium (3485.46 Bq kg^{-1}) were found at Karithura beach of Kollam district.

- The absorbed dose rate, external hazard index and radium equivalent activities are computed. The radium equivalent activities in the beach sands of Kollam district varies from 877.95 Bq kg^{-1} to 3715.87 Bq kg^{-1}, which is higher than the reference limit of 370 Bq kg^{-1} (UNSCEAR 2000).

- The Annual Effective Dose (AED) calculated from the 44 samples collected from the area shows a geometric mean value of 1.04 (GSD 2.03) mSv/y.

- The correlation matrices connecting the activity concentrations of uranium, thorium and potassium and the radiation hazard indices were generated both for the soil samples collected from HBRA and NBRA.

- The presence of radioactive elements along with the trace elements in soil samples were confirmed using ED-XRF and the correlation matrix connecting uranium and thorium with other heavy metals was also generated.

- The study reveals the fact that heavy mineral deposits are confined to the narrow belt of Kollam district that causes enhanced radioactivity in beach sands. The radium equivalent activity, external hazard index, and absorbed dose rate of the surface soil samples along the coastal areas of Kollam district are higher than the internationally accepted limit.

6.2 Inhalation dose

- Indoor radon and thoron levels in Pirayiri region of Palakkad district, Ponnani of Malappuram district, Kappad of Kozhikkode district were investigated by deploying twin cup dosimeters.

- The geometric mean value of radon concentration (25.52 Bq m^{-3}) in Pirayiri-Palakkad is higher than the nationwide average. The estimated thoron concentration in Pirayiri-Palakkad was found to be somewhat higher than the national average 12.2 Bq m^{-3} .

- Radon concentration in the studied coastal areas Ponnani and Kappad are less than the world average value of 40 Bq m^{-3}, reported for dwellings and lies below the limit of (10-60 Bq m^{-3}) UNSCEAR prediction in East Asia. The higher ventilation rate prevents radon build up in these dwellings.

- The equilibrium factor calculated for thoron and its progeny (0.02) in Kappad has been found to be in good agreement with its globally assumed value (0.02).

- The estimated inhalation dose in the monitored areas are below the action level limit (3-10 mSv/y) recommended by International Commission on Radiological Protection (ICRP).

6.3 Future plans

- The baseline data regarding the distribution of heavy metals like Cd, Cr, Ni, Zn etc along the coastal line is to be investigated by extending the the present work using ICP-MS (Inductively coupled plasma mass spectrometry).

- The evaluation of external dose due to radionuclides in soil samples from more quarry areas located in other districts.

- Seasonal variation of radon and thoron concentration in quarry areas like Palakkad, Wayanad etc.

- The radon concentration in drinking water samples in urban and rural areas of Kerala.

Appendix A

Appendix

Table A.1: The radiological parameters

S. No	**Location**	**Sample code**	**Dose ($nGy\ h^{-1}$)**	**AED ($mSv\ y^{-1}$)**	**R_{eq} ($Bq\ kg^{-1}$)**	**H_{ex}**
1	Shanghumugham	SH1	35.05	0.042	74.40	0.20
2		SH2	37.11	0.045	79.66	0.21
3		SH3	41.07	0.050	88.46	0.24
4	Alapuzha	A1	40.80	0.050	88.01	0.24
5		A2	73.51	0.090	161.5	0.43
6		A3	50.33	0.061	108.3	0.29
7	Neendakara Jyothi	NJ1	1019	1.25	2306	6.23
8		NJ2	715	0.877	1616	4.36
9		NJ3	1072	1.314	2425	6.55
10		NJ4	4761	0.584	1074	2.90

Continued on next page

Table A.1 – continued from previous page

S. No	Location	S. code	Dose	AED	R_{eq}	H_{ex}
11		NJ5	1748	2.144	3966	10.71
12		NJ6	1038	1.273	2344	6.33
13		NJ7	1693	2.076	3836	10.36
14		NJ8	700	0.859	1582	4.27
15	Neendakara	N1	1038	1.27	2345	6.33
16		N2	2065	2.53	4679	12.64
17		N3	797	0.978	1804	4.87
18		N4	101	0.123	223.6	0.60
19		N5	1854	2.274	4201	11.35
20		N6	878	1.077	1986	5.36
21		N7	756	0.927	1706	4.61
22		N8	933	1.144	2112	5.70
23		N9	1233	1.512	2793	7.54
24		N10	1288	1.579	2918	7.88
25	Parimanam	P1	1912	2.345	4354	11.76
26		P2	1243	1.524	2816	7.60
27		P3	1183	1.451	2681	7.24
28		P4	951	1.166	2145	5.79
29		P5	892	1.095	2010	5.43
30	Chavara	CH1	1782	2.185	4040	10.91
31		CH2	1274	1.56	2888	7.80

Continued on next page

Table A.1 – continued from previous page

S. No	Location	S. code	Dose	AED	R_{eq}	H_{ex}
32		CH3	260	0.319	581	1.57
33		CH4	432	0.530	974	2.63
34		CH5	532	0.653	1203	3.25
35		CH6	793	0.972	1793	4.84
36		CH7	7296	0.89	1650	4.46
37		CH8	329	0.40	741	2.00
38		CH9	430	0.527	971	2.62
39		CH10	555	0.681	1254	3.38
40	Chavara IRE	CHI1	248	0.304	557	1.50
41		CHI2	163	0.200	364	0.98
42		CHI3	276	0.339	621	1.68
43		CHI4	784	0.961	1774	4.79
44		CHI5	478	0.586	1072	2.90
45	Karithura	K1	1997	2.44	4503	12.15
46		K2	1172	1.43	2624	7.10
47		K3	1313	1.61	2941	7.89
48		K4	1371	1.63	3074	8.31
49		K5	1318	1.61	2959	8.01
50		K6	2732	3.35	6191	16.71
51	Kuzhupilly	KU1	46.45	0.056	100.35	0.27
52		KU2	54.75	0.067	118.14	0.32

Continued on next page

Table A.1 – continued from previous page

S. No	Location	S. code	Dose	AED	R_{eq}	H_{ex}
53		KU3	43.12	0.052	90.94	0.25
54		KU4	53.20	0.065	114.38	0.31
55		KU5	45.18	0.055	96.17	0.26
56	Munampam	M1	34.71	0.042	72.75	0.20
57		M2	34.69	0.042	71.70	0.19
58		M3	25.35	0.031	50.09	0.14
59		M4	31.76	0.038	66.11	0.18
60	Cherai	CHR1	12.89	0.015	26.16	0.07
61		CHR2	21.27	0.026	40.26	0.11
62		CHR3	19.43	0.023	36.72	0.10
63		CHR4	18.47	0.022	34.51	0.09
64		CHR5	19.38	0.023	37.00	0.10
65	Chavakkad	CHV1	19.11	0.023	35.11	0.10
66		CHV2	22.91	0.028	41.27	0.11
67		CHV3	22.14	0.027	40.11	0.11
68		CHV4	17.45	0.021	31.60	0.09
69		CHV5	17.92	0.021	32.57	0.09
70	Vadanapilly	V1	20.38	0.024	38.11	0.10
71		V2	21.10	0.025	39.16	0.11
72		V3	17.07	0.020	30.92	0.08
73		V4	18.63	0.022	34.51	0.09

Continued on next page

Table A.1 – continued from previous page

S. No	Location	S. code	Dose	AED	R_{eq}	H_{ex}
74		V5	20.25	0.024	38.06	0.10
75	Ponnani	PO1	59.71	0.073	129.80	0.35
76		PO2	47.16	0.057	99.19	0.27
77		PO3	53.52	0.065	114.04	0.31
78		PO4	54.02	0.066	115.25	0.31
79	Kappad	KP1	18.52	0.022	35.08	0.09
80		KP2	16.46	0.020	32.00	0.09
81		KP3	18.48	0.022	35.71	0.10
82		KP4	18.57	0.022	36.05	0.10
83	Payyambalam	PY1	20.76	0.025	42.20	0.10
84		PY2	15.10	0.018	29.91	0.08
85		PY3	16.19	0.019	31.55	0.08
86		PY4	15.10	0.018	30.66	0.08
87		PY5	20.24	0.024	41.96	0.11
88	Bekal	B1	12.90	0.015	25.44	0.06
89		B2	10.68	0.013	20.95	0.06
90		B3	13.23	0.016	26.52	0.07
91		B4	14.81	0.018	29.47	0.08
92		B5	15.74	0.019	31.42	0.08

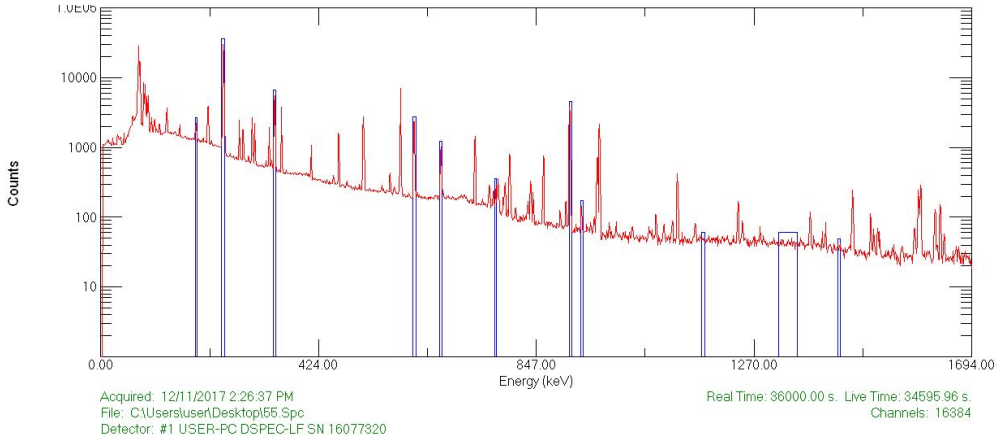

Figure A.1: Sample spectrum 1

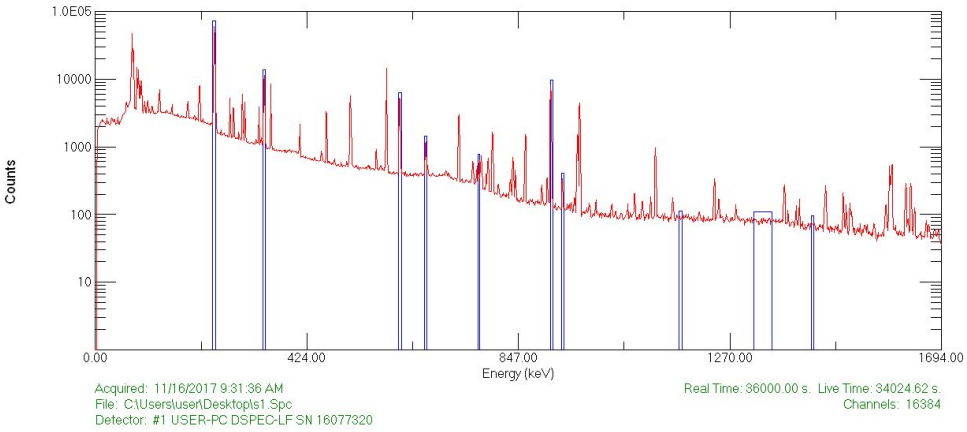

Figure A.2: Sample spectrum 2